AN ABSTRACT OF THE THESIS OF

FRANK ALAN SCHMITTROTH for the DOCTOR OF PHILOSOPHY
(Name) (Degree)

in PHYSICS presented on Oct 7, 1968
(Major) (Date)

Title: A COMPARISON OF EFFECTIVE INTERACTIONS IN NUCLEAR STRUCTURE AND SCATTERING

Redacted for Privacy

Abstract approved:
V. A. Madsen

Effective two-body potentials have been studied for nuclei in the 2s-1d shell and the 1p shell via both structure and scattering calculations. The potential included a central Yukawa force with arbitrary exchange and a tensor force. Calculations were done by use of potential multipole expansions which allow the use of bound single-particle states computed in a Woods-Saxon well.

Effective potential strengths were obtained for nuclear structure by the application of a least squares criterion to effective two-body matrix elements currently available in the literature for the 1p and 2s-1d shells. The prominent features of the potential obtained in this way were strong attractive even strengths and weak repulsive odd strengths. These results were consistent between the two shells. The strength of the tensor force, however was not given consistently.

DWBA calculations which included a tensor force have been

carried out for the following reactions: $C^{14}(p, n)$, $N^{15}(p, n)$ $O^{17}(p, n)$, $O^{18}(p, n)$, $N^{14}(p, p')$, and $C^{14}(He^3, t)$. For the $C^{14}(p, n)$ ground state transition and the analogous (p, p') reaction in N^{14}, the tensor force produced a marked improvement in the fit to the experimental angular distributions and total cross sections. No improvement was found, however, for the (He^3, t) calculation for the same transition, a case poorly fit by the central force calculations also. No significant change was noted in the other reactions.

The effective strengths that were deduced from fitting effective matrix elements were compared to values obtained from DWBA calculations. If the two-body potential is expressed as

$$V = V_{00} + (\vec{\sigma}_1 \cdot \vec{\sigma}_2)V_{10} + (V_{01} + (\vec{\sigma}_1 \cdot \vec{\sigma}_2)V_{11})(\vec{\tau}_1 \cdot \vec{\tau}_2),$$

then, except for the V_{00} strength, good agreement is obtained.

Exchange calculations (knockout) have been made for $C^{14}(p, n)$ and $O^{18}(p, n)$ reactions. The exchange contributions were not large but were quite significant. In particular, they produced an increase in the effective even strengths and a reduction of the effective odd strengths. As a result, a marked improvement in the value of V_{00} is obtained when compared to structure studies. A discrepancy still exists; however, it is thought that core-polarization can remove most of it.

Finally a coupled channel calculation was done for the C^{14}-N^{14} system based on a microscopic model with charge exchange. The results confirmed the validity of the DWBA calculations.

A Comparison of Effective Interactions in Nuclear Structure and Scattering

by

Frank Alan Schmittroth

A THESIS

submitted to

Oregon State University

in partial fulfillment of
the requirements for the
degree of

Doctor of Philosophy

June 1969

APPROVED:

Redacted for Privacy

Associate Professor of Physics

in charge of major

Redacted for Privacy

Chairman of Department of Physics

Redacted for Privacy

Dean of Graduate School

Date thesis is presented Oct 7, 1968

Typed by Clover Redfern for Frank Alan Schmittroth

ACKNOWLEDGMENT

Foremost, thanks are due to Dr. V. A. Madsen for his competent direction and guidance, but even more for innumerable questioning and enlightening discussions.

A debt of gratitude is owed to the cyclotron group at Lawrence Radiation Laboratories where a very fruitful summer was spent. In particular, thanks are due to Dr. J. D. Anderson and Dr. C. Wong for providing much of the data pertinent to this work along with many of the optical parameters used. Mr. Bert Pohl was indispensible numerous times in organizing and operating computer programs essential to this thesis.

Dr. S. M. Austin was kind enough to release data before publication along with optical parameters used in the $N^{14}(p, p')$ results.

Dr. A. K. Kerman must be thanked for information vital to the tensor multipole expansion.

A final note of gratitude must be given to Mr. M. J. Stomp for the coupled channel program he has written, and an extra note of thanks are due for a large effort to obtain an operational program in time for this thesis.

TABLE OF CONTENTS

LIST OF TABLES

LIST OF FIGURES

A COMPARISON OF EFFECTIVE INTERACTIONS IN NUCLEAR STRUCTURE AND SCATTERING

I. INTRODUCTION

Effective interactions in a shell model description of nuclear states have interested physicists for a long time (13, 17, 19). A typical calculation would assume that a nucleus like O^{18} can be described by an inert O^{16} core plus two valence neutrons outside the O^{16} core. A simple residual force is assumed between the valence nucleons, and the wave functions are calculated with the assumption that only a few shell model levels are important (the 2s-1d shell in this example). Recently, there have been two important developments in structure calculations. First, an approach, which parameterizes matrix elements rather than a specific residual potential (2, 5, 11), has had marked success in predicting various first order transition rates and moments. Second, calculations which attempt to compute the effective interaction starting from free nucleon-nucleon forces look very hopeful (8, 23). A large amount of information is also now available on the effective force in inelastic and quasi-inelastic scattering (4, 6, 28, 31, 25).

This work attempts to relate current efforts in both structure and scattering calculations. An effective potential is used, which allows calculation and comparison of matrix elements for different shells. It also allows comparison of scattering amplitudes with

nuclear structure matrix elements. Central forces with arbitrary exchange have been included in all of the calculations. Also, motivated by the anomolous behavior of the C^{14}(p, n) reaction (4, 41), a tensor force has been included in both scattering and structure computations. This anomalous behavior is analogous and closely related to the abnormally slow C^{14} beta-decay reaction (32, 29). Structure calculations consist primarily of deducing effective potentials from existing effective two-body nuclear matrix elements. Scattering calculations include a survey of the effect of the tensor force in DWBA calculations, calculation of exchange effects in DWBA, and coupled channel calculations including tensor forces.

All the calculations are confined to the 1p and 2s-1d shells. One reason is that the effective matrix elements mentioned above, from which a potential is deduced, are given for this region. Calculations with these effective matrix elements indicate that a shell model approach for the 1p and 1d-2s regions is appropriate and useful (2, 5, 11). In addition, there is scattering data for this region from which one can deduce the effective forces (4, 6, 41). In particular, angular distributions and total cross sections for (p, n) reactions, along with some (p, p') and (He^3, t), are calculated for transitions in C^{14}, N^{15}, O^{17}, and O^{18}. Exchange effects are examined for the C^{14}(p, n) and O^{18}(p, n) reactions. Coupled channel calculations are done for the C^{14}-N^{14} system. Most of the scattering data is in the 10-20 MeV

region, and the calculations are likewise done for these energies.

Formal expressions and computer codes have been obtained to carry out the above calculations. A multipole expansion for the two-body tensor force has been obtained. The multipole expansion for the tensor force as well as central forces allows the calculation of bound state kernels, $\left\langle \varphi_{j_2 m_2}(r_1) \middle| v(r_1 - r_0) \middle| \varphi_{j_1 m_1} \right\rangle$, where the bound states, φ, are computed in a Saxon-Woods potential. v is the two-body interaction. This kernel is used to calculate two-body matrix elements. It is also used in a larger program which computes kernels from configuration-mixed shell-model states. These configuration-mixed kernels are convenient for use as coupled-channel coupling matrix elements and in DWBA calculations.

II. INTRODUCTION TO EFFECTIVE FORCES

A goal of this work is to compare the effective forces found in nuclear structure with those in scattering. Although general reasons for the need to introduce effective forces are known (8, 9), quantitative calculations of them are very difficult. Also, effective forces do not necessarily arise from the same reasons for scattering as for structure. These considerations make one ask whether or not a meaningful comparison can be made. It is not even obvious what it is that should be compared.

The problem has been studied in nuclear structure for some time. Brueckner first succeeded in calculating an effective interaction for nuclear matter which was well-behaved (9). Free nucleon-nucleon potentials have a hard core which gives infinite matrix elements for unperturbed states (18, 24). An effective interaction, G, may be defined by $G\varphi = V\psi$ (8) where φ is an unperturbed two-nucleon state, V is the true nucleon-nucleon potential and ψ is the correlated two-nucleon wave function. Correlations are produced by the Pauli exclusion principle as well as the hard cores. The matrix elements of G for unperturbed states, then, are finite, unlike those for V. This theory has suffered troubles and refinements, but is a starting point for many calculations. Kuo and Brown have extended the calculations to finite nuclei (23), namely O^{18}. They

calculate an effective interaction for the two valence neutrons of O^{18} from the free nucleon-nucleon Hamada-Johnston potential (18). An important feature of their calculation is that of core-polarization contributions to the effective potential. Core-polarizations must be introduced because of the truncated shell-model space in which the nuclear wave functions are calculated. In the case of O^{18}, the wave functions are described entirely as neutrons in the 1d-2s shell. The true physical wave functions are more complicated. However, the complication is absorbed as a modification of the effective force due to core-polarizations. The core-polarization terms calculated by Kuo and Brown are three particle-one hole states in O^{18}, and they produce dramatic improvement in the theoretical fit to the energy spectra. Since this effect appears to be important, one might expect the effective force to change as the core changes. Specifically, one would not be too surprised if the effective force differed in the 1p shell and the 2s-1d shell.

For a nucleon-nucleus scattering interaction, just as for nuclear structure, the hard cores in the potential must still be considered in finding an effective interaction. The effect of the exclusion principle will certainly be different for scattering than for nuclear matter and depends on the energy of the incident particle. At energies high compared to the Fermi energy of the nucleus, many intermediate states are available for the interacting particles, and the interaction

should approach a free nucleon-nucleon interaction. At low energies, the exclusion principle is more important and the effective interaction will change. Core polarizations have been shown by Love and Satchler to be important in scattering calculations (26). The philosophy is similar to Kuo and Brown's work (23). Namely, one wants an interaction that takes account of core excitations in intermediate states, while the model wave functions used are those of simple shell-model states for the valence nucleons outside an inert core. However, while Kuo and Brown consider one particle-one hole excitations of the core, Love and Satchler use a collective vibrational model to describe the excitations. Another trouble that besets a comparison of effective forces in scattering and structure is the problem of a scattering theory. An effective force deduced from cross-sections using a DWBA theory may be taking up deficiencies of the DWBA calculation. Two immediate troubles are nuclear distortions produced by channel coupling and exchange effects.

The point of view taken in this work is empirical. Effective forces deduced from empirical data for the 1p shell will be compared with those for the 2s-1d shell. Also, a comparison will be made between the effective forces deduced from structure with those deduced from scattering. The possibility of exchange effects and channel coupling modifying the effective force as deduced from a DWBA calculation will be examined by explicit calculations.

III. THEORETICAL FORMALISMS

Coupling Matrix Elements

In a coupled-equation formalism, the total wave function, ψ, is expanded in a product basis set of functions which consist of nuclear wave functions times projectile wave functions. Explicitly (37),

$$\psi = \frac{1}{r} \sum_{\substack{Jn \\ j_n \ell_n}} R_{Jn\ell_n j_n}(r)[\mathcal{Y}_{\ell_n j_n}, \Phi_{I_n}]_{JM} \tag{3.1}$$

where

$$[\mathcal{Y}_{\ell_n J_n}, \Phi_{I_n}]_{JM} = \sum_{\substack{m_j \\ M_n}} C(j_n I_n J; m_j M_n M) \mathcal{Y}_{\ell_n j_n m_j} \Phi_{I_n M_n} \tag{3.2}$$

and

$$\mathcal{Y}_{\ell_n j_n m_j} = [i^{\ell_n} Y_{\ell_n}, \Sigma_s]_{j_n m_j}. \tag{3.3}$$

Φ_{I_n} is the nuclear wave function for channel n with nuclear spin I_n. Σ_s represents the spin and isospin parts of the projectile wave function with spin s. $R_{Jn\ell_n j_n}$ are the radial wave functions for the projectile whose center of mass is at r. The angular momentum parts of the wave function are coupled to good total angular momentum to reduce the amount of coupling necessary. With this form of ψ, the Schrodinger equation, $H\psi = E\psi$, becomes (37)

$$\left[-\frac{\hbar^2}{2m}\frac{d^2}{dr^2} + \frac{\ell_n(\ell_n+1)}{r^2} + V_{nn}(r) - E + E_n \right] R_{J n \ell_n j_n}(r)$$

$$= -\sum_{\substack{n' \neq n \\ \ell_{n'} j_{n'}}} V_{nn'}(r) R_{J n' \ell_{n'} j_{n'}}(r) \qquad (3.4)$$

where

$$V_{n'n}(r) = \left\langle [\mathcal{Y}_{\ell_{n'} j_{n'}}, \Phi_{I_{n'}}]_{JM} \middle| V \middle| [\mathcal{Y}_{\ell_n j_n}, \Phi_{I_n}]_{JM} \right\rangle . \qquad (3.5)$$

A microscopic description will now be given for the coupling matrix elements $V_{n'n}$. In practice, optical potentials will be used for the diagonal terms, V_{nn}. If $V_{n'n}$ is written in detail, one finds

$$V_{n'n} = \Sigma C(j_n I_n J; m_j M_n M) C(j_{n'} I_{n'} J; m'_j M_{n'} M)$$
$$\times C(\ell_n s j_n; m_\ell m_s m_j) C(\ell_{n'} s j_{n'}; m_{\ell'} m'_s m'_j)$$
$$\times i^{(\ell_n - \ell_{n'})} \int Y_{\ell_{n'} m'_\ell} Y_{\ell_n m_\ell} K(\vec{r}) d\hat{r} \qquad (3.6)$$

where

$$K(\vec{r}) = \left\langle \Phi_{I_{n'} M_{n'}} \Sigma_{s m'_s} \middle| V \middle| \Phi_{I_n M_n} \Sigma_{s m_s} \right\rangle . \qquad (3.7)$$

V may be written as the sum of two-body potentials representing the effective interaction, $V = \Sigma_{ij} v(i, j)$. i and j refer to nucleon coordinates in the nucleus and projectile respectively. In second-quantized notation, V may be written

$$V(r) = \Sigma \left\langle \varphi_{j_2 m_2 a_2}(1)\chi_{\bar{\nu}_2 \bar{a}_2}(0)\left| v(1,0) \right| \right.$$

$$\times \left. \varphi_{j_1 m_1 a_1}(1)\chi_{\bar{\nu}_1 \bar{a}_1}(0) \right\rangle$$

$$\times a^{\dagger}_{j_2 m_2 a_2} a_{j_1 m_1 a_1} C^{\dagger}_{\bar{\nu}_2 \bar{a}_2} C_{\bar{\nu}_1 \bar{a}_1} \qquad (3.8)$$

The $a^{\dagger}$ operators create single-particle bound states of the nucleus,

$$\varphi_{jma} = a^{\dagger}_{jma} | 0 \rangle . \qquad (3.9)$$

j is the angular momentum of the state while m is the z-component. a is the z-component of isospin, $a = 1/2$ for neutrons and $-1/2$ for protons. The $C^{\dagger}$ operators create the spin-isospin part of the projectile nucleon wave functions,

$$\chi_{\nu_2 a_2} = C^{\dagger}_{\nu_2 a_2} | 0 \rangle \qquad (3.10)$$

The two-body matrix element in the above equation is integrated over all co-ordinates except the position co-ordinate, r, for the projectile. It is thus a function of r. Scattering operators, A_{IK} and C_{IK}, are now defined by (28)

$$C^{\dagger}_{\bar{\nu}_2 \bar{a}_2} C_{\bar{\nu}_1 \bar{a}_1} = \sum_{I'K'} C\left(\tfrac{1}{2}\tfrac{1}{2} I'; \bar{\nu}_1 \bar{\nu}_2 - K'\right)(-)^{1/2-\bar{\nu}_1} C_{I'K'}(\bar{a}_1 \bar{a}_2) \qquad (3.11)$$

$$a^{\dagger}_{j_2 m_2 \alpha_2} a_{j_1 m_1 \alpha_1} = \sum_{IK} C(j_1 j_2 I;\ m_1 - m_2 - K)(-)^{j_1 - m_1} A_{IK}(j_1 j_2 \alpha_1 \alpha_2). \tag{3.12}$$

$K(\vec{r})$ may now be written as

$$\begin{aligned} K(\vec{r}) = \sum_{\substack{j_2 m_2 \alpha_2 \\ j_1 m_1 \alpha_1}} \sum_{\bar{\nu}_2 \bar{\alpha}_2 \bar{\nu}_1 \bar{\alpha}_1} \sum_{\substack{IK \\ I'K'}} & C(j_1 j_2 I;\ m_1 - m_2 - K)(-)^{j_1 - m_1} \\ & \times C(\tfrac{1}{2}\tfrac{1}{2} I';\ \bar{\nu}_1 - \bar{\nu}_2 - K')(-)^{1/2 - \bar{\nu}_1} \\ & \times \left\langle \Phi_{I_{n'} M_{n'}} \middle| A_{IK}(j_1 j_2 \alpha_1 \alpha_2) \middle| \Phi_{I_n M_n} \right\rangle \left\langle \Sigma_{s m'_s} \middle| C_{I'K'}(\alpha_1 \alpha_2) \middle| \Sigma_{s m_s} \right\rangle \\ & \times \left\langle \varphi_{j_2 m_2 \alpha_2} \chi_{\bar{\nu}_2 \bar{\alpha}_2} \middle| v(1,0) \middle| \varphi_{j_1 m_1 \alpha_1} \chi_{\bar{\nu}_1 \bar{\alpha}_1} \right\rangle. \end{aligned} \tag{3.13}$$

As in Reference (28), it is convenient to define spectroscopic amplitudes as reduced matrix elements of the scattering operators,

$$\begin{aligned} & S(II_n I_{n'};\ j_1 j_2 \alpha_1 \alpha_2) C(I_n I_{n'} I;\ M_n - M_{n'} - K)(-)^{I_n - M_n} \\ & = \left\langle \Phi_{I_{n'} M_{n'}} \middle| A_{IK} \middle| \Phi_{I_n M_n} \right\rangle, \end{aligned} \tag{3.14}$$

$$\begin{aligned} & \bar{S}(SI',\ \bar{\alpha}_1 \bar{\alpha}_2) C(SSI';\ m_s - m'_s - K')(-)^{S - m_s} \\ & = \left\langle \Sigma_{s m'_s} \middle| C_{I'K'} \middle| \Sigma_{s m_s} \right\rangle \end{aligned} \tag{3.15}$$

If a multipole expansion for the potential exists, it is then convenient to reduce the two body matrix element in Equation (3.13) by defining

z, such that the quantity

$$a(\vec{r}) \equiv \left\langle \varphi_{j_2 m_2 a_2} \chi_{\bar{\nu}_2 \bar{a}_2} \middle| V \middle| \varphi_{j_1 m_1 a_1} \chi_{\bar{\nu}_1 \bar{a}_1} \right\rangle$$

$$= \sum_{\substack{LN \\ II' \\ KK'}} (-)^N Y_{L-N}(\hat{r}) C(II'L;\ KK'N) C(j_1 j_2 I;\ m_1 - m_2 - K)(-)^{j_1 - m_1}$$

$$\times C\left(\frac{1}{2}\frac{1}{2} I';\ \bar{\nu}_1 - \bar{\nu}_2 - K'\right)(-)^{1/2 - \bar{\nu}_1} z(II'L;\ j_1 j_2 a_1 a_2;\ |r|) \tag{3.16}$$

It is not hard to show that the above form is quite general. The expression for z will be given explicitly for central and tensor two-body forces. If the last three equations are substituted into Equation (3.13) for K and a few simple orthogonality sums are performed, one then finds

$$K(\vec{r}) = \sum_{\substack{II' \\ KK' \\ LN}} (-)^N Y_{L-N}(\hat{r}) C(II'L;\ KK'N) C(I_n I_{n'} I;\ M_n - M_{n'} - K)(-)^{I_n - M_n}$$

$$\times C(SSI';\ m_s - m'_s - K')(-)^{S - m_s} X(II'L, I_n, I_{n'}, S\,|r|), \tag{3.17}$$

where

$$X(\Pi'L;\ I_n I_{n'},\ S,\ |r|) = \sum_{\substack{j_1 j_2 \\ \alpha_1 \alpha_2 \\ \bar{\alpha}_1 \bar{\alpha}_2}} S(\Pi_n I_{n'};\ j_1 j_2 \alpha_1 \alpha_2) \bar{S}(I's:\ \bar{\alpha}_1 \bar{\alpha}_2)$$

$$\times\ z(\Pi'L;\ j_1 j_2 \alpha_1 \alpha_2 \bar{\alpha}_1 \bar{\alpha}_2;\ |r|). \qquad (3.18)$$

Equation (3.17) for K now can be substituted into Equation (3.6) for $V_{n'n}$. After a certain amount of Racah algebra, one obtains the following expression for $V_{n'n}$:

$$V_{n'n} = \sum_{\Pi'L} i^{(\ell_n - \ell_{n'})} \langle \ell_{n'} \| Y_L \| \ell_n \rangle \hat{L} \hat{j}_n \hat{j}_{n'} \hat{\Pi}\hat{\Pi}' (-)^{I' + j_{n'} + I_n - J}$$

$$\times\ W(j_n j_{n'} I_n I_{n'}; IJ) \begin{pmatrix} \ell_n & S & j_n \\ L & I' & I \\ \ell_{n'} & S & j_{n'} \end{pmatrix} X(\Pi'L;\ I_n I_{n'} S,\ |r|) \qquad (3.19)$$

where $\hat{L} = \sqrt{2L+1}$. The reduced matrix element follows the convention of Messiah (29, Vol. 2, p. 573).

This expression for $V_{n'n}$ is very general and is analogous to similar expressions for the collective model (10, 37). The collective coupling interaction may be written as

$$V_{n'n} = \sum_N (-)^N Y_{L-N} Q_{LN} v_L(r) \qquad (3.20)$$

where Q_{LN} is an operator in the space of the collective model of the nucleus, and $v_L(r)$ gives the spatial dependence. In this case, it is not hard to show that

$$X(\Pi'L;\ I_n I_{n'},\ S,\ |r|) = \frac{\hat{S}}{\hat{L}}\, v_L(r)\delta_{I'0}\delta_{IL}\ \langle I_{n'} \| Q_L \| I_n \rangle \qquad (3.21)$$

The isospin dependence of X will now be examined in more detail. First assume that the isospin dependent part of the effective two-body force, V, may be factored from the space-spin part of the potential, V_o,

$$V(1, 0) = V_o(1, 0)V_{\mathcal{I}}(1, 0). \qquad (3.22)$$

Normally, $V_{\mathcal{I}}$ is either equal to 1 or $\vec{\tau}_1 \cdot \vec{\tau}_0$. Co-ordinates 1 and 0 refer to nuclear- and projectile-nucleon co-ordinates. A new z_o may be defined by factoring out the isospin part of the matrix element that is implicit in the z defined in Equation (3.16),

$$z(\Pi'L;\ j_1 j_2 a_1 a_2 a'_1 a'_2,\ |r|)$$

$$= z_o(\Pi'L;\ j_1 j_2 a_1 a_2,\ |r|)\ \langle a_2(1)\bar{a}_2(0)|V_{\mathcal{I}}(1, 0)|a_1(1)\bar{a}_1(0)\rangle \qquad (3.23)$$

where

$$|a_1(1)a_1(0)\rangle = |a_1(1)\rangle\ |\bar{a}_1(0)\rangle \qquad (3.24)$$

is a product state. $|a_1(i)\rangle$ is a spinor in co-ordinate i which

represents an isospin wave function with z-component a_1. Since the spatial dependence of bound states may differ for protons and neutrons, z_o may depend on a_1 and a_2.

For the case of good isospin, new spectroscopic amplitudes may be defined (28),

$$\bar{S}(I'S;\ \tau'T') = \frac{\langle \Sigma_{ST'} \| C_{I'\tau} \| \Sigma_{ST'} \rangle}{\hat{I}'\hat{\tau}'} \tag{3.25}$$

for the projectile and

$$S(I I_{n'} I_n;\ T_n T_{n'} \tau;\ j_1 j_2) = \frac{\langle \Phi_{I_{n'} T_{n'}} \| A_{I\tau} \| \Phi_{I_n T_n} \rangle}{\hat{I}\hat{\tau}} \tag{3.26}$$

for the nucleus where the matrix elements are reduced in space-spin and isospin space. T' is the projectile isospin. T_n and $T_{n'}$ are the initial and final isospins of the target nucleus. The scattering operators A and C have been appropriately generalized,

$$A_{IK\tau\rho}(j_1 j_2) = \sum_{a_1 a_2} C(\tfrac{1}{2}\tfrac{1}{2}\tau;\ a_1 - a_2 - \rho)(-)^{1/2-a_1} A_{IK}(j_1 j_2 a_1 a_2) \tag{3.27}$$

$$C_{I'K'\tau'\rho'} = \sum_{\bar{a}_1 \bar{a}_2} C(\tfrac{1}{2}\tfrac{1}{2}\tau';\ \bar{a}_1 - \bar{a}_2 - \rho')(-)^{1/2-\bar{a}_1} C_{I'K'}(\bar{a}_1 \bar{a}_2). \tag{3.28}$$

It follows from these definitions that

$$\bar{S}(I'S;\ \bar{a}_1\bar{a}_2) = \sum_{\tau'\rho'} C(\tfrac{1}{2}\tfrac{1}{2}\tau';\ \bar{a}_1\text{-}\bar{a}_2\text{-}\rho')(-)^{1/2-\bar{a}_1}$$

$$\times\ C(T'T'\tau';\ \bar{p}_n\text{-}\bar{p}_{n'}\text{-}\rho')(-)^{T'-\bar{p}_n}\bar{S}(I'S;\ \tau'T'), \tag{3.29}$$

where $\bar{p}_n$ and $\bar{p}_{n'}$ are the initial and final z components of projectile isospin. If this identity is substituted, along with the factored form for z, into Equation (3.18) for X, one obtains

$$X(\Pi'L,\ I_nI_{n'},\ S,\ |r|)$$

$$= \sum_{j_1j_2} \sum_{\substack{a_1a_2 \\ \tau'\rho'}} S(\Pi_nI_{n'};\ j_1j_2a_1a_2)\bar{S}(I'S,\ \tau'T')$$

$$\times\ z_o(\Pi'L;\ j_1j_2a_1a_2|r|)\,\mathcal{A}(a_1a_2;\ \tau'\rho')$$

$$\times\ C(T'T'\tau';\ \bar{p}_n\text{-}\bar{p}_{n'}\text{-}\rho')(-)^{T'-\bar{p}_n} \tag{3.30}$$

where

$$\mathcal{A}(a_1a_2;\ \tau'\rho')$$

$$= \sum_{\bar{a}_1\bar{a}_2} C(\tfrac{1}{2}\tfrac{1}{2}\tau';\ \bar{a}_1\text{-}\bar{a}_2\text{-}\rho')(-)^{1/2-\bar{a}_1}\ \langle a_2\bar{a}_2|V\ |a_1\bar{a}_1\rangle. \tag{3.31}$$

If z is independent of a_1 and a_2, then, in exactly the

same fashion, X may be re-expressed for the case where both the target isospin and the projectile isospin are good. In that case,

$$X(\Pi'L;\ I_n I_{n'};\ T_n T_{n'},\ S,\ |r|)$$

$$= \sum_{j_1 j_2} \sum_{\substack{\tau\rho \\ \tau'\rho'}} S(\Pi_n I_{n'};\ T_n T_{n'} \tau;\ j_1 j_2) \bar{S}(I'S;\ \tau' T')$$

$$\times z(\Pi'L;\ j_1 j_2,\ |r|)\, \mathcal{A}(\tau\rho;\ \tau'\rho')$$

$$\times C(T'T'\tau';\ \bar{p}_n - \bar{p}_{n'} - \rho')(-)^{T' - \bar{p}_n}$$

$$\times C(T_n T_{n'} \tau;\ P_n - P_{n'} - \rho)(-)^{T_n - P_n}, \qquad (3.32)$$

where P_n and $P_{n'}$ are initial and final z components of target isospin which correspond to total isospin T_n and $T_{n'}$. See Reference (28) for details. The factor $\mathcal{A}$ is

$$\mathcal{A}(\tau\rho;\ \tau'\rho') = \sum_{a_1 a_2} C(\tfrac{1}{2}\tfrac{1}{2}\tau;\ a_1 - a_2 - \rho)\, \mathcal{A}(a_1 a_2,\ \tau'\rho') \qquad (3.33)$$

The factor $\mathcal{A}$, which appears in the above expressions, is essentially a reduced matrix element for the isospin part of the two-body matrix elements. For the case of definite target isospin, $\mathcal{A}(\tau\rho,\ \tau'\rho')$ has the following values:

$$2\delta_{T'0}\delta_{\rho'0}\delta_{T0}\delta_{\rho 0} \qquad \text{for} \quad V_\alpha = 1$$

and

$$2(-)^{\rho}\delta_{T1}\delta_{T'1}\delta_{\rho,-\rho'} \qquad \text{for} \quad V_\alpha = \vec{\tau}_1 \cdot \vec{\tau}_2.$$

For the case of non-definite isospin, $\mathcal{A}(a_1 a_2; T'\rho')$ has the following values:

$$\sqrt{2}\,\delta_{a_1 a_2}\delta_{T'0}\delta_{\rho'0} \qquad \text{for} \quad V_\alpha = 1$$

and

$$\sqrt{6}\,\delta_{T'1}C(\tfrac{1}{2}1\tfrac{1}{2};\ a_2\rho' a_1) \qquad \text{for} \quad V_\alpha = \vec{\tau}_1 \cdot \vec{\tau}_2.$$

DWBA Expressions

Although the above expressions for X were developed in the context of a coupled-channel formalism, they are also a useful way to express DWBA amplitudes. The DWBA amplitude for inelastic scattering is (28)

$$\begin{aligned} A &= \langle \chi_f^{(-)} | K | \chi_i^{(+)} \rangle \\ &= \sum_{\substack{\Pi\Pi'L \\ KK'N}} Y^*_{LN} C(\Pi\Pi' L;\ KK'N) C(I_n I_{n'} I;\ M_n - M_{n'} - K)(-)^{I_n - M_n} \\ &\quad \times C(SSI';\ m_s - m'_s - K')(-)^{S - m_s} \\ &\quad \times \langle \chi_f^{(-)} | Y_{LN} X(\Pi\Pi' L;\ I_n I_{n'},\ S,\ |r|) | \chi_i^{(+)} \rangle, \end{aligned} \tag{3.34}$$

where $\chi_i^{(+)}$ and $\chi_f^{(-)}$ are initial and final distorted waves. For unpolarized states, the amplitude may be squared and summed and averaged over initial and final states to obtain

$$\frac{d\sigma}{d\Omega} = \left(\frac{2m}{4\pi\hbar^2}\right)^2 \frac{k_f}{k_i} \frac{1}{(2I_n+1)(2S+1)} \sum_{\Pi' LN} \left| \left\langle \chi_f^{(-)} \middle| Y_{LN} X \middle| \chi_i^{(+)} \right\rangle \right|^2. \tag{3.35}$$

Appropriate statistical factors have also been added (28).

Calculation of Two-body Matrix Elements by Means of Multipole Expansions

If a multipole expansion for the potential exists, the two-body matrix element, $M = {}_{AN}\left\langle j_3 j_4 JT \middle| V \middle| j_1 j_2 JT \right\rangle_{AN}$, may be conveniently expressed in terms of a quantity, z, already defined for use in scattering form factors (Equation (3.16)). V is the two-body potential. $|j_1 j_2 JT\rangle_{AN}$ is a two-particle state coupled to good total angular momentum J and isospin T:

$$|j_1 j_2 JT\rangle_{AN} = \sqrt{\frac{2}{1+\delta_{j_1 j_2}}} \left(\frac{1-P_{12}}{2}\right) |j_1 j_2 JT\rangle \tag{3.36}$$

where

$$|j_1 j_2 JT\rangle = \sum_{m_1 m_2} C(j_1 j_2 J;\ m_1 m_2 M) |j_1 m_1\rangle\, |j_2 m_2\rangle\, |TP\rangle \tag{3.37}$$

and

$$|TP\rangle = \sum_{a_1 a_2} C(\tfrac{1}{2}\tfrac{1}{2}T; a_1 a_2 P)|\tfrac{1}{2}a_1\rangle\,|\tfrac{1}{2}a_2\rangle\,. \tag{3.38}$$

j_1 and j_2 are the single-particle angular momenta. The subscript, AN, indicates the state is antisymmetric and normalized. $|j_i m_i\rangle$ are the single-particle states. $|\tfrac{1}{2}a_i\rangle$ are the corresponding isospin spinors. m_i and a_i are z components of angular momenta and isospin. P_{12} exchanges all co-ordinates in states 1 and 2.

Apply P_{12} to Equation (3.37) to see that

$$P_{12}|j_1 j_2 JT\rangle = (-)^{1-T}(-)^{j_1+j_2-T}|j_2 j_1 JT\rangle\,, \tag{3.39}$$

so that

$$\begin{aligned} M &= {}_{AN}\langle\, j_3 j_4 JT|V|j_1 j_2 JT\,\rangle_{AN} \\ &= \left[\frac{2}{(1+\delta_{j_1 j_2})}\,\frac{2}{(1+\delta_{j_3 j_4})}\right]^{1/2}\langle j_3 j_4 JT|V\,\frac{(1-P_{12})}{2}|j_1 j_2 JT\rangle \\ &= \Delta_j\{\langle j_3 j_4 JT|V|j_1 j_2 JT\rangle + (-)^{j_1+j_2-J-T}\langle j_3 j_4 JT|V|j_2 j_1 JT\rangle\} \end{aligned} \tag{3.40}$$

where

$$\Delta_j = \left[\frac{1}{(1+\delta_{j_1 j_2})}\,\frac{1}{(1+\delta_{j_3 j_4})}\right]^{1/2}\,. \tag{3.41}$$

The first term in M is the direct term and the second is the exchange. Both may be calculated in the same fashion, and only the direct term, M_D, will now be considered. Factor the isospin part, V_ℓ, from V. $V = V_o V_\ell$. Define $M_T = \langle TP|V|TP\rangle$. M_D then becomes

$$M_D = \langle j_3 j_4 JT|V|j_1 j_2 JT\rangle$$

$$= M_T \sum C(j_3 j_4 J;\ m_3 m_4 M) C(j_1 j_2 J;\ m_1 m_2 M)$$

$$\times C(\ell_2 \tfrac{1}{2} j_2;\ n_2 \nu_2 m_2) C(\ell_4 \tfrac{1}{2} j_4;\ n_4 \nu_4 m_4)$$

$$\times \langle j_4 \ell_4 n_4 | a(\vec{r}) | j_2 \ell_2 n_2\rangle . \qquad (3.42)$$

$|j\ell n\rangle = Y_{\ell n} R_{\ell j}$ is the space part of the wave function. The spin part, χ_ν is contained in $a(\vec{r})$ which was defined by Equation (3.16). Any isospin dependence of $a(\vec{r})$ has been taken to be in M_T. If Equation (3.16) for $a(\vec{r})$ is substituted into Equation (3.42), and if the factor $\langle \ell_4 n_4 | Y_{LN} | \ell_2 n_2\rangle$ is evaluated, then one obtains a sum over eight Clebsch-Gordan coefficients. The sum can be done to give a Racah coefficient and 9-j coefficient. The final result is

$$M_D = M_T \sum_{II'L} \left[z R^{j_1 j_3}_{j_2 j_4} \langle \ell_4 \| Y_L \| \ell_2\rangle \hat{L}\hat{I}\hat{I}'\hat{j}_2\hat{j}_4 (-)^{I+I'} \right.$$

$$\left. \times W(j_1 J I j_4;\ j_2 j_3) \begin{pmatrix} j_2 & \frac{1}{2} & \ell_2 \\ j_4 & \frac{1}{2} & \ell_4 \\ I & I' & L \end{pmatrix} \right] , \qquad (3.43)$$

where

$$ {}_{z}R^{j_1 j_3}_{j_2 j_4} = \int_0^\infty R^{*}_{\ell_4 j_4} R_{\ell_2 j_2} z(II'L;\ j_1 j_3 | r |) r^2 dr. \qquad (3.44) $$

The same expression can be used for the exchange term, M_E. The final expression is

$$ M = {}_{AN}\langle j_3 j_4 JT | V | j_1 j_2 JT \rangle_{AN} $$

$$ = \Delta_j M_T [M_D + (-)^{j_1 + j_2 - J - T} M_E] \ . \qquad (3.45) $$

M_T has the following values:

$$ M_T = 1 \qquad \text{for} \quad V_\ell = 1 \quad \text{and} $$

$$ M_T = \delta_{T1} - 3\delta_{T0} \qquad \text{for} \quad V_\ell = \tau_1 \cdot \tau_2 . $$

Tensor Force Multipole Expansion

The usual tensor force is defined by

$$ V_T(\tau_1 \cdot \tau_2) \equiv V_{12} S_{12} (\vec{\tau}_1 \cdot \vec{\tau}_2) \qquad (3.46) $$

where

$$ V_{12} = \left[\frac{1}{(\alpha r)^2} + \frac{1}{(\alpha r)} + \frac{1}{3} \right] \frac{e^{-\alpha r}}{\alpha r} \qquad (3.47) $$

and

$$S_{12} = \frac{3(\vec{\sigma}_1 \cdot \vec{r})(\vec{\sigma}_2 \cdot \vec{r})}{r^2} - \vec{\sigma}_1 \cdot \vec{\sigma}_2$$

$$= \sqrt{\frac{24\pi}{5}} \sum_{\beta} S_{2\beta} Y^*_{2\beta}(\hat{r}) . \qquad (3.48)$$

The second-rank spin tensor S_2 is defined by

$$S_{20} = \sqrt{\frac{2}{3}} (3S_z^2 - S^2) \qquad (3.49)$$

with $\vec{S} = \vec{S}_1 + \vec{S}_2$. The desired multipole expansion for the spatial part of V_T has the form

$$V_{12}(r) Y_{2\beta}(\hat{r}) = \sum_{\substack{LN \\ \lambda\mu}} f_{L\lambda}(r_1, r_2) C(L\lambda 2; N\mu\beta) Y_{\lambda\mu}(\hat{r}_2) Y_{LN}(\hat{r}_1) \qquad (3.50)$$

where

$$\vec{r} = \vec{r}_2 - \vec{r}_1 .$$

First note that[1]

$$V_T = \frac{1}{a^2} \left[(\sigma_1 \cdot \nabla)(\sigma_2 \cdot \nabla) - \frac{(\sigma_1 \cdot \sigma_2)}{3} \nabla^2 \right] \frac{e^{-ar}}{ar} \qquad (3.51)$$

from Reference (12, p. 437).

---

[1] This approach to the tensor force expansion is due to A. Kerman in a private communication.

Now Fourier transform the Yukawa force,

$$\frac{e^{-\alpha r}}{r} = \frac{1}{(2\pi)^3}\int \frac{4\pi}{(\alpha^2+q)^2}\, e^{i\vec{q}\cdot\vec{r}}\, d^3q \tag{3.52}$$

Then Equation (3.51) becomes

$$S_{12}V_{12} = \frac{1}{a^3}\left[(\vec{\sigma}_2\cdot\vec{\nabla})(\vec{\sigma}_1\cdot\vec{\nabla}) - \frac{\vec{\sigma}_1\cdot\vec{\sigma}_2}{3}\vec{\nabla}^2\right]\left(\frac{1}{2\pi}\right)^3\int \frac{4\pi}{a^2+q^2}\, e^{i\vec{q}\cdot\vec{r}}\, d^3q \tag{3.53}$$

Differentiating inside the integral gives

$$S_{12}V_{12} = \sqrt{\frac{24\pi}{5}}\sum_{\beta}(-)^{\beta}S_{2-\beta}Y_{2\beta}(\hat{r})V_{12}(r)$$

$$= -\frac{1}{6\pi^2\alpha^3}\int \frac{q^2}{a^2+q^2}\left[\frac{3(\vec{\sigma}_1\cdot\vec{q})(\vec{\sigma}_2\cdot\vec{q})}{q^2} - (\vec{\sigma}_1\cdot\vec{\sigma}_2)\right] e^{i\vec{q}\cdot\vec{r}}\, d^3q \tag{3.54}$$

$$= \sqrt{\frac{24\pi}{5}}\sum_{\mu}(-)^{\mu}S_{2-\mu}\left[-\frac{1}{6\pi^2\alpha^3}\int \frac{q}{a^2+q^2}\, Y_{2\mu}(\hat{q})e^{i\vec{q}\cdot\vec{r}}\, d^3q\right]. \tag{3.55}$$

By comparing coefficients of $S_{2\beta}$, one finds

$$V_{12}(r)Y_{2\beta}(\hat{r}) = -\frac{1}{6\pi^2\alpha^3}\int \frac{q^2}{a^2+q^2}Y_{2\beta}e^{i\vec{q}\cdot\vec{r}}\, d^3q \tag{3.56}$$

Write $e^{i\vec{q}\cdot\vec{r}} = e^{i\vec{q}\cdot\vec{r}_2}\, e^{-i\vec{q}\cdot\vec{r}_1}$ and separately expand each plane wave in terms of spherical bessel functions, $j_\ell(qr)$:

$$V_{12}Y_{2\beta} = -\frac{(4\pi)^2}{6\pi^2 a^3} \sum_{\substack{\ell_1 m_1 \\ \ell_2 m_2}} i^{(\ell_2-\ell_1)} Y_{\ell_2 m_2}(\hat{r}_2) Y_{\ell_1 m_1}(\hat{r}_1)$$

$$\times \int_0^\infty \frac{q^2}{a^2+q^2} j_{\ell_1}(qr_1) j_{\ell_2}(qr_2) q^2 dq$$

$$\times \int Y^*_{\ell_2 m_2}(\hat{q}) Y_{2\beta}(\hat{q}) Y_{\ell_1 m_1}(\hat{q}) d\hat{q}. \qquad (3.57)$$

The last integral is

$$\langle \ell_2 m_2 | Y_{2\beta} | \ell_1 m_1 \rangle = \frac{(-)^{\ell_1 - m_1}}{\sqrt{5}} (-)^{\ell_1+\ell_2} C(\ell_1 \ell_2 2; -m_1 m_2 \beta)$$

$$\times \langle \ell_2 \| Y_2 \| \ell_1 \rangle \qquad (3.58)$$

A little manipulation yields

$$V_{12}Y_{2\beta} = \sum_{\substack{\ell_1 \ell_2 \\ m_1 m_2}} f_{\ell_1 \ell_2}(r_1 r_2) C(\ell_1 \ell_2 2; m_1 m_2 2) Y_{\ell_2 m_2}(\hat{r}_2) Y_{\ell_1 m_1}(\hat{r}_1) \qquad (3.59)$$

where

$$f_{\ell_1 \ell_2} = \frac{A}{a^3} \int_0^\infty \frac{q^4}{a^2+q^2} j_{\ell_1}(qr_1) j_{\ell_2}(qr_2) dq \qquad (3.60)$$

with

$$A = -(-)^{\ell_2} i^{(\ell_2-\ell_1)} \frac{8}{3\sqrt{5}} \langle \ell_2 \| Y_2 \| \ell_1 \rangle . \qquad (3.61)$$

These results give the desired multipole expansion. It yet remains to evaluate $f_{\ell_1\ell_2}$.

Consider first the case where $r_2 > r_1$. Now use

$$2j_{\ell_2} = h^{(1)}_{\ell_2} + h^{(2)}_{\ell_2}$$

where $h^{(1)}_{\ell_2}$ and $h^{(2)}_{\ell_2}$ are spherical Hänkel functions of the first and second kind. $f_{\ell_1\ell_2}$ can then be written

$$f_{\ell_1\ell_2} = \frac{A}{a^3}\int_0^\infty \frac{q^4}{a^2+q^2}\left(\frac{1}{2}\right)\left(h^{(1)}_{\ell_2}(qr_2)+h^{(2)}_{\ell_2}(qr_2)\right)j_{\ell_1}(qr_1)dq. \qquad (3.62)$$

The matrix element $\langle \ell_2 \| Y_2 \| \ell_1 \rangle$ implies $(-)^{\ell_2+\ell_1} = +1$. Note the following relations:

$$j_\ell(x) = (-)^\ell j_\ell(-x), \quad h^{(2)}_\ell(x) = (-)^\ell h^{(1)}_\ell(-x).$$

The above integral can now be written

$$f_{\ell_1\ell_2} = \frac{A}{2a^3}\int_0^\infty \frac{q^4}{a^2+q^2}\left[h^{(1)}_{\ell_2}(qr_2)j_{\ell_1}(qr_1)+h^{(1)}_{\ell_2}(-qr_2)j_{\ell_1}(-qr_1)\right]dq$$

$$= \frac{A}{2a^3}\int_{-\infty}^\infty \frac{q^4}{a^2+q^2}\, h^{(1)}_{\ell_2}(qr_2)j_{\ell_1}(qr_1)dq \qquad (3.63)$$

This integral may be evaluated by contour integration. The contour

for $r_2 > r_1$ may be closed in the upper half-plane. The contour does not contribute in that region since the exponential in $h^{(1)}_{\ell_2}(qr_2)$, namely e^{iqr_2} will damp those in $j_{\ell_1}(qr_1)$ for $r_2 > r_1$. The Clebsch-Gordan coefficient insures $\ell_1 - \ell_2 \geq -2$, so that the integrand is well-behaved at the origin. The integral is simply, $2\pi i$ times the residue at $q = i\alpha$:

$$f_{\ell_1\ell_2} = \frac{A}{2\alpha^3}(2\pi i)\frac{(i\alpha)^4}{(2i\alpha)} h^{(1)}_{\ell_2}(i\alpha r_2) j_{\ell_1}(i\alpha r_1)$$

$$= \frac{\pi A}{2} h^{(1)}_{\ell_2}(i\alpha r_2) j_{\ell_1}(i\alpha r_1) \qquad (3.64)$$

for

$$r_2 > r_1.$$

A similar procedure may be followed for $r_2 < r_1$ which gives

$$f_{\ell_1\ell_2}(r_1 r_2) = \frac{\pi A}{2}\begin{cases} h^{(1)}_{\ell_2}(i\alpha r_2) j_{\ell_1}(i\alpha r_1) & r_2 > r_1 \\ h^{(1)}_{\ell_1}(i\alpha r_1) j_{\ell_2}(i\alpha r_2) & r_2 < r_1. \end{cases} \qquad (3.65)$$

The assumption of a one-pion-exchange force makes V_{12} quite singular at the origin, $V_{12} \sim \frac{1}{r^3}$. This is not likely to be valid in practice, and V_{12} has been regularized to give the potential

$$\text{Reg } V_{12}(\alpha r) = V_{12}(\alpha r) - (\frac{\beta}{\alpha})^3 V_{12}(\beta r) \qquad (3.66)$$

with

$$\beta > \alpha.$$

For small r, $\text{Reg } V_{12} \sim \frac{1}{r}$. $\text{Reg } V_{12}$ was used for all calculations in this work.

Bound State Form Factors

The defining relation for z is given by Equation (3.16). z is a type of reduced two-body matrix element and forms an important part of the form-factor for various matrix elements in this work (see Equations (3.18, 3.44)).

To obtain an expression for z,

$$a(\vec{r}) = \left\langle \varphi_{j_2 m_2 a_2} \chi_{\bar{\nu}_2 \bar{a}_2} \middle| V \middle| \varphi_{j_1 m_1 a_1} \chi_{\bar{\nu}_1 \bar{a}_1} \right\rangle \tag{3.67}$$

is first evaluated. For a central force of the form

$$V = \frac{e^{-\alpha r}}{\alpha r} (a \vec{\sigma}_1 \cdot \vec{\sigma}_2 + b), \tag{3.68}$$

the result for a(r) is

$$a_C(\vec{r}) = \sum_{\substack{LN \\ II' \\ KK'}} \frac{1}{\hat{L}} Y_{L-N} \hat{j}_1 \hat{j}_2 \left\langle \ell_2 \| Y_L \| \ell_1 \right\rangle g_L^{j_1 j_2}(r) \hat{I}\hat{I}'$$

$$\times (-)^{j_1 + m_2 + I' + 1/2 + \bar{\nu}_2} (-)^{I + I' - L} C(j_1 j_2 I;\ m_1 - m_2 - K)$$

$$\times C(II'L;\ KK'N) C(\tfrac{1}{2}\tfrac{1}{2}I';\ \bar{\nu}_1 - \bar{\nu}_2 - K')$$

$$\times \begin{pmatrix} j_1 & \frac{1}{2} & \ell_1 \\ j_2 & \frac{1}{2} & \ell_2 \\ I & I' & L \end{pmatrix} (2)(\delta_{I'1} a + \delta_{I'0} b). \tag{3.69}$$

Review the section for coupling matrix elements for a discussion of any isospin dependence. Direct comparison of Equations (3.16) and (3.69) gives z immediately for a central force:

$$z_C(II'L;\ j_1 j_2, r) = (-)^{I-L} \frac{\hat{j}_1 \hat{j}_2 \hat{I}\hat{I}'}{\hat{L}} \left\langle \ell_2 \| Y_L \| \ell_1 \right\rangle$$

$$\times g_L^{j_1 j_2}(2)(\delta_{I'1} a + \delta_{I'0} b) \begin{pmatrix} j_1 & \frac{1}{2} & \ell_1 \\ j_2 & \frac{1}{2} & \ell_2 \\ I & I' & L \end{pmatrix} \tag{3.70}$$

z will now be found for the tensor force

$$V_T(r) = \sqrt{\frac{24\pi}{5}} \sum_{\beta} S_{2\beta} Y^*_{2\beta}(\hat{r}) V_{12}(\hat{r}) \tag{3.71}$$

where

$$Y_{2\beta}V_{12} = \sum_{\substack{LN \\ \lambda\mu}} f_{L\lambda}(r_1 r_0)C(L\lambda 2;\ N\mu\beta)Y_{\lambda\mu}(\hat{r}_1)Y_{LN}(\hat{r}_0). \qquad (3.72)$$

The first step, as for the central force, is to evaluate $a(\vec{r})$, Equation (3.16). The bound states, φ_{jm} in $a(\vec{r})$ are decoupled so that the spin and space parts of V_T can be separately evaluated. At the same time, if Equation (3.71) is inserted into Equation (3.16), one finds for $a(\vec{r})$,

$$\begin{aligned} a_T = & \sum_{\substack{n_1 n_2 \\ \nu_1 \nu_2}} C(\ell_1 \tfrac{1}{2} j_1;\ n_1 \nu_1 m_1)C(\ell_2 \tfrac{1}{2} j_2;\ n_2 \nu_2 m_2) \\ & \times \sum_{\beta} \sqrt{\frac{24\pi}{5}} \left\langle \chi_{\nu_2}\chi_{\bar{\nu}_2} \middle| S_{2\beta} \middle| \chi_{\nu_1}\chi_{\bar{\nu}_1} \right\rangle \\ & \times \left\langle R_{\ell_2 j_2} Y_{\ell_2 n_2} \middle| V_{12} Y^*_{2\beta} \middle| Y_{\ell_1 n_1} R_{\ell_1 j_1} \right\rangle . \end{aligned} \qquad (3.73)$$

By use of Equation (3.72), the factor which contains the spatial dependence may be written as

$$\begin{aligned} M_L &= \left\langle R_{\ell_2 j_2} Y_{\ell_2 n_2} \middle| V_{12} Y^*_{2\beta} \middle| Y_{\ell_1 n_1} R_{\ell_1 j_1} \right\rangle \\ &= \sum_{LN} C(L\lambda 2;\ N\mu-\beta)(-)^{\beta} g^{j_1 j_2}_{L\lambda}(r) \left\langle \ell_2 n_2 \middle| Y_{\lambda\mu} \middle| \ell_1 n_1 \right\rangle Y_{LN}(\hat{r}) \end{aligned} \qquad (3.74)$$

where

$$g_{L\lambda}^{j_1 j_2}(r) = \int_0^\infty R^*_{\ell_2 j_2}(r_1) R_{\ell_1 j_1}(r_1) f_{L\lambda}(r_1, r) r_1^2 dr_1. \quad (3.75)$$

The spin part will now be evaluated. First couple both the initial and final pairs of spin states to good total spins, S_1 and S_2. The spin matrix element becomes

$$M_s = \left\langle \chi_{\nu_2} \chi_{\bar{\nu}_2} | S_{2\beta} | \chi_{\nu_1} \chi_{\bar{\nu}_1} \right\rangle$$

$$= \sum_{\substack{S_1 \mu_1 \\ S_2 \mu_2}} C(\tfrac{1}{2}\tfrac{1}{2} S_1;\ \nu_1 \bar{\nu}_1 \mu_1)\, C(\tfrac{1}{2}\tfrac{1}{2} S_2;\ \nu_2 \bar{\nu}_2 \mu_2) \left\langle S_2 \mu_2 | S_{2\beta} | S_1 \mu_1 \right\rangle \quad (3.76)$$

where

$$|S\mu\rangle = \sum_{\nu \bar{\nu}} C(\tfrac{1}{2}\tfrac{1}{2} S;\ \nu \bar{\nu} \mu) |\chi_\nu \chi_{\bar{\nu}}\rangle \quad (3.77)$$

and $S = 0$ and 1.

The Wigner-Eckart theorem yields

$$\left\langle S_2 \mu_2 | S_{2\beta} | S_1 \mu_1 \right\rangle = \frac{C(S_1 2 S_2;\ \mu_1 \beta \mu_2)}{\sqrt{3}} \left\langle S_2 \| S_2 \| S_1 \right\rangle . \quad (3.78)$$

The defining relation for $S_{2\beta}$ gives $2\sqrt{5}$ for the reduced matrix element. Note that only $S_1 = S_2 = 1$ can contribute since $S_{2\beta}$ is a second rank tensor. The tensor force may scatter only between

triplet spin states. M_s now becomes

$$M_s = \sum_{\mu_1 \mu_2} C(\tfrac{1}{2}\tfrac{1}{2}1;\ \nu_1 \bar{\nu}_1 \mu_1) C(\tfrac{1}{2}\tfrac{1}{2}1;\ \nu_2 \bar{\nu}_2 \mu_2) C(1\,2\,1;\ \mu_1 \beta \mu_2) 2\sqrt{\frac{5}{3}}\,. \tag{3.79}$$

Now recouple the spins in M_s:

$$M_s = \sum_{\substack{\bar{S}\bar{\mu} \\ I'K'}} 6\bar{S}I' \begin{pmatrix} \frac{1}{2} & \frac{1}{2} & \bar{S} \\ \frac{1}{2} & \frac{1}{2} & I' \\ 1 & 1 & 2 \end{pmatrix} C(\bar{S}I'2;\ \bar{\mu}K'\beta)$$

$$\times C(\tfrac{1}{2}\tfrac{1}{2}\bar{S};\ \nu_1 - \nu_2 - \bar{\mu})(-)^{1/2-\nu_1}$$

$$\times C(\tfrac{1}{2}\tfrac{1}{2}I';\ \bar{\nu}_1 - \bar{\nu}_2 - K')(-)^{1/2-\bar{\nu}_1} \tag{3.80}$$

The 9-j symbol is a definite number, 1/9, since the only value that $\bar{S}$ or I' can have is 1.

Now apply the Wigner-Eckart theorem to the matrix element in M_L, Equation (3.74), and substitute M_s and M_L into Equation (3.73) to obtain

$$a_T = 2\sqrt{\frac{24\pi}{5}} \sum_{\substack{LN \\ \lambda\mu}} \sum_{\substack{\bar{\mu}K' \\ \beta}} g_{L\lambda}^{j_1 j_2}(r) Y_{LN}(\hat{r}) \frac{1}{\ell_2} \langle \ell_2 \| Y_\lambda \| \ell_1 \rangle$$

$$\times (-)^{\beta} C(L\lambda 2;\ N\mu - \beta) C(\tfrac{1}{2}\tfrac{1}{2}I';\ \bar{\nu}_1 - \bar{\nu}_2 - K')(-)^{1/2-\nu_1} \times$$

$$\left[\times \sum_{\substack{n_1 n_2 \\ \nu_1 \nu_2}} C(\ell_1 \tfrac{1}{2} j_1;\ n_1 \nu_1 m_1) C(\ell_2 \tfrac{1}{2} j_2;\ n_2 \nu_2 m_2) \right.$$

$$\left. \times C(\tfrac{1}{2} \tfrac{1}{2} \bar{S};\ \nu_1 - \nu_2 - \bar{\mu})(-)^{1/2-\nu_1} C(\ell_1 \lambda \ell_2;\ n_1 \mu n_2) \right]. \quad (3.81)$$

The sum in brackets gives,

$$[\quad] = \sum_{IK} \hat{j}_1 \hat{\hat{I}} \hat{\ell}_2 \sqrt{3} \begin{pmatrix} \ell_1 & \frac{1}{2} & j_1 \\ \lambda & \bar{S} & I \\ \ell_2 & \frac{1}{2} & j_2 \end{pmatrix} C(\lambda \bar{S} I;\ \mu \bar{\mu} K)(-)^{j_1 - m_1} \frac{\hat{j}_2}{\hat{I}}$$

$$\times C(j_1 j_2 I;\ m_1 - m_2 - K) \quad (3.82)$$

Now use

$$\sum_{\mu \beta \bar{\mu}} C(\lambda\, 2 L;\ \mu \beta - N) C(\bar{S} I' 2;\ \bar{\mu} K' \beta) C(\lambda \bar{S} I;\ \mu \bar{\mu} K)$$

$$= (-)^{I+I'-L} \sqrt{5}\, \hat{I} W(I' \bar{S} L \lambda;\ 2I) C(I' I L;\ K' K - N) \quad (3.83)$$

to obtain

$$a_T = \sum_{\substack{LN \\ IK \\ I'K'}} (-)^N Y_{L-N} C(I I' L;\ K K' N) C(j_1 j_2 I;\ m_1 - m_2 - K)(-)^{j_1 - m_1}$$

$$\times C(\tfrac{1}{2} \tfrac{1}{2} I';\ \bar{\nu}_1 - \bar{\nu}_2 - K')(-)^{1/2-\bar{\nu}_1} \times$$

$$\times \sum_{\lambda} 12\sqrt{\frac{10\pi}{3}}\,(-)^{L}\,\frac{\hat{j}_1\hat{j}_2\hat{I}\hat{I}'}{\hat{L}}\,\delta_{I'0}\,\langle \ell_2 \| Y_\lambda \| \ell_1 \rangle\, g_{L\lambda}^{j_1 j_2}$$

$$\times W(11L\lambda;\ 2I) \begin{pmatrix} \ell_1 & \frac{1}{2} & j_1 \\ \lambda & 1 & I \\ \ell_2 & \frac{1}{2} & j_2 \end{pmatrix} . \qquad (3.84)$$

A comparison with Equation (3.16) immediately gives

$$z_T(II'L;\ j_1 j_2,\ |r|) = \sum_{\lambda} 12\sqrt{10\pi}\,(-)^{L}\,\frac{\hat{j}_1\hat{j}_2\hat{I}}{\hat{L}}\,\delta_{I'0}\,\langle \ell_2 \| Y_\lambda \| \ell_1 \rangle$$

$$\times\, g_{L\lambda}^{j_1 j_2} W(11L\lambda;\ 2I) \begin{pmatrix} \ell_1 & \frac{1}{2} & j_1 \\ \lambda & 1 & I \\ \ell_2 & \frac{1}{2} & j_2 \end{pmatrix} . \qquad (3.85)$$

for the tensor force.

IV. EFFECTIVE POTENTIAL IN STRUCTURE

Review of Some Calculations Using a 2-body Force in Light Nuclei

There have been numerous shell model calculations employing a residual 2-body force (13, 17, 19-21, 38, 39). Inglis (19) first made a comprehensive study of structure in light nuclei (A=5, A=17). His approach was primarily to make theoretical fits to the available energy spectra. One important conclusion, that he reached, was that the jj shell-model coupling scheme, successful in heavier nuclei, was unsatisfactory. At least an intermediate coupling model, intermediate between LS and jj-coupling, was needed. He also examined in some detail the problem of the beta-decay rate in C^{14} which experimentally is anomalously slow. The transition is from the 0^+ ground state of C^{14} to the 1^+ ground state of N^{14}, and is thus an allowed Gamow-Teller transition. The slow rate can only be explained by a cancellation of wave functions, which results in a near zero nuclear transition matrix element. Inglis showed, that if the wave functions for C^{14} and N^4 are described by two holes in the 1p-shell, then it is impossible for any central plus spin-orbit residual interaction to give wave functions which produce the necessary cancellation. The alternatives are a tensor force in the residual interaction, and, or configuration mixing of other shells in the wave functions.

The possibility of a tensor force has been studied extensively

by Visscher and Ferrell (39). They assume that the C^{14} and N^{14} ground-state wave functions may be described as two holes in the 1p-shell. Wave functions are then found using a residual potential with central, spin-orbit, and tensor terms. They find that, with the inclusion of the tensor force, the experimental beta-decay rate can be achieved; and, at the same time, the ground-state energy level of C^{14} and the ground state and first two excited states of N^{14} can be fit. They further test the wave functions by calculating M1 and E2 rates among the same levels. If E2-enhancement is assumed, there is reasonable agreement with experiment.

Another study of the N^{14} nucleus has been made by True (38). He uses a central residual potential nearly identical to the central part of the Visscher-Ferrell force. If he assumes that N^{14} consists of an inert C^{12} core with two extra valence nucleons which can move in the $1p_{1/2}$, $2s_{1/2}$, $1d_{5/2}$ and the $1d_{3/2}$ orbitals, he is able to give shell model assignments in agreement with experiment to nearly all levels in N^{14} up to 10.5 MeV excitation.

An application of the residual potential approach has been made to the 2s-1d shell by Inoue et al. (20, 21). They use a very general two-body potential which includes central, spin-orbit, and tensor forces, all of which include exchange forces. The potential parameters are varied to obtain a fit to the energy spectra of O^{18}, F^{18}, O^{19}, and Ne^{20}. The wave functions which result from the parameter fit,

are tested against beta-decay rates and electromagnetic data. With some exceptions, there is reasonable agreement with experimental observations. After a discussion of two applications of the effective-matrix-element approach, a more detailed discussion of the actual potential parameters used in the above calculations will be given.

Effective-Matrix-Element Approach

One reason for using a parameterized residual potential is to see if some nuclei may be understood in terms of a simple shell model, that is, where the nucleus is described by a few interacting valence nucleons in shells outside an inert core which produces the shell-model potential. Any failures of this approach might be due to a residual potential which was not correct. It is possible, however, that a simple shell-model scheme will not work, that agreement with experiment cannot be attained no matter how general the residual potential is. In order to test the shell-model description rather than the residual potential, calculations have been made which treat the two-body matrix elements as parameters (2, 5, 11). In this way no restriction is placed on the potential, and the success or failure of the calculation rests on the assumption that the wave functions may be described in a truncated shell-model space.

In second-quantized notation, the shell-model Hamiltonian may be written,

$$H = \sum_i \epsilon_i a_i^\dagger a_i + \frac{1}{2} \sum_{ijk\ell} V_{ij,k\ell} a_j^\dagger a_i^\dagger a_k a_\ell, \qquad (4.1)$$

where the $a_i^\dagger$'s create holes or particles depending on the case being considered (see Appendix). The ϵ_i are single-particle energies which correspond to the single-particle wave functions φ_i for the shell-model Hamiltonian h_i, $h_i\varphi_i = \epsilon_i\varphi_i$. The $V_{ij,k\ell}$ are two-body matrix elements of the residual potential.

$$V_{ij,k\ell} = \langle \varphi_i\varphi_j | V(1,2) | \varphi_k\varphi_\ell \rangle \qquad (4.2)$$

The problem is solved in a truncated space, which means that only a few φ_i's are considered. For example, the 1p shell has two states, the $1p_{1/2}$ and $1p_{3/2}$. From these, one can obtain 15 two-body matrix elements and two single-particle energies which gives 17 parameters (11). Once these parameters are determined, then the Hamiltonian in the truncated space is completely determined, and wave functions may be calculated.

Cohen and Kurath (11) do the effective matrix element calculation for the 1p shell. In order to determine the 17 parameters, they do a least squares fit to the experimental energy levels of nuclei from $A = 6$ to $A = 14$. In other words they minimize

$$\chi^2 = \Sigma [E - E_{exp}]^2 \qquad (4.3)$$

where the sum is over all the energy levels. Two well known levels were omitted, namely the 4^+ in Be^8 and the 0^+ excited state in C^{12} at 7.65 MeV. Inclusion of the 0^+ state produces a large increase in χ^2, and they believe the state is not well described by a 1p-shell model.

The resulting wave functions are tested by calculating magnetic-dipole moments, beta-decay rates, and M1-transition strengths. In general, the agreement with experiment is excellent. Later work indicates that some E2 enhancement is produced by the wave functions, but not enough (30). One very satisfying result is the prediction of the anomolously small beta-decay rate in C^{14}. A comparison of their results with those of Amit and Katz (2) indicates that the choice of energy levels being fit is quite critical to the results.

If they assume a potential with the general form of the Hamada-Johnston (18) potential, but without the hard cores, Cohen and Kurath are able to express the two-body matrix elements in terms of one-body matrix elements in the relative co-ordinate system of the pair of particles. This method enables them to show that the qualitative features of their potential are similar to the Hamada-Johnston potential. One interesting result is that a very short-range dependence is indicated for the singlet-even part of the force, much like a pairing force.

Arima et al. (5) apply the effective matrix element method to the 1d-2s shell exactly as Cohen and Kurath did for the 1p shell. In

this case, energy levels in Ne^{20}, F^{20}, O^{20}, F^{19}, O^{19}, O^{18}, and F^{18} are fit. The 1.7 MeV state in F^{18} disrupts the fit and is left out. The $T = 1$ effective two-body matrix elements are well determined by the oxygen data alone. Inclusion of the flourine and neon isotopes in the fit changes these matrix elements by less than 200 keV. The matrix elements themselves are on the order of two MeV. The $T = 0$ matrix elements are more sensitive. Their values depend on which Ne^{20} levels are included and can become completely ridiculous if a bad choice of levels is made. They note that all the $T = 1$ and three of the $T = 0$ matrix elements are well enough determined to make meaningful comparisons with other data. A comparison is made with the theoretical reaction matrix elements of Kuo and Brown (23) and rough agreement is noted. The theoretical and empirical matrix elements differ by about 20-30% for those matrix elements which are well determined. Again, as with Cohen and Kurath, the resulting wave functions are tested against beta-decay rates and electromagnetic data. Overall agreement is reasonable; although, there are a number of cases where it is necessary to include core excitations or consider the $1d_{3/2}$ level to explain the data. They confined their calculations to the $2s_{1/2}$ and $1d_{5/2}$ levels. For the particular case of the F^{18} ground state beta-decay transition to O^{18}, the correct value is obtained. Earlier calculations by Elliot and Flowers (13) and also by Kuo and Brown (24) which also used 2s-1d shells-model wave functions

gave an ft value too low for the same transition.

Potential Strengths Determined from Effective Matrix Elements

A straight forward method for extracting an effective potential from a set of effective two-body matrix elements is now given. It was noted above that Cohen and Kurath found an effective potential in order to compare their results with the Hamada-Johnston potential. They made explicit use of the harmonic oscillator states in order to reduce their two-body matrix elements to one-body harmonic oscillator integrals. A primary goal of the present work is to compare effective forces in nuclear structure and scattering. Scattering calculations are more sensitive to the bound state wave functions than are structure calculations (22); so that, it is more important to use bound states calculated in a Woods-Saxon potential. For single-particle excitations, the form factor which enters the DWBA amplitude is,

$$g_L^{j_1 j_2}(r) = \int \varphi^*_{j_2}(r_1)\varphi_{j_1}(r_1)v_L(r_1, r)r_1^2 dr_1 \qquad (4.4)$$

where the φ's are bound state wave functions and v_L is a coefficient of the multipole expansion for the force. For a central force,

$$V(|r-r_1|) = \sum_{LN} Y^*_{LN}(\hat{r}_1)Y_{LN}(\hat{r})v_L(r_1, r). \qquad (4.5)$$

Chapter III gives a more complete development of the multipole expansion. A more meaningful comparison between effective potentials for structure and for scattering will be made if the nuclear two-body matrix elements are calculated from the same bound state form-factor that enters the scattering calculation. The result, derived in Chapter III, is

$$\langle j_3 j_4 JT|V|j_1 j_2 JT\rangle = \sum_{II'L} C(II'L) \left\langle \varphi_{j_3} \left| g_L^{j_4 j_2} \right| \varphi_{j_1} \right\rangle + \text{exchange.} \qquad (4.6)$$

In this form the nuclear two-body matrix elements are coupled to good spin and isospin J and T, and the potential is conveniently written as

$$V = \sum_{AB} P_{AB} V_{AB} v_C(\alpha r) + V_T S_{12}(\tau_1 \cdot \tau_2) v_T(\alpha_T r) \qquad (4.7)$$

where the P_{AB} and V_{AB} are projection operators and strengths respectively for the central potential. The four operators, P_{AB}, are P_{TE}, P_{TO}, P_{SE}, and P_{SO} and project onto triplet-even, triplet-odd, singlet-even, and singlet-odd states respectively. V_T is the tensor strength while $S_{12}(\tau_1 \cdot \tau_2)$ is the tensor operator times a $\tau_1 \cdot \tau_2$ isospin dependence.

$$v_C = \frac{e^{-\alpha r}}{\alpha r} \qquad (4.8)$$

and

$$v_T = E(\alpha r) - (\frac{\beta}{\alpha})^3 E(\beta r) \qquad (4.9)$$

where

$$E(\alpha r) = (\frac{1}{3}+\frac{1}{\alpha r}+\frac{1}{(\alpha r)^2})\frac{e^{-\alpha r}}{\alpha r} \ . \qquad (4.10)$$

v_T is discussed in Chapter III.

Given a set of ranges and potential strengths and appropriate bound state parameters, the computer then calculates the two-body matrix elements for bound states in a Woods-Saxon potential. The computer code was checked against a table of 15 $T = 0$ and $T = 1$ two-body matrix elements listed by Arima et al. (5) for a Yukawa force with a Rosenfeld exchange mixture (33, p. 233). The bound states were harmonic-oscillator states in the 2s-1d shell.

In order to find the set of potential strengths which yield the best fit to a given set of two-body matrix, a least-squares criterion is used. Specifically,

$$\delta = \sum_{i=1}^{N} (y_i - m_i)^2 \qquad (4.11)$$

is minimized, where $\{m_i\}$ $(i=1, N)$ is the set of empirical matrix elements and $\{y_i\}$ are the values of the two-body matrix elements calculated for a given set of potential strengths $\{V_s\}$.

$(V_1, V_2, V_3, V_4, V_5) \equiv (V_{TE}, V_{SE}, V_{TO}, V_{SO}, V_T)$. Because the effective potential depends linearly on the potential strengths, so do the calculated matrix elements $\{y_i\}$.

$$y_i = \sum_{s=1}^{5} a_{is} V_s \tag{4.12}$$

where a_{is} is the value of the i-th matrix element computed by setting all the V's equal to zero except for $V_s = 1$. Now, δ is minimized with respect to the potential strengths, $\{V_s\}$.

$$\frac{\partial \delta}{\partial V_s} = 0, \quad s = 1, 5. \tag{4.13}$$

This set of five equations for the five potential strengths easily becomes

$$\sum_{S'} A_{ss'} V_{s'} = B_s \tag{4.14}$$

where

$$A_{ss'} = \sum_i a_{is} a_{is'} \tag{4.15}$$

and

$$B_s = \sum_i a_{is} m_i. \tag{4.16}$$

Thus, for a given set of empirical matrix elements, the best choice of

potential strengths is found by first calculating all the a_{is}'s. The above set of equations is then solved for the V_s's. In practice, obvious modifications may be made to find the best set of $\{V_s\}$ for $s = 1, 4$ with $V_5 \equiv V_T = 0$, or any other fixed value.

Effective Potential Strengths in the 1p and 2s-1d Shells

First an effective potential for the 1p-shell was extracted from Kurath's effective matrix elements. The inverse range used for the central force was $\alpha = .578\ \text{fm}^{-1}$ while $(\alpha_T, \beta_T) = (.709, 3.)$ for the tensor ranges. The wave functions used were harmonic oscillator functions with an exponential dependence,

$$\sim e^{-1/2(\gamma r)^2}$$

where

$$\gamma = .595\ \text{fm}^{-1}.$$

(α_T, β_T) are the two ranges that enter the tensor force. Table 1 summarizes the primary results. Each row gives the potential strengths that result in the best effective potential. α, γ, N, and $\Delta = \frac{10}{N} \sum_i \delta_i^2$ are also listed, where N is the number of matrix elements used in the fit.

The first Kurath fit was to all 15 1p-shell matrix elements denoted by (8-16) 2BME by Cohen and Kurath (11). The strong

Table 1. Potential strengths determined from effective matrix element fit and comparison with other potentials.

Description	α	γ	N	V_{TE}	V_{SE}	V_{TO}	V_{SO}	V_T	$\frac{10}{N}\Sigma\delta_i^2$
CK fit[a]	.578	.595	15	-28.6	-24.5	7.4	8.1	3.7	3.8
CK fit[a]	.578	.595	9	-27.7	-27.7	-24.0	4.4	15.4	4.1
CK fit with fixed tensor	.578	.595	15	-28.8	-22.9	10.0	11.8	-10.	4.6
	.578	.595	15	-28.7	-24.1	8.1	9.1	0.	3.9
	.578	.595	15	-28.6	-25.3	6.2	6.4	10.	4.0
Arima[b] fit	.638	.510	11	-42.0	-24.4	13.0	-90.6	-25.5	1.0
Arima[b] fit	.638	.510	8	---	-25.1	12.9	---	-23.1	1.2
Arima fit with fixed tensor	.638	.510	11	-43.0	-28.8	12.2	-83.8	-10.	1.2
	.638	.510	11	-43.7	-31.7	11.8	-79.5	0.	1.5
	.638	.510	11	-44.4	-34.6	11.3	-75.2	10.	1.8
CK (short range)	2.	.595	15	-489.	-391.	399.	565.	3.42	3.6
Other potentials									
VF[c]	.578	.595	--	-51.9	-32.8	0.	0.	11.4	
True[d]	.548	.566	--	-52.0	-32.5	0.	0.	0.	
Inoue[e]	$\lambda = 2/3$		--	-35.0	-27.0	13.5	0.	10.	
Comparison of normalized potentials									
CK	.7	.55	15	-53.2	-45.6	19.5	21.4	3.7	
VF	.7	.55	--	-53.6	-33.9	0.	0.	11.4	
Arima	.7	.55	11	-43.7	-25.4	13.9	-96.5	-25.5	
Inoue	.7	.55	--	-53.2	-41.1	26.5	0.	10.	

[a]Ref. 11.

[b]Ref. 5.

[c]Ref. 39 VF use a Gaussian potential.

[d]Ref. 38 True uses a Gaussian potential

[e]Ref. 19, 20 Inoue et al. use a Yukawa potential.

attractive even potentials and the relatively weak odd potentials are the most prominent features. The tensor strength is also very weak. In view of Visscher and Ferrell's results, the tensor strength seemed small and a fit was made to the nine effective matrix elements which had $(J, T) = (0, 1)$ or $(1, 0)$. The reason for this choice is that the low lying levels in C^{14} and N^{14} which concerned Visscher and Ferrell are $(J, T) = (0, 1)$ or $(1, 0)$ type states. Table 1 shows that the result of the new fit is to increase the tensor strength from 3.7 to 15.4 MeV in closer agreement with Visscher and Ferrell. A precise comparison of the tensor strength used here and of that used by Visscher and Ferrell is not possible, since different spatial dependences of the tensor force are assumed. However, the new fit also changes the V_{TO} strength radically to -24. MeV, and one sees that the choice of matrix elements used in the fit is crucial.

Another fit was made with $\alpha = 2.$ to investigate the effect of range in the central force. The value of Δ in Table 1 shows that the fit is improved by the short range, in agreement with Cohen and Kurath's results. See the Appendix for a discussion of the range dependence of the potential strengths. Also, three runs were made with the tensor strength fixed at $V_T = -10.$, 0., and 10. MeV. Only the central strengths were allowed to vary in these runs. These results will be discussed later.

Exactly as with Cohen and Kurath, an effective potential was

derived for the 2s-1d shell from the matrix elements of Arima et al. (5). In their paper it is pointed out that only the $T = 1$ and three of the $T = 0$ matrix elements listed there are reliable. Two fits were thus made, one to the eight $T = 1$ matrix elements and another which included the three $T = 0$ matrix elements. For the eight parameter fit, the V_{TE} and V_{SO} strengths are undetermined since they correspond to $T = 0$. Again, the even strengths are strongly attractive and V_{TO} is smaller and repulsive. $V_{SO} = -90.5$ MeV is in complete disagreement with the results of Cohen and Kurath. However, the $T = 0$ strengths, V_{TE} and V_{SO}, are determined by only three $T = 0$ empirical matrix elements. If the details of the fitting procedure are investigated, one finds that V_{TE} depends on the sum of the three matrix elements, while V_{SO} depends very strongly on the $(J, T) = (2, 0)$ matrix element. In particular, if the $(2, 0)$ matrix element were changed from -3.70 to -1.25 MeV, V_{SO} would change from $-91.$ to about $+10.$ MeV. The value for V_{TE} should be reliable; although, the value for V_{SO} is not. Inoue et al. find that V_{SO} varies from 0. to 17. MeV and depends strongly on the ground state energy of F^{18}.

If $\frac{10}{N}\sum \delta_i^2$ is considered as a criterion for the quality of a fit, then the fits for the 2s-1d shell are remarkably better than those for the 1p shell. One possible explanation is that an average shell-model potential is better defined for the 2s-1d shell. The 1p shell

includes nuclei from Li^5 to O^{16}, and the single particle wave functions would vary appreciably as one progresses through the shell.

Finally, in Table 1, a comparison is made between the results of Cohen and Kurath, Visscher and Ferrell, Arima, et al. and Inoue et al. In order to make the comparison, all the results were converted to an inverse range of $\alpha = .7$ fm^{-1} and a harmonic-oscillator parameter $\gamma = .55$ fm^{-1}. It was assumed that, $V \sim (\frac{\alpha}{\gamma})^n$ where $n=2.3$, and 3.7 for the even and the odd potential strengths respectively. These values for n were arrived at by a comparison of potential strengths obtained from fits in the 1p shell for two different values of α. This procedure is described in more detail in the Appendix. The central results are in semi-quantitative agreement. The general features to be noted are the strong attractive even potentials and the smaller odd repulsive potentials. V_{SE} is smaller than V_{TE} in all cases; although, the amount varies considerably. Although V_{SO} is very poorly determined, it is consistent with the results to say it has the same sign and magnitude as V_{TO}.

The results of Cohen and Kurath, and Visscher and Ferrell apply to the 1p shell, those of Arima, et al. and Inoue et al. to the 2s-1d shell. Note that a common $\gamma = .55$ fm^{-1} was chosen for both shells in order to allow a comparison of the strengths between the two shells. This value of γ corresponds to an rms radius of 2.87 fm and 3.41 fm for the 1p and 2s-1d shells respectively. These values

were computed from $\sqrt{\langle r^2 \rangle} = \frac{1}{\gamma}[2(n-1)+\ell+\frac{3}{2}]^{1/2}$ where (n, ℓ) are harmonic-oscillator quantum numbers.

The primary results of the calculation with a Woods-Saxon potential are shown in Table 2 along with the previous harmonic-oscillator results. The index, $\Delta = \frac{10}{N}\sum \delta_i^2$, which is a measure of the quality of the least squares fitting procedure, shows a slight improvement in the fit for both the 1p shell and the 2s-1d shell; although, the improvement is more noticeable for the latter. In order to compare the magnitudes of potential strengths, all the results are normalized to an inverse range $\alpha = .7\ \text{fm}^{-1}$ as was done before for the harmonic-oscillator results. Previously, the harmonic-oscillator parameter was chosen to be $\gamma = .55\ \text{fm}^{-1}$ for the purpose of comparison. This value corresponds to rms radii of 2.87 and 3.41 fm for the 1p states and 2s-1d states respectively. The average rms radius for the $1p_{1/2}$ and $1p_{3/2}$ states computed in the Woods-Saxon potential was 2.80 fm. The average rms radius for the $1d_{5/2}$ and $2s_{1/2}$ was 3.90 fm. The potential strengths for the Woods-Saxon calculations were renormalized to correspond to rms radii consistent with the above value of $\gamma = .55\ \text{fm}^{-1}$ (see Appendix for this conversion). These results are displayed in Table 3. One sees that for the central forces the results of the Woods-Saxon calculation are in general agreement with those for the harmonic-oscillator calculation. Recall that V_{SO} is very poorly determined in the 2s-1d shell. The

Table 2. Effect of using a Woods-Saxon potential, W-S, in determining effective potentials compared to using a harmonic-oscillator potential, H. O. (See Chapter 4 for parameter definitions.) $a_T = .7$ and $.71$ for the 2s-1d and 1p shells respectively. $\beta_T = 4.$

	Potential well	V_{TE}	V_{SE}	V_{TO}	V_{SO}	V_T	$\frac{10}{N}\Sigma\delta_i^2$
2s-1d shell (N = 11)							
$a = .7 \quad r = 1.25 \times A^{1/3}$	W-S	-67.7	-49.2	25.5	-126.0	- 2.5	.8
$a = .638 \quad \gamma = .510$	H. O.	-42.0	-24.4	13.0	- 90.7	-25.5	1.0
1p shell (N = 15)							
$a = .71 \quad r = 1.25 \times A^{1/3}$	W-S	-46.7	-38.7	14.0	14.7	3.6	3.7
$a = .578 \quad \gamma = .595$	H. O.	-28.6	-24.6	7.4	8.1	3.7	3.8

Table 3. Renormalized values for Table 2. Potential strengths have been altered to correspond to a common $a = .7$ and $\gamma = .55$. An effective γ is defined for a Woods-Saxon well by considering rms radii.

	Potential well	V_{TE}	V_{SE}	V_{TO}	V_{SO}	V_T
2s-1d shell	W-S	-49.7	-36.2	15.5	---	- 2.5
	H. O.	-43.7	-25.4	13.9	-96.5	-25.5
1p shell	W-S	-51.1	-42.4	16.2	17.0	3.6
	H. O.	-53.2	-45.6	19.5	21.4	3.7

tensor force did not change much for the 1p shell, but changed markedly in the 2s-1d shell.

The Tensor Force in Nuclear Structure

The tensor results in Table 1 show no consistency. The result of the fit to Arima's matrix elements has the opposite sign for the tensor compared to the other results in Table 1. Although the tensor value of Inoue et al. is positive, this result was only chosen to agree with the Hamada-Johnston potential, in order to narrow the range of investigation. To see what the effect of different strengths might be on the overall fit, the tensor force was fixed at values of -10., 0., and 10. MeV while the central strengths were chosen to give the best fit. This procedure was followed for both the Cohen and Kurath, and the Arima et al. sets of matrix elements. The values of Δ indicate that the fit becomes only slightly worse as V_T deviates from the best value. Also note that the central strengths do not vary much as V_T is altered. In general, the additional parameter of the tensor strength gives an improved fit, but not to a significant degree. The fact that the tensor force is not determined in a consistent fashion in the manner of the central strengths does not mean that it is unimportant. It was noted earlier that Visscher and Ferrell found a tensor force was needed to explain the C^{14} beta-decay rate if no configuration mixing from the 2s-1d shell was assumed (39). Their strength is

not inconsistent with the results of the fit to the Cohen and Kurath matrix elements. In particular, it was also noted earlier that if a fit was made to only those $(J, T) = (0, 1)$ and $(1, 0)$ matrix elements, then the tensor strength would increase from 3.7 to 15.4 MeV.

A recent work by Rose, Häusser, and Warburton (32) has confirmed the necessity of a tensor force in the $A = 14$ system. They examine the possibility of configuration mixing from the 2s-1d shell as well as a tensor force in the shell model interaction. They find two important results if configuration mixing is allowed, but if a tensor force is not. First, it is impossible to simultaneously explain the C^{14} $(1^+ \rightarrow 0^+)$ beta-decay result and the 2.31 MeV M1 gamma transition from the first excited state in N^{14}. Second, it is not possible to explain the 3.95 MeV M1 gamma transition from the 1^+ excited state, and at the same time obtain agreement for the E2/M1 mixing ration for the same transition. This latter conclusion is nearly as strong as the beta-decay argument. With a tensor force and some configuration mixing, they obtain reasonable agreement for all the data associated with the low lying levels in the $A = 14$ system.

The calculation of effective potentials for both the 1p and 2s-1d shells has been redone using bound states calculated in a Woods-Saxon potential rather than a harmonic-oscillator potential. One reason is that the Woods-Saxon potential, which goes to zero as the radius of the potential well increases, is more realistic than the

harmonic-oscillator potential. A second reason, which is important for this work, is that it allows a comparison of results between the structure calculations and the scattering calculations. It is more important to use the Woods-Saxon potential in scattering calculations, since they are sensitive to the wave functions (22).

V. EFFECTIVE FORCES IN SCATTERING

DWBA Formalism for the Microscopic Model

As mentioned earlier, defects of a particular scattering theory may be absorbed to some extent by an effective scattering force; so that, the effective force must be defined with respect to a given scattering theory or model. In this work, a microscopic DWBA theory is the model used (16, 28, 34). The cross section is given by,

$$\frac{d\sigma}{d\Omega} \approx \left| \left\langle \chi_f^{(-)} \middle| K \middle| \chi_i^{(+)} \right\rangle \right|^2 \tag{5.1}$$

where $\chi_f^{(-)}$ and $\chi_i^{(+)}$ are the initial and final distorted waves which describe the projectile nucleon.

$$K(r_o) = \left\langle \Phi_f \Sigma_f \middle| V \middle| \Phi_i \Sigma_i \right\rangle \tag{5.2}$$

$K(r_o)$ is the value of the two-body scattering interaction, V, integrated over the target nucleon and projectile spin co-ordinates. Φ_i and Φ_f are the initial and final nuclear wave function, while Σ_i and Σ_f are the corresponding projectile spin wave functions. In the microscopic model Φ_i and Φ_f are configuration-mixed shell-model states formed from single-particle bound states φ_{jm}. Then, $K(r_o)$ may be written as the sum of single-particle form-factors, $g_L^{j_1 j_2}(r_o)$, weighted by coefficients which describe the configuration-

mixed wave functions,

$$K(r_o) \approx \sum_{j_1 j_2} C_{j_1 j_2} g_L^{j_1 j_2}(r_o). \qquad (5.3)$$

$g_L^{j_1 j_2}$ is the same single-particle form-factor which entered the calculation of two-body nuclear matrix elements. See Chapter III for further details. As for structure, V is a two-body interaction which is the sum of central and tensor terms. $V = V_c + V_T$. For structure calculations, V_c was conveniently written as a sum of even and odd, and triplet and singlet strengths.

$$V_c = (P_{TE}V_{TE}+P_{SE}V_{SE}+P_{TO}V_{TO}+P_{SO}V_{SO})v_C(\alpha r) \qquad (5.4)$$

where P_{AB} are the appropriate projection operators. For scattering, it is more convenient to write,

$$V_c = [V_{00}+V_{10}(\vec{\sigma}_1\cdot\vec{\sigma}_2)+(V_{01}+V_{11}(\vec{\sigma}_1\cdot\vec{\sigma}_2))\tau_1\cdot\tau_2]v_C(\alpha r) \quad . \qquad (5.5)$$

The strengths $V_{ST} = (V_{00}, V_{10}, V_{01}, V_{11})$ and $V_{AB} = (V_{TE}, V_{SE}, V_{TO}, V_{SO})$ are simply related by a four-dimensional matrix (see Appendix). The choice of V_{ST} strengths for scattering is due to various selection rules discussed elsewhere in detail (28). For example, a $(J=0, T=1) \rightarrow (J=1, T=0)$ transition would depend only on V_{11}, but on a linear combination of the V_{AB}.

These rules allow the determination of single V_{ST}'s or simple combinations of them, if a judicious choice of nuclear transitions is made.

Review of Known Strengths

Estimates of the central force parameters have been made for a number of cases (4, 6, 25, 31, 35, 41). Satchler has made preliminary studies of more than 20 reactions (35), primarily (p, p') with some (p, n), to determine the effective strengths. These studies include mass regions $A \approx 18$, 50, 90, and 208 at incident proton energies, $E_p \approx 10\text{-}20$ MeV. The primary results follow. A range of $\alpha^{-1} = 1.$ fm was used in a Yukawa potential.

1. $V_0 \approx 150\text{-}200$, except for Pb^{208} where $V_0 \approx 200\text{-}300$ MeV
2. $V_1 < 67$
3. $V_{01} \approx 20\text{-}24$ MeV

V_0 and V_1 are defined by $V_s = (V_{s0} + V_{s1} \vec{\tau}_1 \cdot \vec{\tau}_2)$, $s = 0, 1$. The isospin dependence of V_0 is small; so that, the value of $(\tau_1 \cdot \tau_2)$ should not change the value of V_0 appreciably.

Reif et al. (31) have studied the spin-flip strength, V_1, in the excitation of non-normal parity 1p1h states in O^{16}, S^{32}, and Si^{28} by inelastic proton scattering at about 17 MeV. They have also studied the non-spin-flip strength, V_0, for normal parity states in the

same nuclei. They find strengths consistent with Satchler's values; however, since they use a Gaussian potential with a range $\alpha^{-1} = 1.7$ fm, the comparison is not too meaningful. The ratio V_1/V_0 should be more meaningful. They find for O^{16}, Si^{28}, S^{32} values of V_1/V_0 of .29, .31, and .31 respectively.

P. J. Locard, S. M. Austin, and W. Benerson (25) have studied the Li^7(p, p') and Li^7(p, n) reactions to the first excited $1/2^{(-)}$ states of Li^7 and Be^7 respectively over a range of incident proton energies from 23 to 52 MeV. They have also examined the Li^6(p, p') transition to the $T = 1$ second excited state of Li^6. If a range of $\alpha^{-1} = 1.$ fm is assumed with a Yukawa potential, they find that V_{00} varies from 90 to 113 MeV as the energy varies from 44.7 to 25. MeV. They also find that $V_{11} = 15$ MeV and is independent of energy. Contributions of other parts of the potential are found to be small. They have also carried out distorted wave calculations, using a theoretical effective interaction deduced by McManus (27), which indicates that the V_{00} term contributes about 70% of the Li^7(p, p') cross section and that the V_{11} term contributes 90% of the (p, n) cross section.

A survey of (p, n) reactions in C, N, O, Al, Ti, and Zr isotopes has been made by J. D. Anderson et al. (4) at incident energies in the range, $E \approx 12$-19 MeV. They compute V_{01} and V_{11} strengths where an inverse range, $\alpha = .7$ fm^{-1}, is assumed with a Yukawa interaction. For $L = 0$ transitions, they find values of V_{11} from

4.6 to 8.0 MeV with an average value $V_{11} = 6.5$ MeV. They also find, $V_{01}/V_{11} \approx 3/2$. Quadrupole enhancements are found for a number of $L = 2$ transitions. V_{01} and V_{11} are increased by factors of about 1.5-3.0.

Ball (6) has made an extensive experimental survey of $(He^3, He^{3'})$ and (He^3, t) reactions in p-shell nuclei at energies of 40-50 MeV from which he has deduced effective nucleon-nucleus strengths. He normalizes his results to $\alpha^{-1} = 1.$ fm for a Yukawa potential. There are three features of his data pertinent to this work. First, except for transitions that appear to have quadrupole enhancements, he finds the following strengths overall. $V_{00} \approx 47\text{-}60$, $V_{01} \approx 19\text{-}33$, and $V_{11} \approx 16\text{-}31$ MeV. Second, for those transitions confined to the 1p shell he finds, $V_{00} \approx 60.3$, $V_{01} \approx 20.6$, and $V_{11} \approx 16.5$ MeV. Only magnitudes have been determined. The assumption of a Serber force would give $|V_{10}| = \frac{1}{3}V_{00} \approx 20.1$ MeV. Finally, for the anomalous $C^{14} \rightarrow N^{14}$ ground state transition, he finds $V_{11} = 25.9$ MeV. Also, the DWBA fits to the angular distribution of this latter transition are noticeably worse than other fits he makes.

The foregoing results are summarized in Table 4 for $\alpha^{-1} = 1.$ fm. Consistent values are obtained for V_{01} and V_{11}. Except in the combination $V_1 = V_{10} + (\tau_1 \cdot \tau_2)V_{11}$, V_{10} is undetermined. There is a rather large variation in V_{00}. The results of Locard et al. (25) show that, in contrast to V_{11}, it is energy dependent. Also, Ball

concludes that V_{00} is much smaller for the p-shell than for heavier nuclei, a fact he attributes to core-polarization. However, Satchler's data includes the $O^{18}(p, p')$ reaction, a nucleus just above the 1p shell, from which he deduces $V_0 \approx 205$ MeV. Core-polarization in this reaction will be reviewed in a later section. Only the magnitudes of the strengths have been determined in Table 5, not the signs.

Preliminary Comparison With Structure Calculations

The values of the central strengths deduced above will now be compared to earlier values found by fitting effective matrix elements used in nuclear structure. The values used for the comparison will be those in Table 2 found by fitting 1p-shell and 2s-1d-shell matrix elements, where a Woods-Saxon potential was used for the bound states. The strengths found for both are 1p shell and the 2s-1d shell are to be normalized to a potential with a range $\alpha^{-1} = 1$ fm. It is assumed, as in earlier comparisons (see Appendix) that the even strengths are proportional to $\alpha^{2.3}$, and the odd to $\alpha^{3.7}$. After the normalization to $\alpha = 1.\ \text{fm}^{-1}$ has been made, the even and odd strengths are transformed to the representation used in the scattering discussion. The results of these normalizations are shown in Table 5. Since the value of V_{SO} in Table 2 for the 2s-1d shell is completely unreliable, it was taken equal to $V_{TO} = 25.5$ MeV in the calculation of the values in Table 5. This value was chosen since

Table 4. Potential strengths determined from DWBA studies. Unless noted otherwise, the inverse range is $\alpha = 1.$ fm^{-1}, and the projectile is a proton. Energies are in MeV.

Incident energy	$\|V_{00}\|$	$\|V_{10}\|$	$\|V_{01}\|$	$\|V_{11}\|$	Letter notes reference
10-20	150-200	< 67	20-24	---	a) b) $V_1/V_0 \approx .3$ for 1p1h excitations.
44.7	90			15.	c)
25.	113			15.	c)
12. -19.			9.	~ 6.5	d) $\alpha = .7$
12. -19.			28.	~19.	d) normalized to $\alpha = 1.$
40-50	47-60		19-33	16-31	e) p-shell target nuclei
40-50	60.3		20.6	16.5	e) p-shell transitions

a) Satchler (35).
b) Reif et al. (31), V_0 and V_1 are defined by $V_s = V_{s0} + V_{s1} \vec{\tau}_1 \cdot \vec{\tau}_2$ for $s = 0, 1.$
c) Locard et al. (25).
d) Anderson et al. (4).
e) Ball (6), He^3 projectiles

Table 5. Values of potential strengths from Table 2 transformed to spin-isospin representation. The values are taken from the W-S fit and are normalized to $\alpha = 1.$ assuming that even strengths obey $V_E \sim \alpha^{2.3}$ and odd strengths obey $V_{odd} \sim \alpha^{3.7}$.

Shell	V_{00}	V_{10}	V_{01}	V_{11}
2s-1d	9.9	23.3	33.7	28.5
1p	-4.0	15.6	20.0	18.1

$V_{SO} \approx V_{TO}$ in the 1p shell where the values appear better determined.

The first thing to notice in Table 5 is that V_{00} is not consistent and that both values given disagree completely with the values determined from scattering reactions which are displayed in Table 4. The strength V_{00} is very sensitive to the value of V_{TO}. Explicitly,

$$V_{00} = \frac{1}{16}(3V_{TE}+3V_{SE}+9V_{TO}+V_{SO}). \tag{5.6}$$

And, small variations of V_{TO} would cause large variations of V_{00}. Thus, V_{00} is not well determined if V_{TO} has an appreciable magnitude.

However, the strengths of V_{10}, V_{01}, and V_{11} determined from structure calculations in Table 5 are in good agreement with the results in Table 4. The magnitudes of the values in Table 5 are well within the range of values displayed in Table 4. V_{01} is 10-20% greater than V_{11} in Table 5 in reasonable agreement with Table 4. V_{10} in Table 5 is consistent with the results of Table 4 which gives the value determined from scattering reactions; although, the latter is poorly determined. Finally, note that there is a slight confirmation in Table 4 of the result that the 1p-shell strengths are smaller than those of other shells. However, the greater strengths in the 2s-1d shell in Table 5 depend critically on the Woods-Saxon well radius

used. Recall that $r = 1.25 \times A^{1/3}$ fm was used where $A = 14$ and 18 were taken as typical atomic masses for the 1p shell and 2s-1d shells respectively. One should also note that, although the signs of the potentials are, for the most part, undetermined in DWBA calculations, they are completely specified in Table 5.

Tensor Results and Calculations in DWBA

Since a $\tau_1 \cdot \tau_2$ isospin dependence has been assumed for the tensor force, scattering reactions will now be discussed for reactions which depend on the corresponding central strengths, V_{01} and V_{11}, but do not depend on the V_{00} and V_{10} strengths. If the results of the effective matrix element fits are reliable, then one would not expect to see any effect of a tensor force in scattering where the very large V_{00} strength would predominate even if some other isospin dependence were assumed.

(p, n) reactions in C^{14}, N^{15}, O^{17}, and O^{18} have previously been investigated by means of a central two-body force (4). A comparison of these results will now be made with calculations which include the tensor force. A note on some technical problems is in order at this point. Nearly all the DWBA calculations with a tensor force have been done on the CDC 3300 computor at Oregon State University. However, because of the limited size of this machine a complete DWBA program for it does not exist at present. In order to do the calculations,

distorted waves were first computed by the DRC probram (15) at Lawrence Radiation Laboratory. These distorted waves were stored on punched cards and magnetic tape. DWBA form factors were then computed and combined with the stored DRC distorted waves on the Oregon State machine, with a program called DWBA, to produce total and differential inelastic scattering cross sections. This procedure allowed parameter variations of the form factors, but the distorted waves, once computed, could not be altered. An additional difficulty which involves a variable mesh size in DRC integrations, hampered precise calculations. In order to insure meaningful results, differential cross sections were calculated with both the DRC program and the DWBA program which used the DRC distorted waves. The differential cross sections calculated by the two methods agreed, point by point, in nearly all cases to within 5% when the same parameters were used in both codes for the calculation of the form factors and with the curves normalized to one-another. In addition, a comparison of the cross sections showed that the results of the DWBA code were consistently big by 10-20%. One test was made in which the mesh size difficulties were removed to be certain that the source of the discrepancies was understood. Agreement was good in that case.

Table 6 displays the effect of a tensor force for a number of reactions discussed in Reference (4). The central strengths, V_{01} and V_{11} are set equal to 7. MeV and the tensor force is varied from 0.

Table 6. Total (p, n) cross sections calculated with a tensor force included. The two central strengths, V_{01} and V_{11}, are both 7. MeV. The inverse central and tensor ranges are $a_C = .715$, $a_T = .715$ and $\beta_T = 4.$ fm^{-1}.

E_p	Target nucleus	Transition	II'L	$V_T=0$	$V_T=7.$	$V_T=14$		Exp
13.7	C^{14}	$0^+ \rightarrow 1^+$ (3.95)	110	37.0	36.1	35.2		
			112	.02	2.2	9.6		
			total	37.0	38.3	44.8		~35
18.8	N^{15}	anal.	000	5.95	5.95	5.95		
			110	1.98	1.93	4.36		
			112	.89	.06	.67		
			total	8.82	7.94	10.98		~15
18.8	N^{15}	$\frac{1}{2}^{(-)} \rightarrow \frac{3}{2}^{(-)}$ (6.15)	110	12.72	14.36	16.28		
			112	.09	1.02	3.32		
			202	.52	.52	.52		
			212	.79	2.32	4.86		
			total	14.12	18.22	24.98		~11
13.5	O^{17}	anal.	000	10.79	10.79	10.79		
			110	15.11	14.27	13.72		
			112	.23	.27	1.91		
			202	1.13	1.13	1.13		
			312	2.03	1.52	1.26		
			total	29.29	27.98	28.81		~50
							$V_T=-14$	
11.7	O^{18}	$0^+ \rightarrow 1^+$ (g.s.)	110	21.00	19.07	17.58	26.20	
			112	.33	.38	2.68	7.00	
			total	21.33	19.45	20.26	33.20	~10

to 14. MeV for each transition. These strengths were picked only for comparison purposes. Optimum values for the central strengths were determined in Reference (4). Also, recall that the calculated cross sections are somewhat too big. In particular, the C^{14} cross section, calculated by the DWBA program, is about 20% high while the rest are about 10% high or less. The inverse central range used was $\alpha = .715\ fm^{-1}$. The inverse tensor ranges (see Chapter III for the form of the tensor force) used were $\alpha_T = .715\ fm^{-1}$ and $\beta_T = 4.\ fm^{-1}$. The value used in Reference (4) for V_{11} is 7. MeV for an inverse range $\alpha = .715\ fm^{-1}$. A tensor strength, $V_T \approx 14.$ MeV is comparable to the Visscher-Ferrell tensor strength and to the tensor strength found by fitting the effective matrix elements related to the low-lying states in the $A = 14$ system. Therefore, the strengths used in Table 6 are of reasonable magnitude. The total, spin, and orbital angular-momentum transfers I, I', and L are also given.

A strength of $V_T = 7.$ MeV produces very little change in any of the total cross sections. A strength of $V_T = 14.$ MeV does produce some effect, notably in the $N^{15}(\frac{1}{2}^- \rightarrow \frac{3}{2}^-)$ transition. Two general properties of the tensor force can be seen in Table 6. First, only spin transfers $I' = 1$ are allowed since the spin operators in the tensor force are of rank 1. Secondly, note that the effect of the tensor force compared to the central force is much greater for the $L = 2$

transitions. In particular, this effect is very apparent in the $C^{14}(p,n)$ transition to the 3.95 MeV state in N^{14}.

Figures 1-5 display angular distributions for the reactions in Table 6. For each reaction, the experimental angular distribution is displayed, together with DWBA fits for two values of the tensor strength, $V_T = 7.$ and 14. MeV. The central strengths, V_{01} and $V_{11'}$ are still set equal to 7. MeV. For each figure the $V_T = 0.$ case is displayed by a dotted line, while the $V_T = 14.$ MeV case is shown by a dot-dashed curve. I, I', and L, which are the total, spin, and orbital angular momentum transfers respectively, are also noted. For example in Figure 2, for the $N^{15}(\frac{1}{2}^- \rightarrow \frac{1}{2}^-)$ transition, the $V_T = 0$ case is displayed for two sets of (II'L) which give identical angular distributions. Namely, (II'L) = (000) and (110). The angular distribution for the $V_T = 14$ MeV case is the incoherent sum of contributions from (II'L) = (000) and (110). For this latter case, the individual angular distributions are not identical. In all the figures, only the important (II'L) sets have been shown.

For the $C^{14}(0^+ \rightarrow 1^+)$ (p, n) reaction at 3.95 MeV excitation, and for the two (p, n) reactions in N^{15}, the $\frac{1}{2}^- \rightarrow \frac{1}{2}^-$ and the $\frac{1}{2}^- \rightarrow \frac{3}{2}^-$ transitions, the $V_T = 0$ DWBA fits are in qualitative agreement with experiment as was discussed in Reference (4). The inclusion of a $V_T = 14.$ MeV tensor force does not drastically change this conclusion. Although the $N^{15}(\frac{1}{2}^- \rightarrow \frac{1}{2}^-)$ fit is made worse at zero

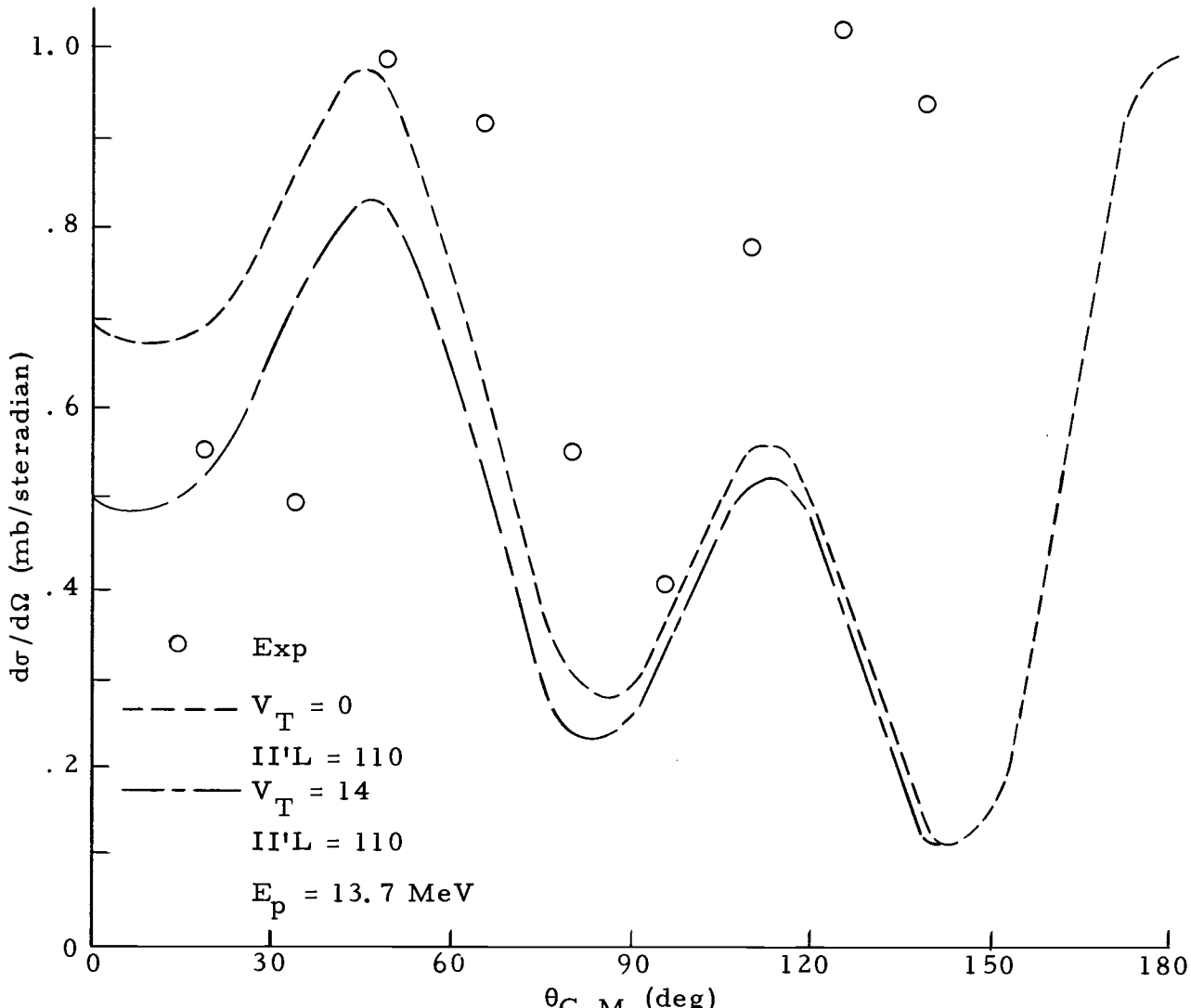

Figure 1. Tensor results for C^{14}(p, n) 3.95 MeV.

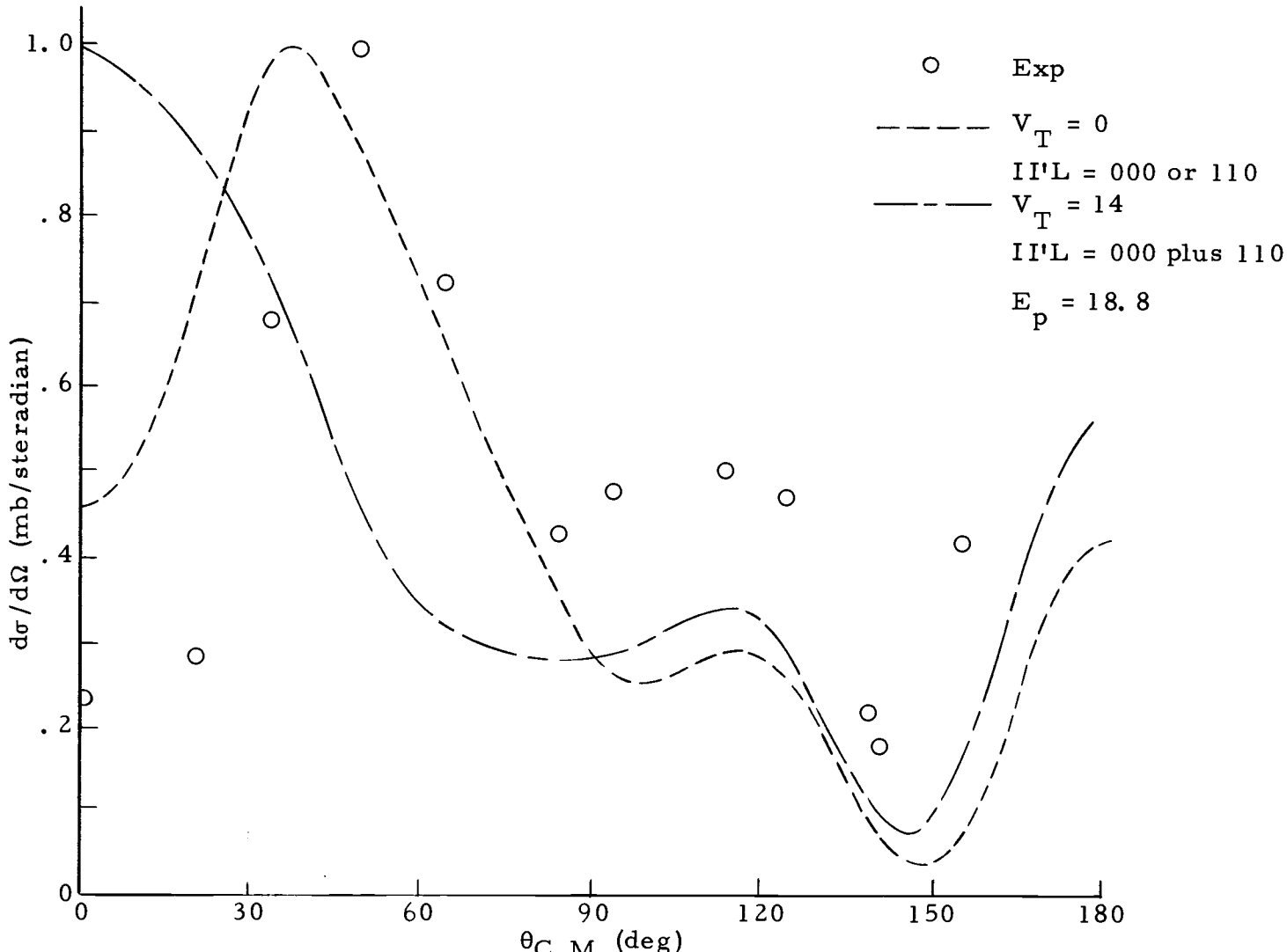

Figure 2. Tensor results for N^{15}(p, n) (anal.).

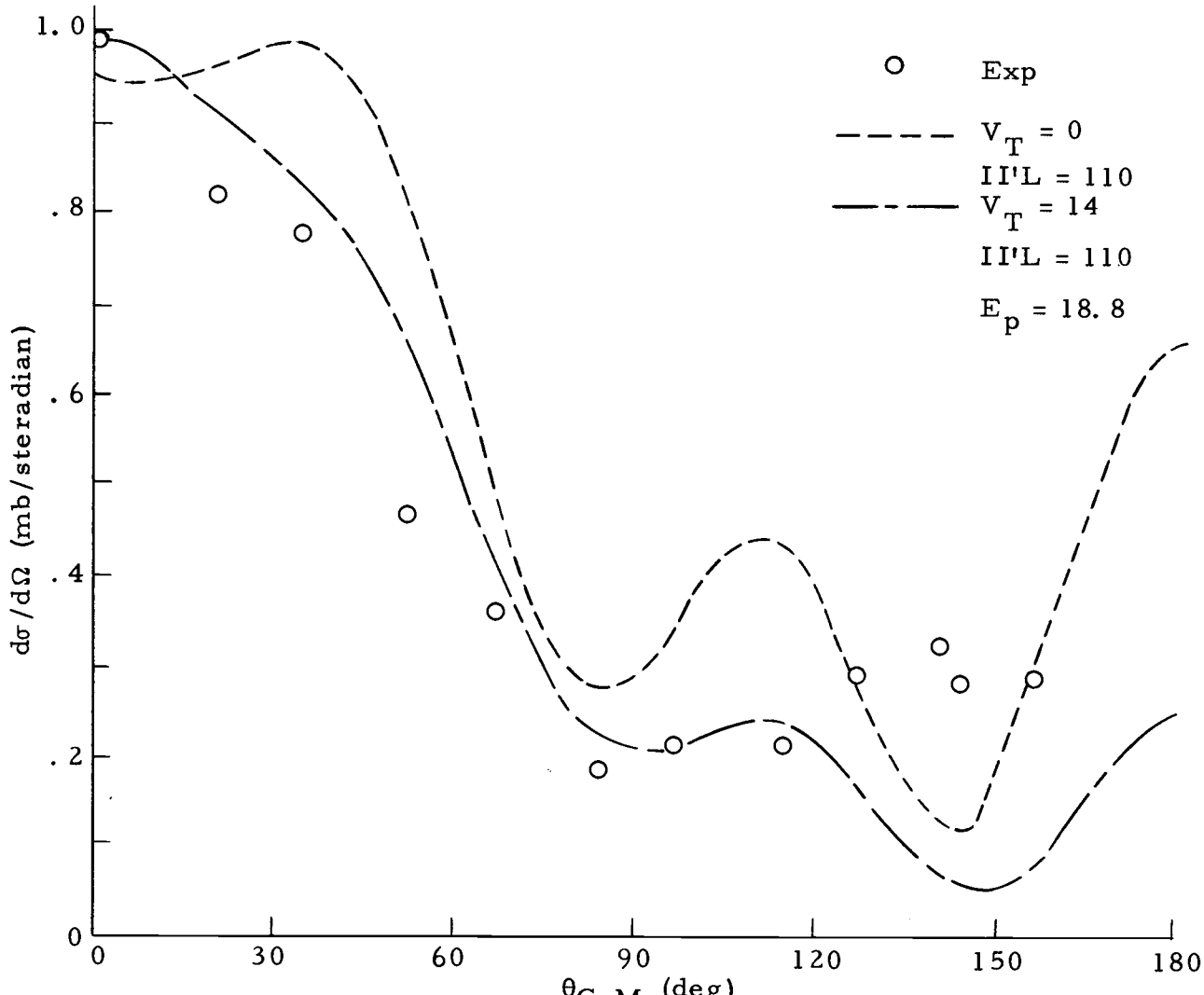

Figure 3. Tensor results for $N^{15}(p, n)$ $(\frac{1}{2}^- \rightarrow \frac{3}{2}^-)$.

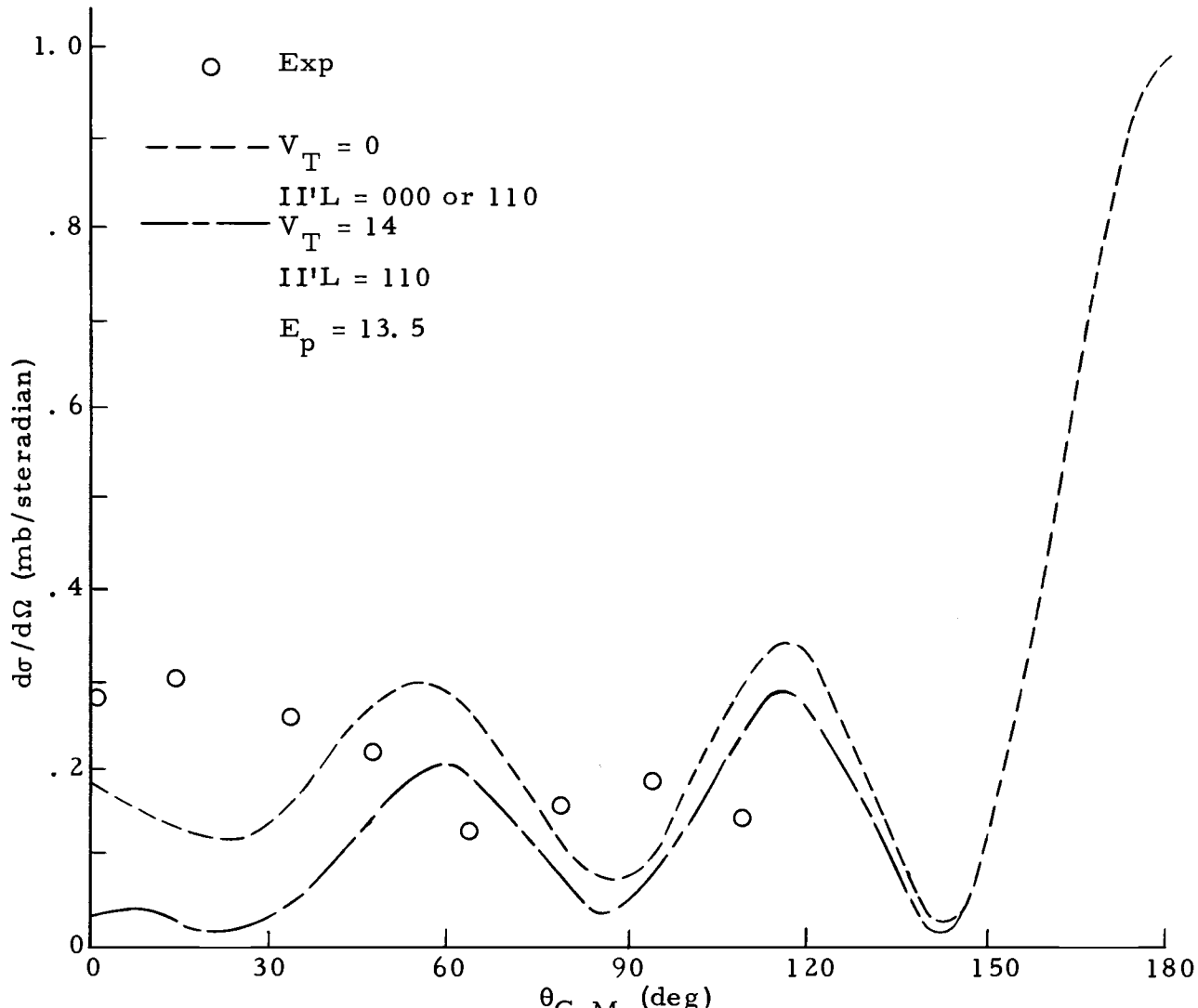

Figure 4. Tensor results for O^{17}(p, n) (anal.).

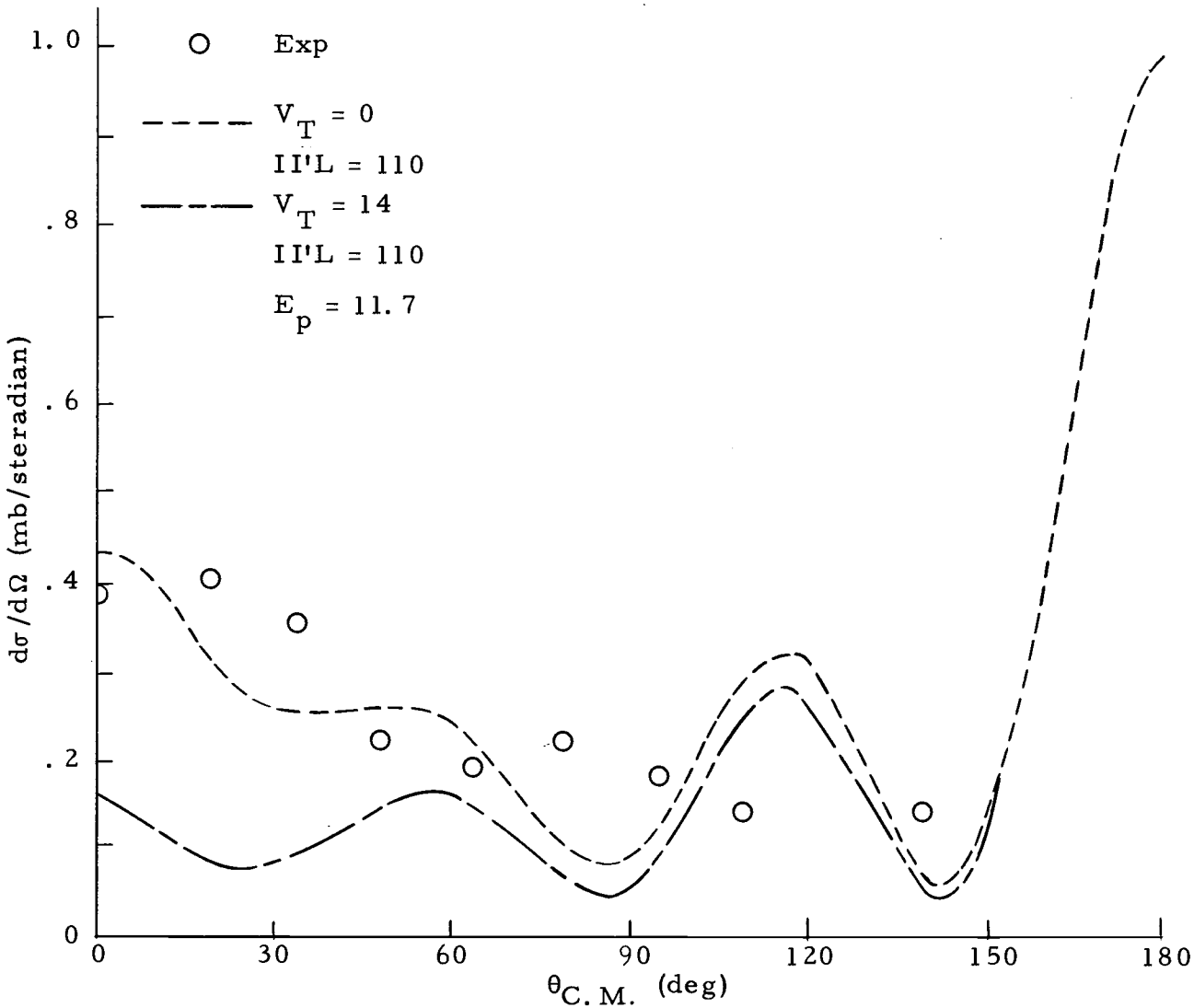

Figure 5. Tensor results for O^{18}(p, n) (g. s.).

degrees.

For the O^{17} and O^{18} reactions, the $V_T = 0$ MeV cases fit the data very badly, a fact already noted in Reference (4). In these cases also, the introduction of a tensor force does not change the nature of the theoretical fits. These fits have all been calculated with the use of distorted waves calculated by the DRC program which does not include a spin-orbit interaction in the distorting potential. The effect of a spin-orbit potential in these reactions is discussed in Reference (4). It is found that the spin-orbit effect produced a noticeable improvement in the oxygen angular distributions. At the same time, the effect is small in the C^{14} and N^{15} calculations which were in better agreement with experiment in the first place.

In general then, the effect of the tensor force in DWBA calculations does not give any consistent improvement. Although, there are some changes in the calculated angular distributions, these changes are not large compared to the overall discrepancies in the fits. The same result is true for the total cross sections. These conclusions are analogous to those found for the structure calculation. Namely, the tensor force does not give consistent improvement for a range of nuclei. Again, as was the case for nuclear structure, this result does not imply that the tensor force is negligible. However, one must look for special cases where the tensor force might be expected to have a more pronounced effect. Such a case will now be examined.

If a central force is assumed for the two-body inelastic scattering operator in a DWBA calculation, then the C^{14} beta-decay transition and the C^{14}(p, n) ground state transition are both produced by the same spin-flip, isospin-flip operator, $\vec{\sigma}\,\vec{\tau}$ (41). However, the same cancellation which produces the small beta-decay rate, implies a small quasi-inelastic scattering cross-section. The experimental cross section is reduced compared to what one would expect if there was no cancellation, but not to the degree predicted. This cancellation of the central force contribution to the (p, n) reaction makes the C^{14}-N^{14} ground state transition an ideal case in which to look for the effects of a tensor force. Actually, because of the spatial dependence of the scattering operator, assumed in this work to be a Yukawa for the central force, the cancellation only occurs completely for zero orbital angular momentum transfers, $L = 0$. Nevertheless, the $L = 2$ multipole, the only other one possible in this case, does not contribute a sufficient amount to explain the experimental cross section without the use of a potential strength which is large compared to the strength needed for other reactions. Also, the angular distribution predicted by the $L = 2$ part of the central force is very poor (4).

The effect of a tensor force will now be examined for the C^{14}(p, n)N^{14} ground state transition, as well as, two other reactions, the $C^{14}(He^3, t)N^{14}$ ground state transition and the N^{14}(p, p')N^{14}

transition to the 2.31 MeV first excited state in N^{14}. The 2.31 MeV state is the analog of the C^{14} ground state, so that the (p, p') reaction is analogous to the (p, n) reaction. These reactions have all been analysed before in terms of a central force DWBA theory[2] (6, 41).

The C^{14}(p, n) and N^{14}(p, p') reactions will be examined first. As in Table 6, a strength $V_{11} = 7.$ for $\alpha = .715$ fm^{-1} was assumed as a basis for comparison. Table 7 displays the total cross sections for $V_T = 0.$, 7., and 14. MeV for both $L = 0$ and 2. For both the (p, n) and (p, p') reactions, a definite improvement is obtained in the total cross section compared to experiment when V_T is non-zero. As noted in Reference (4), in order to obtain agreement with experiment for $V_T = 0$ a value $V_{11} = 22.$ MeV is required. (The computed values in Table 7 for the total cross sections are 10-20% high as noted earlier for Table 6.) This value for V_{11} is clearly out of line compared to the more normal reactions in Table 6. Possible quadrupole enhancement could account for some of the discrepancy; however, in Reference (4) it was shown that the value $V_{11} = 22.$ MeV is high even compared to other $L = 2$ transitions. The tensor force does not help as much in the (p, p') transition. If $V_T = 0$, then $V_{11} = 14.$ MeV is needed to obtain experimental agreement. This value was obtained under the assumption that the

[2] Private communication from S. M. Austin.

Table 7. Tensor force in the $C^{14}(p, n)N^{14}$ ground state transition and the $N^{14}(p, p')N^{14}$ (2.31 MeV) transition. The ranges and strengths are the same as for Table 6.

E_p	Target nucleus	Transition	II'L	$V_T=0$	$V_T=7.$	$V_T=14$	Exp
13.7	C^{14}	$0^+ \rightarrow 1^+$ (g. s.)	110	0	3.66	14.55	
			112	2.50	1.08	2.46	
			total	2.50	4.74	17.01	~18
24.5	N^{14}	$1^+ \rightarrow 0^+$ (2.31)	110	0	.407	1.62	
			112	.294	.121	.26	
			total	.294	.528	1.88	~.7-1.0

N^{14} calculated cross section is too large by the same factor as for C^{14}. The smaller value, $V_{11} = 14.$ MeV, for the (p, p') reaction compared to $V_{11} = 22.$ MeV for the (p, n) reaction might be taken as an energy dependence of V_{11}, since the (p, p') reaction is at nearly twice the energy of the (p, n) reaction. The inclusion of the tensor force, however, removes any need for the implied energy dependence of V_{11}, in agreement with the conclusions by Locard et al. (25). Recent data for the C^{14}(p, n) ground state transition at 18 MeV incident proton energy seems to agree favorably with the N^{14} (p, p') results.[3]

Figures 6 and 7 display experimental and theoretical angular distributions for the reactions discussed in the previous paragraph. The theoretical curves are given for $V_T = 0,\ 14,$ MeV and $V_{11} = 7.$ MeV. For both reactions, there is a big improvement in the fit with the inclusion of a tensor force. The fit is still not outstanding however, and its significance is in doubt. An interesting point is that the $V_T = 14$ MeV, $L = 2$ angular distribution for the C^{14}(p, n) reaction fits the data nearly perfectly. However, as seen in Table 7, the $L = 2$ contribution is small compared to the $L = 0$ contribution for $V_T = 14.$ MeV, and its effect should not be seen.

Ball has measured cross sections and angular distributions for

---

[3] Private communication with J. D. Anderson.

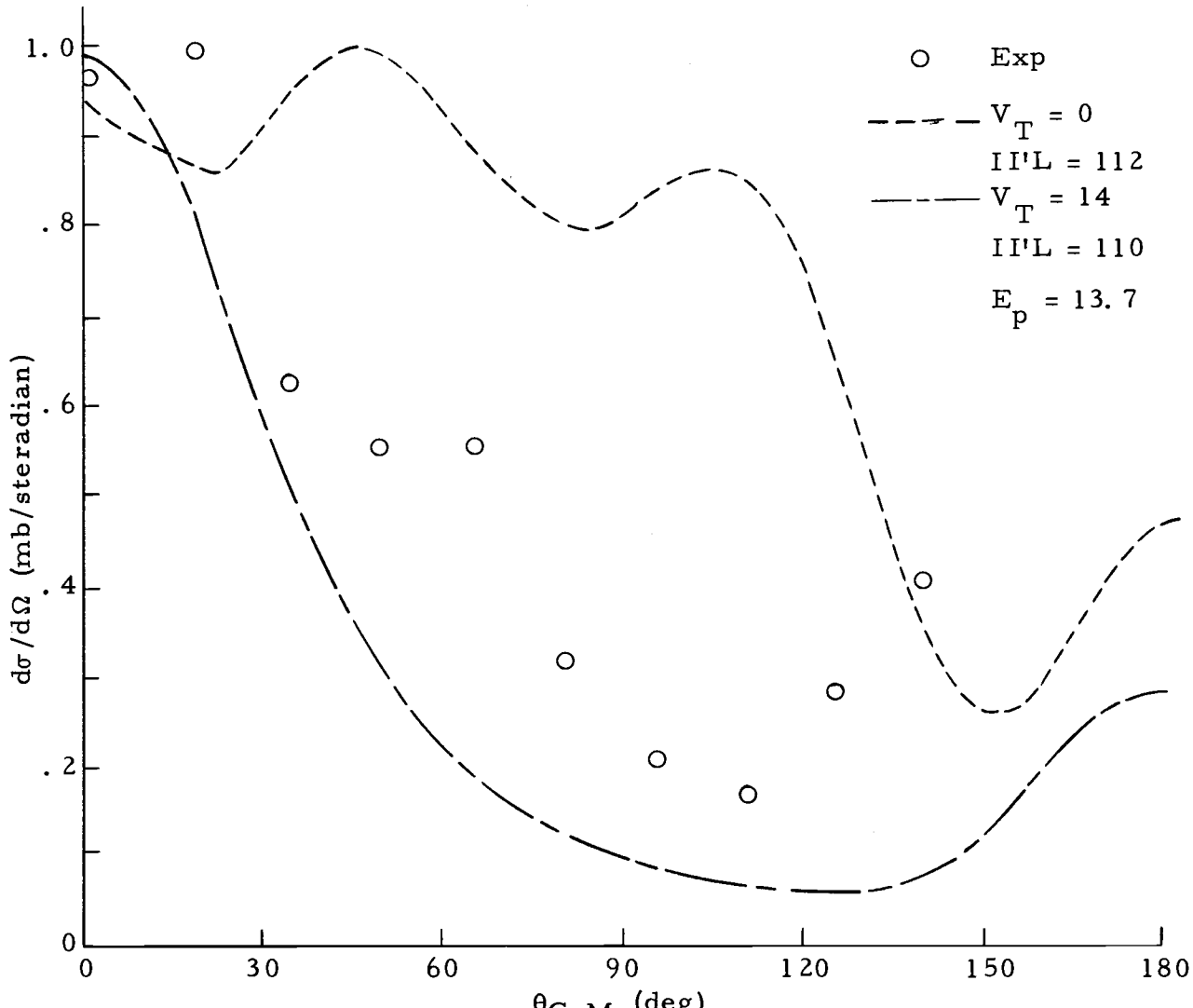

Figure 6. Tensor results for C^{14}(p, n) (g. s.).

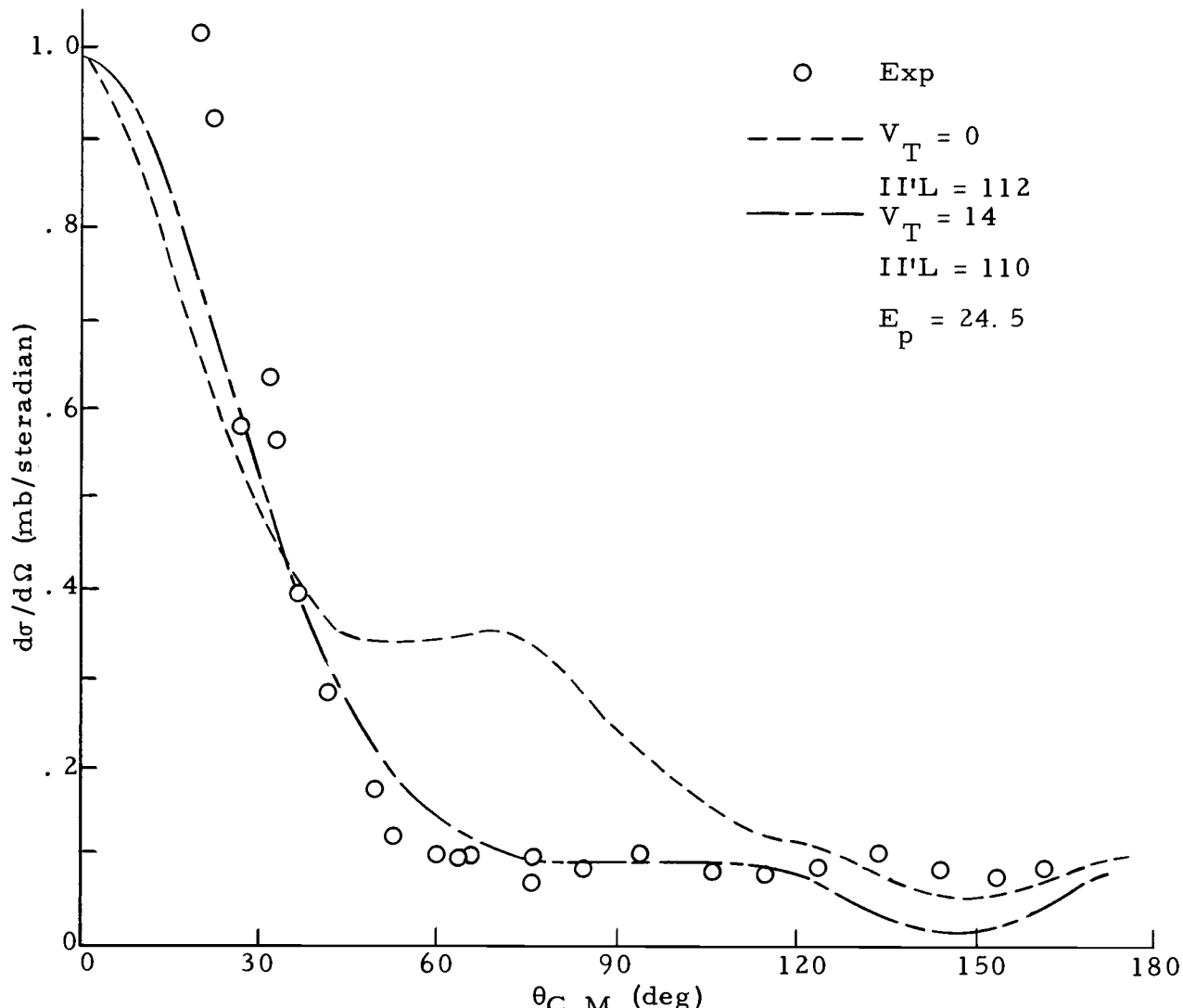

Figure 7. Tensor results for $N^{14}(p, p')$ (2.31).

the $C^{14}(He^3, t)\, N^{14}$ ground state transition and the $N^{14}(He^3, He^{3\prime})N^{14}$ transition to the first excited state corresponding to the (p, n) and (p, p') reactions just discussed (6). He has also examined the analogous reaction to O^{14}, the $N^{14}(He^3, t)O^{14}$ ground state transition. Incident He^3 energies were about 45 MeV. Total cross sections for the three reactions are mutually consistent, and the angular distributions are very similar. A central force DWBA fit to the $C^{14}(He^3, t)$ reaction did not fit the data (6). For all three reactions, he found that $V_{11} = 24 \pm 1$ MeV corresponding to $\alpha = 1.\ fm^{-1}$. If $V \propto \alpha^3$ is assumed, the strength corresponding to $\alpha = .715\ fm^{-1}$ is $V_{11} \sim 9.$ MeV. This value does not seem large. However, it is more meaningful to compare this value with other values obtained from his He^3 reactions. From Table 4, one sees that V_{11} is ≈ 16.5 MeV for transitions in the p shell corresponding to $\alpha = 1.\ fm^{-1}$. Thus, by this standard, the above value of $V_{11} \approx 24.$ MeV is considerably enhanced.

Tensor force calculations were made for the $C^{14}(He^3, t)$ reaction at 44.8 MeV. As in previous discussion, the calculations were done for $V_{11} = 7$ MeV with $V_T = 0$ and 14 MeV. The results, shown in Figure 8, are discouraging. The central force fit has its minimum more than 10° too early. This difficulty has already been noted by Ball (6). The fit with the tensor force is also bad. A smaller value of the tensor force was tried and gives a result intermediate

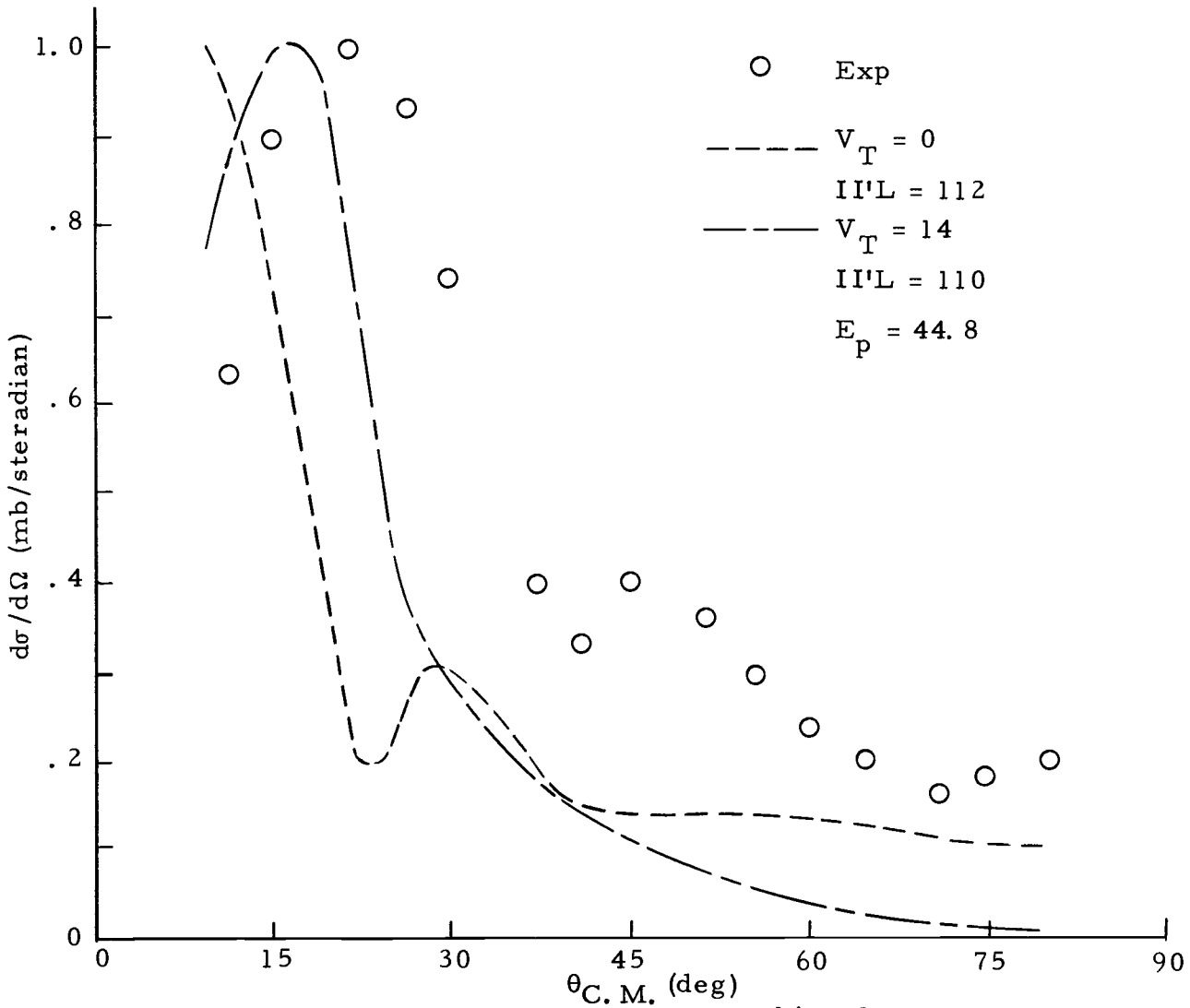

Figure 8. Tensor results for $C^{14}(He^3, t)$ (g. s.).

to those shown. The effect of the tensor force on the total cross section is very similar to the results for the (p, p') and (p, n) reactions already discussed. For $V_T = 7.$ and 14. MeV, the total cross section is increased by the factors 1. 37 and 4. 04 respectively. These increases are enough to obtain the experimental cross sections without any assumption of $L = 2$ enhancement.

Exchange Calculations and Results

Exchange effects will now be studied for the C^{14} and O^{18}(p, n) reactions which have just been discussed. A detailed discussion of exchange in DWBA has been given by Amos, Madsen, and McCarthy (3). They include contributions of the knockout term in addition to the usual direct term calculated in a direct reaction theory. They give the following expression for the inelastic scattering amplitude:

$$M = N \left\langle \chi_f^{(-)}(0) \Phi_{J_f}^{M_f}(\xi_o) \middle| V(0,1) \middle| \chi_i^{(+)}(0) \Phi_{J_i}^{M_i}(\xi_o) \right\rangle$$

$$- N \left\langle \chi_f^{(-)}(0) \Phi_{J_f}^{M_f}(\xi_o) \middle| V(0,1) \middle| \chi_i^{(+)}(1) \Phi_{J_i}^{M_i}(\xi_1) \right\rangle \qquad (5.7)$$

where the first term is the usual direct reaction amplitude, and the second term is the knockout term. N is the number of target nucleons. $\chi_i^{(+)}(0)$ is the incident distorted wave described by space, spin and isospin coordinates, $\vec{r}_0$, $\vec{\sigma}_0$, $\vec{\tau}_0$. $\Phi_{J_i}^{M_i}(\xi_o)$ represents the

target state described by co-ordinates 1 through N excluding the 0 co-ordinates. The co-ordinates 1 and ξ_1 have analogous meanings. V(0, 1) is a central two-body potential with arbitrary exchange.

$$V = \sum_{S,\,T=0}^{1} W_{ST} P_{ST}$$

where the P_{ST} are the singlet or triplet and even or odd state projectors and the W_{ST} are the corresponding strengths. In terms of previous notation,

$$(P_{10}, P_{01}, P_{11}, P_{00}) \equiv (P_{TE}, P_{SE}, P_{TO}, P_{SO}).$$

W_{ST} should not be confused with V_{ST} used earlier, where the V_{ST} referred to spin and isospin-flip strengths. In particular,

$$\begin{aligned} V &= W_{10} P_{TE} + W_{01} P_{SE} + W_{11} P_{TO} + W_{00} P_{SO} \\ &= V_{00} + V_{10}(\vec{\sigma}_1 \cdot \vec{\sigma}_2) + \vec{\tau}_1 \cdot \vec{\tau}_2 (V_{01} + V_{11} \vec{\sigma}_1 \cdot \vec{\sigma}_2). \end{aligned} \tag{5.8}$$

For definite total, spin, and orbital angular momentum transfers (I, I', L) and isospin transfer τ, the differential cross section for transitions from state i to state f is proportional to the square of a sum of single-particle transition amplitudes.

$$\frac{d\sigma}{d\Omega} \approx \sum_{M} \left| \sum_{\substack{j_1 j_2 \\ \tau}} C_{i\to f}^{j_1 j_2}(II'L,\tau) \sum_{TS} D_{i\to f}^{TS}(I'\tau) W_{ST} \right.$$

$$\left. \times \left[F_{LM}^{j_1 j_2} - (-)^{T+S} G_{LM}^{j_1 j_2} \right] \right|^2 \qquad (5.9)$$

j_1 and j_2 denote single-particle states in the initial and final nucleus respectively. j_i includes the usual (nlj) single-particle quantum numbers. The $C_{i\to f}^{j_1 j_2}$ contain configuration-mixing coefficients which describe the nuclear states. Both the $C_{i\to f}^{j_1 j_2}$ and $D_{i\to f}^{j_1 j_2}$ contain various coupling coefficients, which give rise to various selection rules mentioned later. See Reference (3) for details. W_{ST} are the potential strengths defined above. $F_{LM}^{j_1 j_2}$ is proportional to the usual single particle transition rate. For a Wigner force,

$$F_{LM}^{j_1 j_2} \approx \left\langle \chi_f^{(-)}(\vec{r}_0) \middle| Y_{LM}(\hat{r}_0) g_L^{j_1 j_2}(r_0) \middle| \chi_i^{(+)}(\vec{r}_0) \right\rangle \qquad (5.10)$$

where the χ's are the distorted waves and $g_L^{j_1 j_2}$ is the single-particle form factor. $G_{LM}^{j_1 j_2}$ is the corresponding amplitude which arises from the knockout term of the DWBA amplitude. It is defined to be equal to $F_{LM}^{j_1 j_2}$ in the limit of zero range.

As mentioned already the $C_{i\to f}^{j_1 j_2}$'s and $D_{i\to f}^{j_1 j_2}$'s in Equation (5.9) give rise to selection rules, just as for non-exchange scattering.

Some of these are the following:

$$\Delta(IJ_iJ_f), \quad \Delta(I', S, S), \quad \Delta(II'L), \quad \Delta(\tau T_i T_f)$$

where I I', L, and τ are the total, spin, oribtal, and isospin transfer quantum numbers respectively. J_i and J_f are the initial and final nuclear spins, while T_i and T_f are the initial and final isospin quantum numbers. S is the projectile spin. Δ indicates that a triangle relation must be satisfied. Three reactions will be considered, each of which is from $J_i = 0$, $T_i = 1$ to $J_f = 1$, $T_f = 0$, the $O^{18}(p, n)$ ground state transition and the $C^{14}(p, n)$ transitions to the ground and second excited states of N^{14}. The above selection rules imply $I = \tau = 1$. In addition, I' and L may have the following values:

I'	L
0	1
1	0
1	1
1	2

Parity requires that for the direct terms in the 1p shell, only $L = 0$ and 2 are allowed. This rule arises from a nuclear one-body matrix element which has 1p initial and final bound states.

The same procedure was used for both the O^{18} and C^{14} reactions. Total and differential cross-sections were calculated for both the direct and exchange terms alone. These cross sections were also

calculated for the case where the direct and exchange terms contribute coherently. Only even components of the force have been considered, that is, where the phase between $F_{LM}^{j_1 j_2}$ and $G_{LM}^{j_1 j_2}$, $(-)(-)^{T+S}$, is positive. In particular, the even strengths were chosen equal and the odd strengths were 0.

$$W_{10} \equiv V_{TE} = -56.\ \text{MeV} \quad W_{11} \equiv V_{TO} = 0. \tag{5.11}$$

$$W_{01} \equiv V_{SE} = -56.\ \text{MeV} \quad W_{00} \equiv V_{SO} = 0. \tag{5.12}$$

These values correspond to $V_{01} = V_{11} = 7.$ MeV where as before, V_{01} and V_{11} are the strengths of $\vec{\tau}_1 \cdot \vec{\tau}_2$ and $(\vec{\sigma}_1 \cdot \vec{\sigma}_2)(\vec{\tau}_1 \cdot \vec{\tau}_2)$. Calculations, that are referred to as direct or exchange alone, were done by setting either $G_{LM}^{j_1 j_2}$ or $F_{LM}^{j_1 j_2}$ to zero respectively.

The effect on the angular distributions of varying the range of the potential was studied for both the direct and exchange contributions independently. Figures 9-14 display, in pairs, these angular distributions for three transitions, the $L = 0$ $O^{18}(p, n)$ ground transition, and the $(L = 0$ and $2)$ contributions to the $C^{14}(p, n)$ transition to the 3.95 MeV state in N^{14}. Each figure displays the results for $\alpha = .5$, $.7$, and $3.$ fm^{-1}. The most striking feature is the almost complete independence of the exchange angular distributions on α. In all cases, they are very similar to the short-range direct angular distributions. (As mentioned above, the exchange and direct curves must

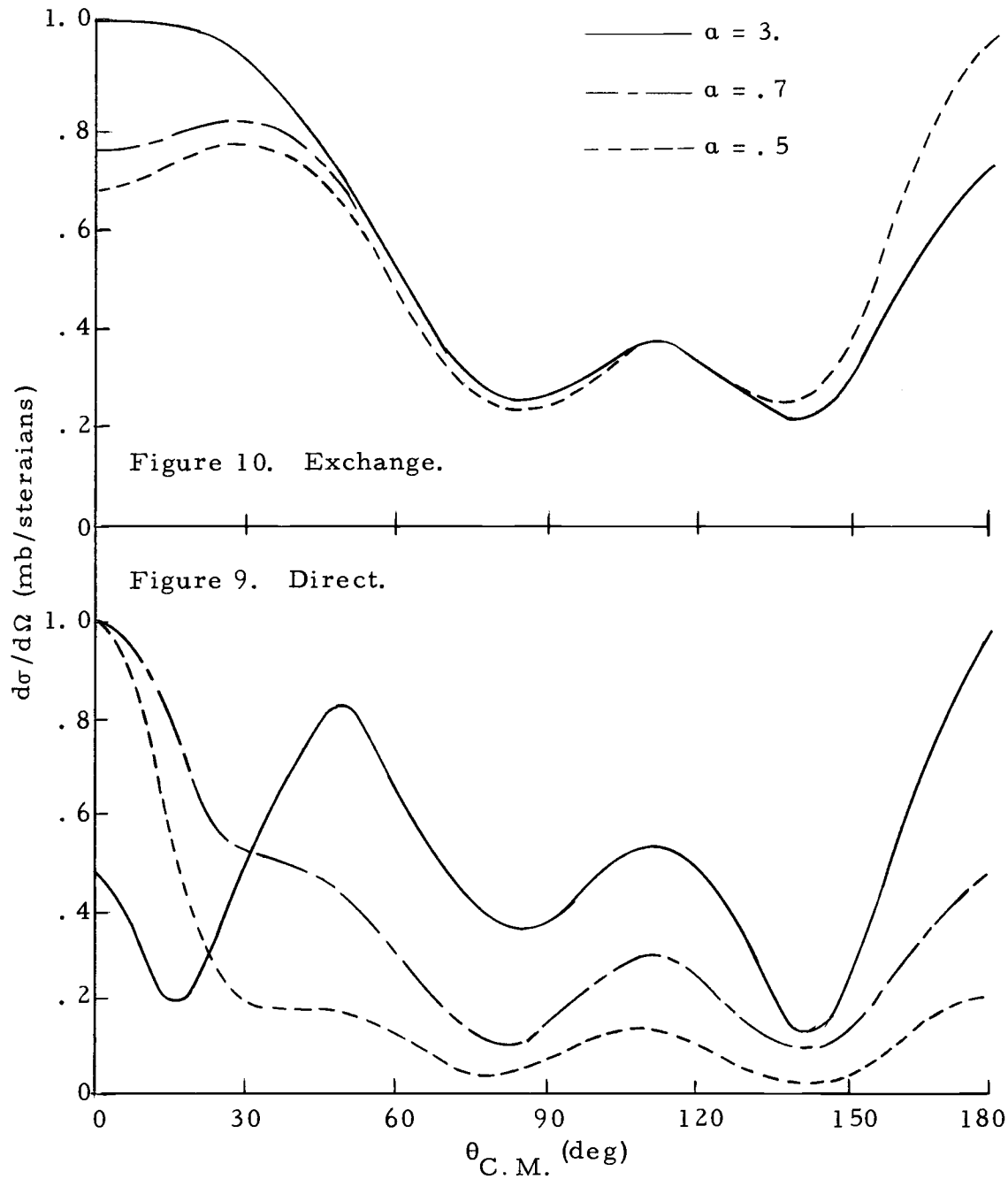

Figure 9, 10. Effect of range for direct and exchange calculations for C^{14}(p, n) (3. 95) L = 0.

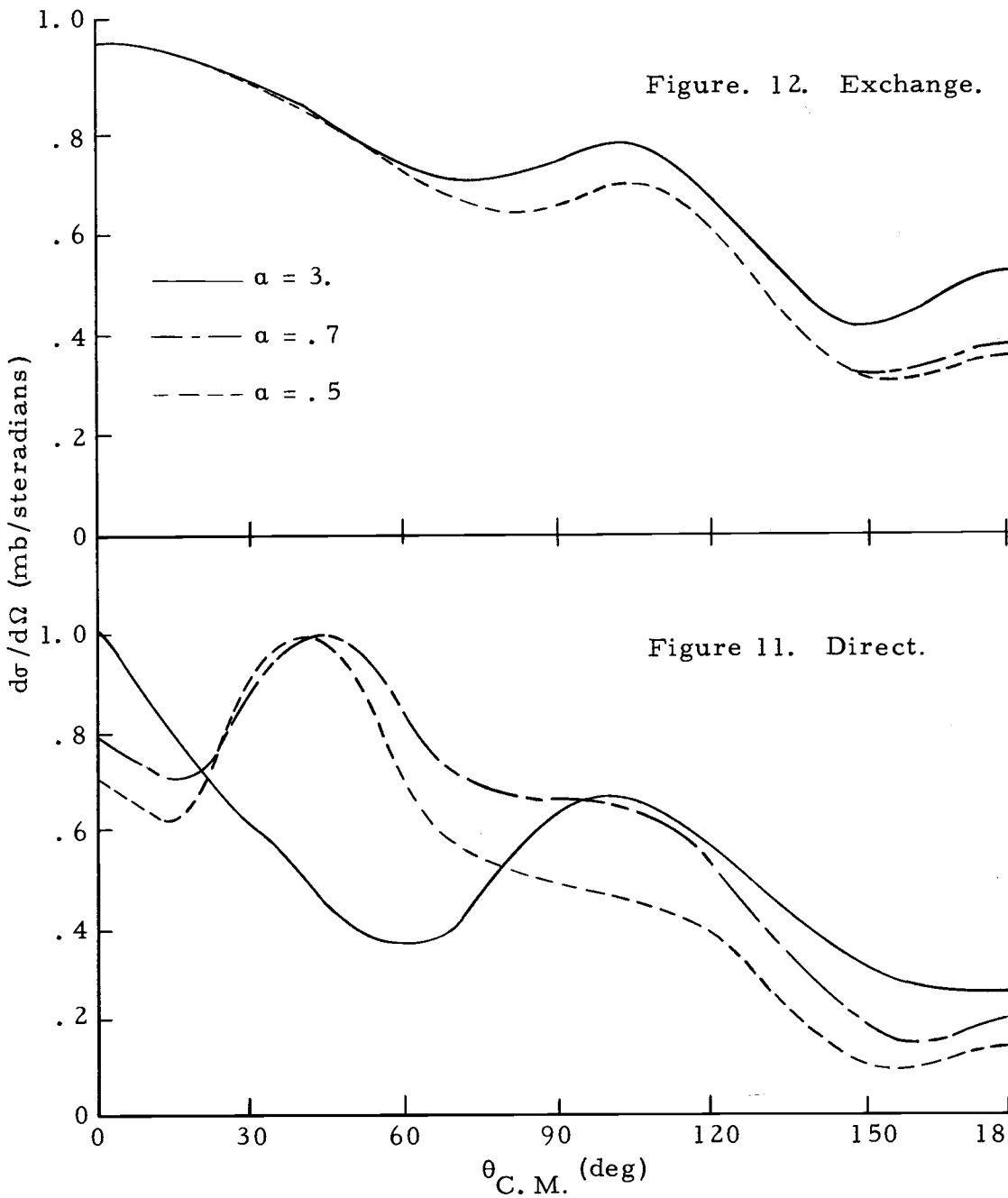

Figure 11, 12. Effect of range for direct and exchange calculations for C^{14}(p, n) (3. 95) L = 2.

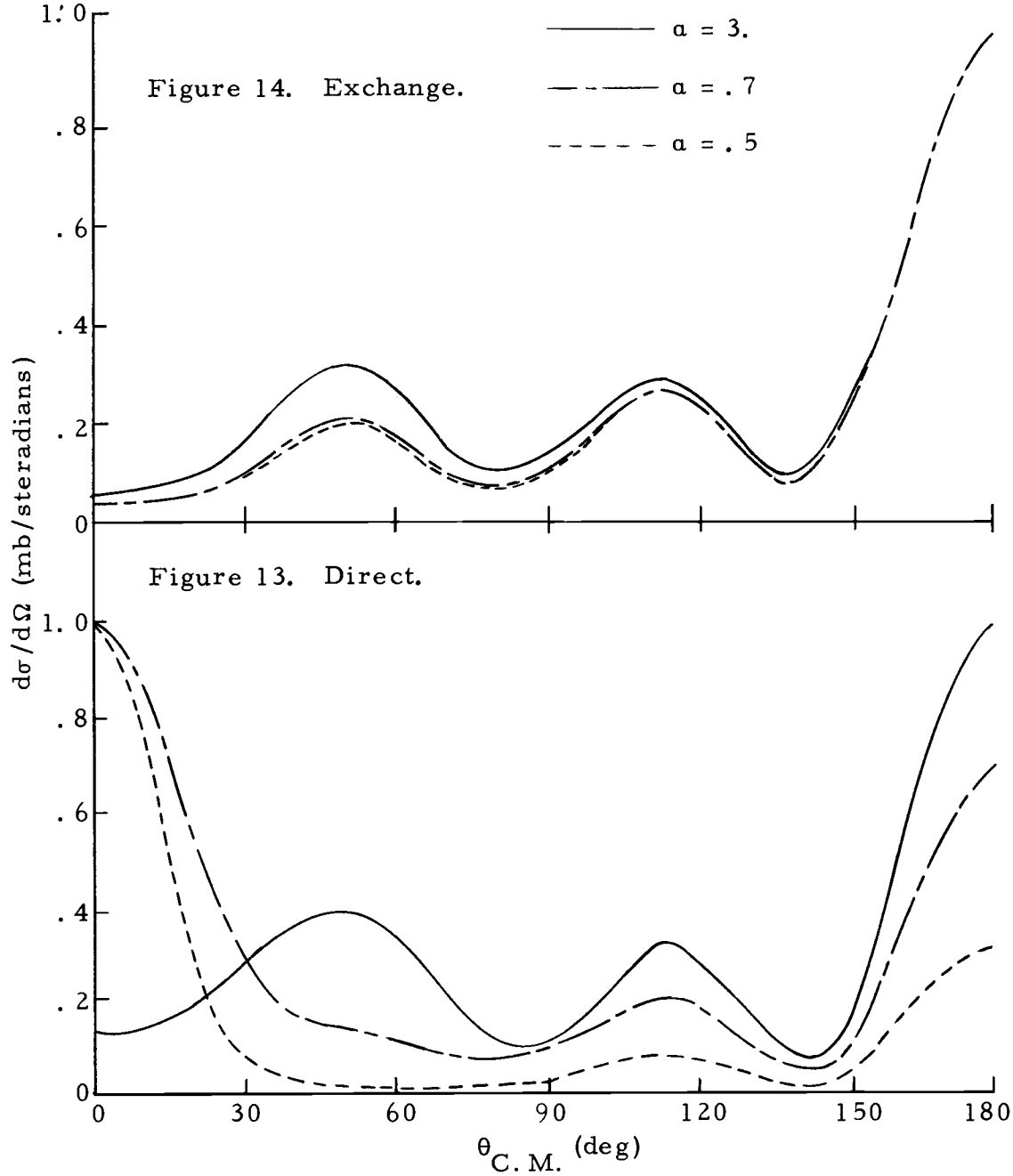

Figure 13, 14. Effect of range for direct and exchange calculations for O^{18}(p, n) (g. s.) L = 0.

be identical at zero-range.) This independence of α for the exchange curves means, that as long as the direct angular distributions are not too different from the shape they would have for short ranges, then the direct and exchange angular distributions will be similar. One sees from the figures that the direct angular distributions deviate appreciably from the short-range shapes only near 0° and 180°.

Figures 15-17 compare the angular distributions of the direct results, the exchange results, and the coherent contribution of both together for the same three reactions, the $L = 2$ $C^{14}(p, n)$ ground state transition, the $L = 0$ $C^{14}(p, n)$ transition to the 3.95 MeV state in N^{14}, and for the $L = 0$ $O^{18}(p, n)$ ground state transition. The direct, exchange, and combined results are labeled by idex = 1, 2, 3 for each curve respectively. The inverse range, α, is .7 fm^{-1}. As noted in the discussion of range dependence, the independent direct and exchange results are very similar, except near 0° and 180°. In addition, the coherent contributions of direct and exchange are close to an average of the independent contributions, which indicates that the relative phase of the direct and exchange amplitudes must be relatively constant, as well as the magnitudes being alike.

The direct angular distributions shown in Figures 15-17 differ somewhat from the results already discussed for these same transitions. First, the optical potentials used were not always the same. And second, the exchange code does not include any effect due to

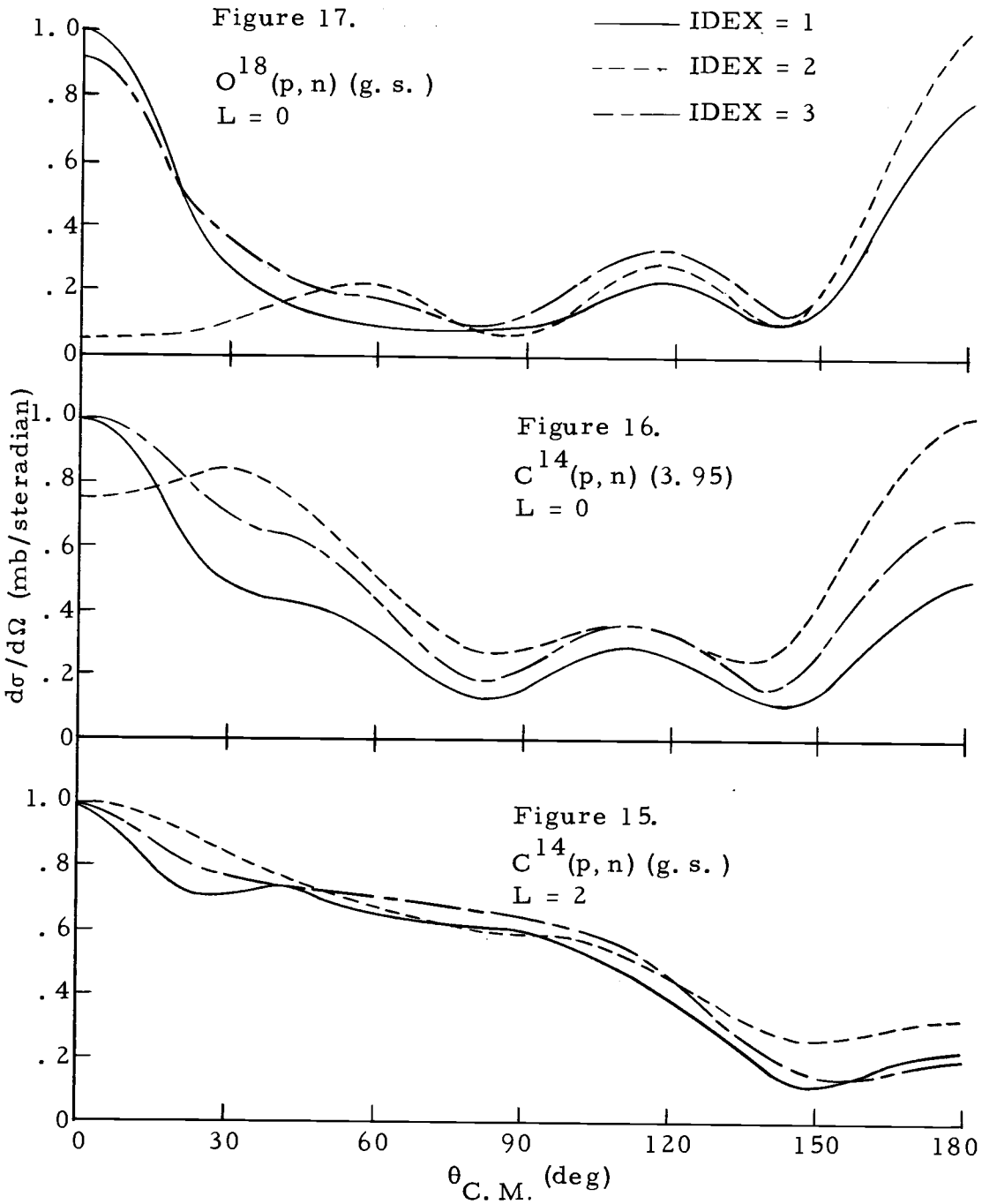

Figure 15-17. Comparison of exchange and direct angular distributions for $a = .7$ fm^{-1}.

recoil while the DRC code does.

Total cross sections have been found for all possible sets of transfer quantum numbers with the exception of $L = 1$ transfers in the $O^{18}(p, n)$ reaction. These are shown in Table 8 for the $L = 0, 2$ transitions. First note the small values of the total cross section for the $L = 0$ ground state transition in C^{14}. This point has already been mentioned for the direct term. The small result depends on the sum

$$\sum_{j_1 j_2} C_{i \to f}^{j_1 j_2}$$

being near zero in Equation 5. 9 and on the assumption that the $F_{LM}^{j_1 j_2}$ are relatively independent of j_1 and j_2 for the p shell. Thus, to the extent that the $G_{LM}^{j_1 j_2}$ are also independent of j_1 and j_2, the exchange term will also give a small result for the $L = 0$ transition.

For the normal $L = 0$ transitions, the O^{18} ground state transition, and the C^{14} transition to the 3. 95 MeV state in N^{14}, the exchange contribution is small compared to the direct. The amount is non-negligible; however, and the coherent sum of exchange and direct is appreciably enhanced over the direct value alone. Again, because $F_{LM}^{j_1 j_2}$ and $G_{LM}^{j_1 j_2}$ are equal for zero-range, the exchange is more noticeably for $\alpha = 3.\ fm^{-1}$. For the $L = 2$ transitions, the

exchange terms are more important than they are for the $L = 0$ ones.

Table 9 shows the enhancement in a quantitative fashion. Let D and E be the direct and exchange amplitudes, so that the direct and exchange angular distributions are given by $|D|^2$ and $|E|^2$ respectively. $|D+E|^2$ gives the angular distribution for the coherent sum of direct and exchange contributions. For each transition, the enhancement, α_L, may be defined by $\alpha_L^2 = \sigma_{D+E}/\sigma_D$ where $\sigma_D = \int |D|^2 d\Omega$ is the total cross section for the direct term. σ_{D+E} is defined similarly. α_L is L dependent. Average values of α_L from Table 9 are $\alpha_0 = 1.27$ and $\alpha_2 = 1.79$. Recall that these enhancements are for even forces, where V_{TO} and V_{SO} were chosen to be zero. This assumption makes the relative phase of $F_{LM}^{j_1 j_2}$ and $G_{LM}^{j_1 j_2}$, $(-)(-)^{T+S}$, equal to $+1$. The following identities allow the calculation of the cross-section for odd forces. That is, where $F_{LM}^{j_1 j_2}$ and $G_{LM}^{j_1 j_2}$ add with opposite signs.

$$|D \pm E|^2 = |D|^2 + |E|^2 \pm 2\mathrm{Re}(DE^*)$$

$$\sigma_{D+E} = \sigma_D + \sigma_E + y \qquad (5.13)$$

$$\sigma_{D-E} = \sigma_D + \sigma_E - y$$

where

$$y = \int 2\mathrm{Re}(DE^*) d\Omega \quad .$$

Table 8. Direct and exchange cross sections in the $C^{14}(p, n)$ and $O^{18}(p, n)$ reactions. Direct, exchange, and direct plus exchange cross sections are denoted by IDEX equal to 1, 2, and 3 respectively for each of three ranges, three transitions, and two orbital angular momentum transfers. Only relative magnitudes are important.

		$\alpha = .5$			$\alpha = .7$			$\alpha = 3.$		
	IDEX	1	2	3	1	2	3	1	2	3
$C^{14}(p, n)$	G. S.; L=0	3.03×10^{-3}	9.77×10^{-4}	6.42×10^{-3}						
$E_p = 13.7$	G. S.; L=2	5.18	3.95	16.93	1.542	1.354	5.42	.001856	.001969	.00761
	3.95; L=0	117.0	4.39	161.8	20.2	1.618	32.5	.00980	.00371	.0248
	3.95; L=2	.0509	.0327	.1517	.01354	.01101	.0464	1.994×10^{-5}	1.417×10^{-5}	6.547×10^{-5}
$O^{18}(p, n)$	G. S.; L=0	75.0	2.46	100.8	12.04	.828	18.7	2.65×10^{-3}	1.604×10^{-3}	8.35×10^{-3}
$E_p = 11.7$	G. S.; L=2	.802	.324	1.969	.207	.0957	.558	1.379×10^{-4}	1.120×10^{-4}	4.99×10^{-4}

Table 9. Enhancement factors, α_L and β_L, due to exchange. α_L and β_L are shown for the same transitions that appear in Table 8 for $\alpha = .7\ fm^{-1}$. (See Chapter V for a discussion of the table.)

		σ_D	σ_E	y	σ_{D+E}	σ_{D-E}	α_L	β_L
$C^{14}(p, N)$	G. S.; L=2	1.542	1.354	2.524	5.42	.372	1.876	.493
	3.95; L=0	20.2	1.618	10.68	32.5	11.14	1.269	.752
	3.95; L=2	.01354	.01101	.0218	.0464	.00275	1.851	.451
$O^{18}(p, n)$	G. S.; L=0	12.04	.828	5.83	18.7	7.04	1.246	.764
	G. S.; L=2	.207	.0957	.255	.558	.048	1.641	.482

The equation for σ_{D+E} gives a value for y which in turn can be used to find σ_{D-E}. An enhancement, β_L, for odd forces may be defined in the same fashion as for α_L. Namely $\beta_L^2 = \sigma_{D-E}/\sigma_D$. β_L is given along with α_L in Table 9. Average values for β_L are, $\beta_0 = .758$ and $\beta_2 = .475$. Just as the even forces are enhanced by α_L, the odd forces are diminished by β_L.

Earlier, the strengths V_{00}, V_{10}, V_{01}, and V_{11}, as determined from fitting effective matrix elements were compared with values obtained from DWBA fits to various scattering reactions. The two sets of strengths were given in Tables 5 and 4 respectively. Since, the exchange effects are non-negligible, at least for the reactions just studied, it is of interest to see how the inclusion of the exchange amplitudes affects the potential strengths determined from DWBA calculations. However, since almost all calculations up to the present time have not included exchange (4, 6, 25, 31, 35, 41), a different point of view will be taken. Rather than redetermine the values in Table 4 by the inclusion of exchange, a new effective force with modified strengths will be defined; such that, a direct DWBA calculation with the modified strengths will give the same results as a calculation with unmodified strengths which includes the exchange amplitude. The possibility of mocking-up the results which include exchange, by simply changing the strengths in a pure direct calculation, depends critically on the following fact: the most important effect of exchange is

to change the magnitude of the cross-section and not the angular distribution. It may be that the contribution of exchange to the total cross section will be consistent with the present results for other reactions; although, the angular distribution is not. In that case a direct calculation with altered strengths may give correct total cross sections, but not the correct angular distributions. Only calculations for a wider range of nuclei can answer the question.

The enhancements of the even and odd strengths, α_L and β_L will now be used to modify the effective potential strengths, given in Table 2, determined from the effective-matrix-element fits. These modified strengths are to be considered as effective strengths for direct DWBA calculations and can be compared directly with the results in Table 4. The procedure is the following and is applied independently to the potentials determined from both the 1p and 2s-1d shells given in Table 2. First, for each shell and the appropriate L, the even and odd strengths are multiplied by α_L and β_L respectively. These altered even and odd strengths are then normalized to a range $\alpha^{-1} = 1.$ fm. with the assumption that the even and odd strengths are proportional to $\alpha^{2.3}$ and $\alpha^{3.7}$ respectively. Finally, a transformation is made from the even-odd potential representation to the spin and isospin representation.

$$(V_{TE}, V_{SE}, V_{TO}, V_{SO}) \rightarrow (V_{00}, V_{10}, V_{01}, V_{11}).$$

The results of the enhancement by α_L and β_L are shown in Table 10 for both shells and $L = 0, 2$. Table 11 gives the results of Table 10 renormalized to $\alpha = 1.\ fm^{-1}$, and in terms of the $(V_{00}, V_{10}, V_{01}, V_{11})$ strengths.

Table 11, which contains the potential strengths determined from effective matrix elements and by the inclusion of exchange enhancement, may now be compared to Tables 5 and 4. Table 5 does not include exchange enhancement and Table 4 contains strengths determined from direct DWBA calculations. A comparison of Tables 11 and 5 shows that for the V_{10}, V_{01}, and V_{11} strengths there is very little $L = 0$ enhancement due to exchange effects in either the 1p or 2s-1d shell. For these same strengths, there is some $L = 2$ enhancement of about 20-30%. The new values of these strengths are still consistent with the experimental results in Table 4. Also increased values of V_{01} and V_{11} for $L = 2$ transitions have been noted in other studies (4, 6). The most encouraging aspect of the new values in Table 11 is the increased magnitudes for the values of V_{00} compared to the results in Table 5. In fact, in Table 5, the values of V_{00} for the two shells did not even have a consistent sign. The new values of V_{00} are still small in magnitude compared to the experimental values, but the inclusion of exchange has produced a marked improvement in the agreement. Finally, note that for the $L = 2$ transitions, V_{00} is increased far more than the other three

strengths.

The $L = 2$ enhancements just mentioned must not be confused with the usual meaning of $L = 2$ or quadrupole enhancement. The normal meaning of $L = 2$ enhancement originates in the experimental fact that E2 gamma-transition rates are, normally, many times greater than would be expected for a single-particle nuclear transition (40). This fact is explained by a collective model of the nucleus and is often described in terms of effective charges. Inelastic scattering transitions are described, in the collective model, by the same rank 2 tensor which describes the E2 transitions. And so, for those states which have enhanced E2 rates, the inelastic scattering cross-section is likewise enhanced. The enhancement discussed in the preceding paragraph, however, is not due to any property of the nucleus, but is the result of an attempt to obtain correct experimental scattering cross-sections with the use of a pure direct DWBA theory. The effect of ignoring the exchange amplitude has been absorbed by a modification of the potential strengths. This type of $L = 2$ enhancement would affect a pure single particle transition since it is not a nuclear property. At the same time, the effect is not pertinent except in the context from which it arises, specifically, in a direct inelastic scattering calculation.

A reminder and a comment which have effects on the interpretation of the strengths in Table 11 are in order. First, the meaning of

the relative strengths between the 1p and 2s-1d shell is somewhat uncertain, since this relative strength depends on the nuclear sizes chosen for the two shells. Second, in the calculation of V_{00} from the even and odd strengths, V_{00} is quite sensitive to the V_{TO} strength. A small increase in the magnitude of V_{TO} for V_{TO} positive can reduce the magnitude of V_{00} a disproportionate amount (see Appendix).

$L = 1$ contributions to the total cross-sections were calculated and are given in Table 12 for the C^{14}(p, n) reactions to the ground and to the 3.95 MeV states in N^{14}. For these transitions, $I = 1$ and $I' = 0, 1$. A comparison of these values, with the corresponding values in Table 13 for the $L = 0$ and 2 contributions, shows that the $L = 1$ values are negligible. The $L = 1$ contributions are pure exchange, since they are parity forbidden for the direct terms.

Core Polarization

The importance of core-polarization in relation to this work will now be discussed. Although the inclusion of exchange gave a marked improvement in the values of V_{00} determined from effective matrix elements, those values are still small compared to the experimental values in Table 4, determined from scattering studies. The values of V_{00} determined from effective matrix elements were about 20. and 60. MeV for $L = 0$ and 2 transitions respectively.

Table 10. Enhancement of effective potentials by α_L and β_L. Initial values are taken from rows 1 and 3 of Table 2. The even and odd strengths have been multiplied by α_L and β_L respectively for L = 0 and 2. V_{SO} was set equal to V_{TO} for 2s-1d.

		V_{TE}	V_{SE}	V_{TO}	V_{SO}
(2s-1d W-S α = .7)	Initial value	-67.7	-49.2	25.5	25.5
	L = 0	-85.1	-61.8	19.3	19.3
	L = 2	-121.1	-88.0	9.2	9.2
(1p W-S α = .71)	Initial value	-46.7	-38.7	14.0	14.7
	L = 0	-58.7	-48.6	10.6	11.1
	L = 2	-83.5	-69.2	5.0	7.0

Table 11. Values of effective strengths in Table 10 normalized to α = 1. and transformed to spin-isospin representation.

	L	V_{00}	V_{10}	V_{01}	V_{11}
(2s-1d)	0	-17.4	23.3	36.5	29.9
	2	-67.5	24.6	43.4	34.0
(1p)	0	-20.6	16.6	22.1	19.6
	2	-51.4	18.8	26.7	23.6

Table 12. Total exchange cross sections for L = 1 for the C^{14}(p, n) ground state and 3.95 MeV transitions. $V_{01} = V_{11}$ = 7. MeV. α = .7.

II'	g. s.	3.95 MeV
10	.07	.11
11	.01	.09

In the low-energy region, 10-20 MeV, the values deduced by Satchler (35) were about 150-200 MeV and even larger. These values were deduced from a range of nuclei that include (p, p') scattering from O^{18}, Zr^{90}, Ti^{50}, and Pb^{208}. Core-polarization can remove part of this discrepancy.

Often, in the calculation of transition rates or scattering cross-sections, it is assumed that only one or a few valence nucleons participate in the transition. Core-polarization is a means which implicitly includes the effect of other nucleons in the nucleus. These other nucleons are often referred to as the core. Core-polarization often takes the form of effective charges (26). If the effect of all nucleons in a nucleus could be calculated, the idea of core-polarization would not be needed. Satchler and Love (26) have recently studied the effect of core-polarization in the determination of effective potentials for inelastic scattering. They used, as a measure of the polarization, E2 transition strengths, which are normally much larger than single-particle transition rates. They find, that if core-polarization is included, the V_{00} strength may be reduced to 70-100 MeV rather than 200 MeV. With this reduction, the values of V_{00} as deduced from scattering and from effective matrix elements are in much closer agreement; although, there is still a discrepancy.

If the reduced values of V_{00}, which do not include core-polarization, are compared with values of V_{00} as deduced from

effective matrix elements, then, to be consistent, core-polarization effects should not be included in the effective matrix elements. That is, suppose effective matrix elements, which do not include any effect of core-polarization, were used to calculate wave functions from which E2 rates could be found. Then the calculated E2 rates should be too small. For the case of the 1p shell and the effective matrix elements of Cohen and Kurath, the calculated E2 rates are indeed too small. Effective charges are needed for neutrons and protons of $e_p = e(1+\beta)$ and $e_n = \beta e$ where $\beta \approx .5$ (Ref. 30). There is some justification, then, for the comparison of values of V_{00}, as deduced from effective matrix elements, with the reduced values of V_{00} found from scattering studies.

VI. COUPLED CHANNEL CALCULATIONS

To check for additional defects of the reaction theory, in the deduction of effective potentials, a coupled-channel calculation has been made for the $A = 14$ system. It was shown earlier, for example, that neglect of exchange had several important effects. DWBA is only an approximation to the coupled-channel calculation and in some cases has been shown to give markedly different results (10, 37).

Because the computer calculation is long and expensive, comprehensive surveys are impractical. The $A = 14$ system is suitable for a number of reasons. The $C^{14}(p, n)$ ground state transition is weak and, just as it was a place to look for tensor force effects, it is a place where coupling effects might be seen. A reasonable amount of scattering data is available for this system (4, 41). A set of wave functions is available which appear to adequately describe the low-lying levels (39). And finally, the number of functions, that are necessary to couple, is not large.

Four channels were coupled, the C^{14} ground state, the N^{14} ground state and the two lowest excited states in N^{14} at 2.31 and 3.95 MeV (see Figure 21). The channel description must include the state of the projectile which was a proton for the C^{14} channel and, in order to conserve charge, a neutron in the N^{14} channels. All possible couplings were included, and all diagonal coupling terms were described

by an optical potential (see Appendix). The code to calculate the off-diagonal elements is described in the Appendix, while the integration of the coupled equations was done by a code at Oregon State University.[4] This code includes spin-orbit coupling in the optical potential. Computer time for this problem is about 20 minutes on the Oregon State CDC 3300 computer.

The values chosen for V_{10}, V_{01}, and V_{11} were 7., 9.5, and 8.0 MeV respectively. These are rounded values obtained from the structure values in Table 2 for the 1p shell. The strengths were normalized for $\alpha = .715$ fm^{-1}. Also, although the effect of exchange in a coupled-channel calculation is not understood, the values were renormalized for $L = 0$ exchange contributions. This same procedure gives a value for V_{00} of -14. MeV. However, on the basis of other evidence (Table 4), $V_{00} = -60.$ MeV was used instead. V_T, taken to be 14. MeV, was picked for the tensor strength since it has been shown to give a reasonable description for the C^{14}(p, n) ground state transition (see Table 7 and discussion of the tensor force).

The first column in Table 13 gives the total cross sections found with the coupled-channel method along with corresponding DWBA values for the C^{14}(p, n) ground state and 3.95 MeV transitions. The effect of coupling in these two transitions is negligible, if one

[4] Written by M. J. Stomp.

Table 13. Coupled-channel cross sections. All values in millibarns. $\alpha = \alpha_T = .715$ fm^{-1}; $\beta_T = 4.$ fm^{-1}.

	Run 1[a]	Run 2[b]	DWBA[c]
C^{14} (reaction)	721.	----	----
C^{14}(p, n) ($0^+ \rightarrow 1^+$) (g. s.)	12. 8	12. 2	17. 0
C^{14}(p, n) ($0^+ \rightarrow 1^+$) (3. 95)	35. 7	36. 2	44. 8
N^{14}(n, n') ($1^+ \rightarrow 0^+$) (3. 95)	13. 9	22. 0	----
N^{14}(n, n) (elastic)	828.		

[a] $V_{00} = -60.$ $V_{10} = 7.$ $V_{01} = 9.5$ $V_{11} = 8.$ $V_T = 14.$

[b] Same as (a) except $V_{10} = 30.$

[c] $V_{11} = 7.$ $V_T = 14.$ (Recall that DWBA results are ~20% high for the C^{14}(p, n) (3. 95) transition.)

remembers that the theoretical DWBA values were about 20% high (see section on tensor force calculations). A comparison of the angular distributions for the DWBA and coupled-channel calculations is given for the two transitions in Figures 18 and 19. Again, the effect of coupling is negligible. Most of the difference seen, is more likely due to the inclusion of the spin-orbit potential in the coupled-channel calculation.

Any coupling effect on the C^{14}(p, n) ground state transition was expected to result from coupling to the N^{14}(n, n') 3. 95 MeV transition. The experimental value for the N^{14}(p, p') cross section is ~ 23 mbrns at 14.1 MeV incident proton energy. In view of this value, the N^{14}(n, n') coupled-channel value, 13.9 mbrns, shown in Table 13 (see Figure 20) seems small. In order to detect possible effects of this transition on the C^{14}(p, n) ground state transition, its theoretical value was artifically boosted by increasing V_{10} from 7. to 30. MeV. The 3. 95 MeV transition in N^{14} is the only coupling affected by a change of V_{10}. The value for the N^{14}(n, n') transition was raised to 22. 0 mbrns. But there was almost no effect on the C^{14}(p, n) ground state transition. One must conclude, therefore, that the DWBA calculations made for the C^{14}(p, n) reactions are about as accurate as the coupled-channel calculations. Spin-orbit effects for this system appear small, but non-negligible in agreement with other work (4).

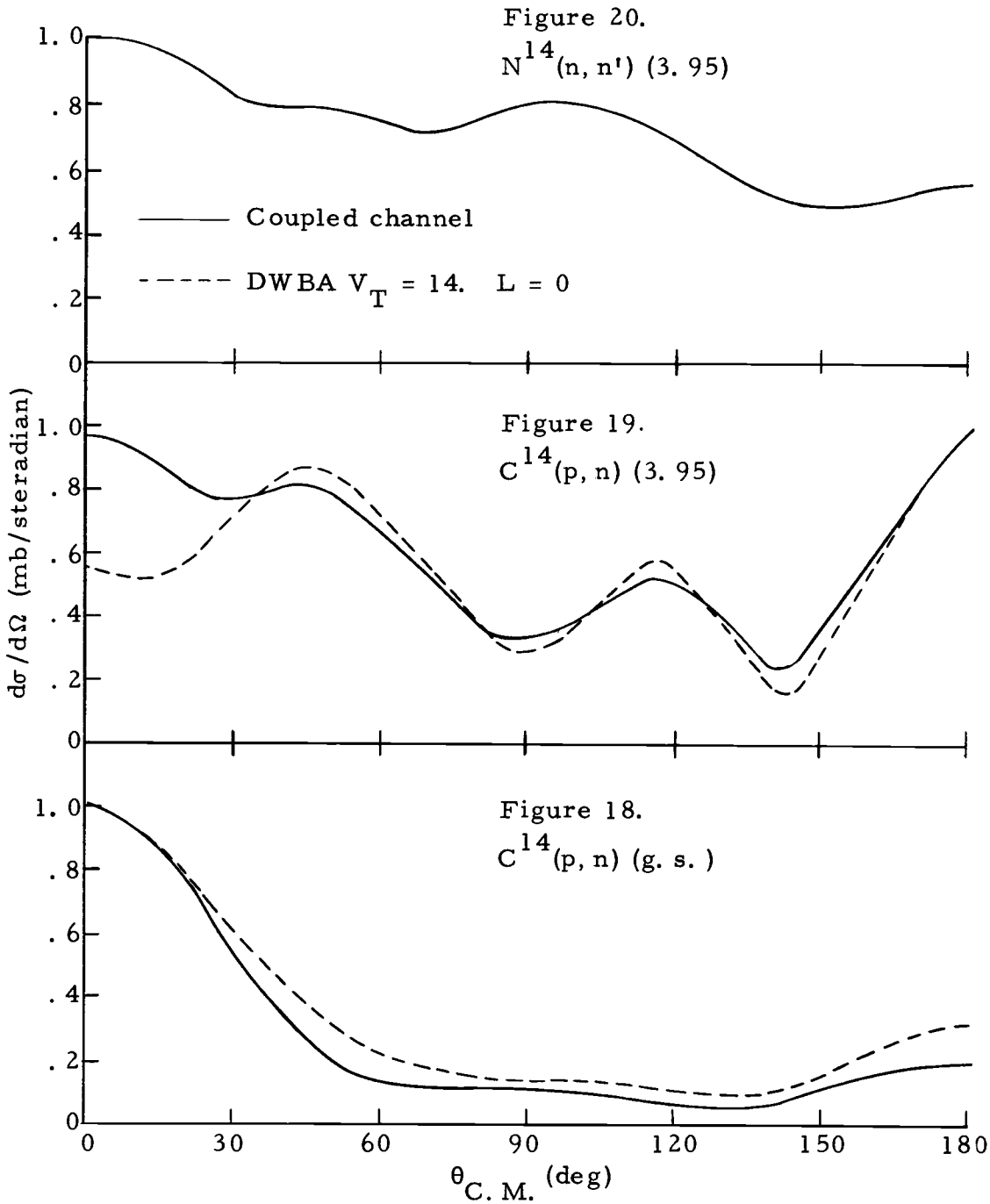

Figure 18-20. Coupled channel results and comparison with DWBA in A = 14.

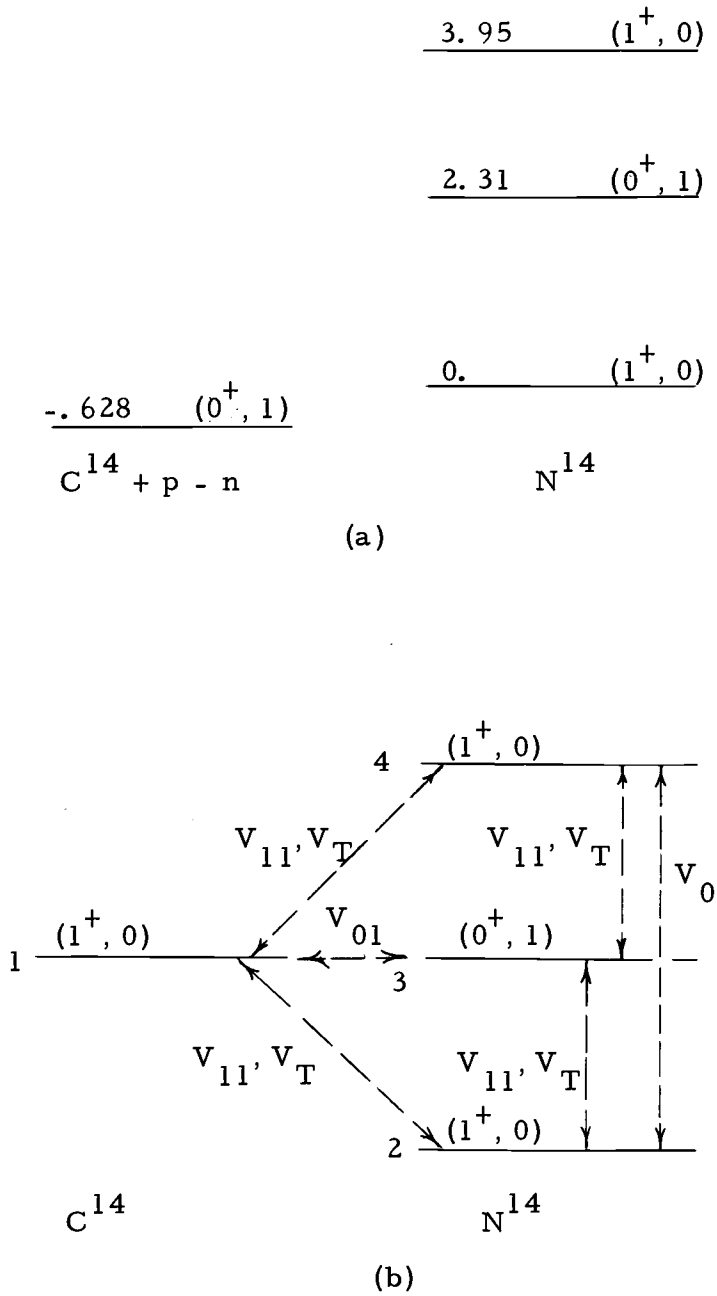

Figure 21. Low energy levels in C^{14} and N^{14}. (a) (J^{π}, T) and energies in MeV are shown; (b) The potential strengths which contribute to each are given, and channel numbers are noted to the left of each channel.

VII. SUMMARY

Effective potentials have been extracted from two independent sets of effective matrix elements, one set for the 1p shell (11), and the other for the 2s-1d shell (5). These potentials were then compared to values obtained by DWBA calculations from various scattering data. Several factors which could alter the DWBA results, and thus affect the comparison, were noted or investigated. These were exchange effects, core-polarization, and channel-coupling.

For both the 1p and 2s-1d shells, the central potentials, which were well determined, were found to have strong attractive even strengths and weak repulsive odd strengths (see Table 2). The comparison of the values obtained from individual shells was very reasonable, although a precise comparison was not necessarily meaningful. Unlike the central potentials, the tensor strength did not appear well-determined, and its values were not consistent for the two shells. These results are consistent with other determinations of the tensor strength however (39).

The potential strengths determined from effective matrix elements were found to be in good agreement with the spin and isospin-flip strengths, V_{10}, V_{01}, and V_{11} determined from DWBA calculations. They did not, however, give a reasonable value for the pure Wigner strength, V_{00}. The inclusion of exchange in DWBA calculations for the O^{18}(p, n) and C^{14}(p, n) reactions was used to define new

effective potentials for DWBA without exchange. These new potentials showed a dramatic improvement in the value obtained for V_{00} compared to the values obtained from scattering without a significant change in the agreement of the three other central strengths. This effect was L dependent, and the values predicated for V_{00} were greater in magnitude for $L = 2$ transitions than for $L = 0$ transitions. Core-polarization was also noted to give some improvement in the value for V_{00}.

The procedure which obtains strengths from effective matrix elements gives an unambiguous determination of the signs of the strengths which are needed in coupled-channel calculations.

Coupled-channel calculations were made for the $A = 14$ system. There were no noticeable effects due to coupling on either the $C^{14}(p, n)$ ground state transition or the transition to the 3.95 MeV excited state in N^{14}.

The tensor force was used in a survey of DWBA calculations. The effect in most reactions was not significant. A big improvement was noted in the results for the $C^{14}(p, n)$ ground state and $N^{14}(p, p')$ 2.31 MeV transitions. The $C^{14}(He^3, t)$ results remained in serious disagreement with experiment.

BIBLIOGRAPHY

1. Ajzenberg-Selove, F. and T. Lauritsen. Energy levels of light nuclei. VI. Nuclear Physics 11:1-340. 1959.

2. Amit D. and A. Katz. Effective interaction calculations of energy levels and wave functions in the nuclear 1p shell. Nuclear Physics 58:388-406. 1964.

3. Amos, D. A., V. A. Madsen and I. E. McCarthy. Antisymmetrized distorted-wave approximation for nucleon-nucleus scattering. Nuclear Physics A94:103-128. 1967.

4. Anderson, J. D. et al. Effective two-body force inferred from the (p, n) reaction on ^{17}O, ^{18}O, ^{27}Al, and other light nuclei. Livermore, California, Lawrence Radiation Laboratory, 1968. (Submitted to the Physical Review)

5. Arima, A. et al. A shell-model study of the isotopes of O, F, and Ne. Nuclear Physics A108:94-112. 1968.

6. Ball, Gordon Charles. An investigation of the (^{3}He, t) and (^{3}He, $^{3}He'$) reactions on 1p shell nuclei. Ph. D. thesis. Berkeley, University of California, 1968. 143 numb. leaves.

7. Bauer, R. W. et al. Elastic scattering of 7 to 14 MeV neutrons from nitrogen. Nuclear Physics A93:673-682. 1967.

8. Brown, G. E. Unified theory of nuclear models and forces. 2d rev. ed. Amsterdam, North-Holland, 1967. 259 p.

9. Brueckner, K. A. Many-body problem for strongly interacting particles. II. Linked cluster expansion. Physical Review 100: 36-45. 1955.

10. Buck, B. Calculation of elastic and inelastic proton scattering with a generalized optical model. Physical Review 130:712-726. 1963.

11. Cohen, S. and D. Kurath. Effective interactions for the 1p shell. Nuclear Physics 73:1-24. 1965.

12. DeBenedetti, Sergio. Nuclear interactions. New York, John Wiley, 1964. 636 p.

13. Elliot, J. P. and B. H. Flowers. The structure of the nuclei of mass 18 and 19. Proceedings of the Royal Society of London 229:536-563. 1955.

14. Federman, P. and I. Talmi. Coexistence of shell model and deformed states in oxygen isotopes. Physics Letters 19:490-493. 1965.

15. Gibbs, W. R. et al. Direct reaction calculation. Washington, D. C., 1964. 44 p. (National Aeronautics and Space Administration. Technical Note. NASA TN D-2170)

16. Glendenning, Norman K. and Marcel Veneroni. Inelastic scattering based on a microscopic description of nuclei. Physical Review 144:839-853. 1966.

17. Gupta, Raj K. and P. C. Sood. Effective interactions in C^{14}. Physical Review 152:917-923. 1966.

18. Hamada, T. and I. D. Johnston. A potential model representation of two-nucleon data below 315 MeV. Nuclear Physics 34: 382-403. 1962.

19. Inglis, D. R. The energy levels and the structure of light nuclei. Reviews of Modern Physics 25:390-450. 1953.

20. Inoue, T. et al. The structure of the sd-shell nuclei. I. C^{18}, F^{18}, O^{19}, F^{19} and Ne^{20}. Nuclear Physics 59:1-32. 1964.

21. _____ The structure of the sd-shell nuclei. III. Effect of non-central interactions. Nuclear Physics A99:305-320. 1967.

22. Johnson, B. B., L. W. Owen and G. R. Satchler. Shell-model form factors for the $^{90}Zr(p, p')$ reaction. Physical Review 142: 748-757. 1966.

23. Kuo, T. T. S. and G. E. Brown. Structure of finite nuclei and the free nucleon-nucleon interaction, and application to ^{18}O and ^{18}F. Nuclear Physics 85:40-86. 1966.

24. Lassila, K. E. et al. Note on a nucleon-nucleon potential. Physical Review 126:881-882. 1962.

25. Locard, P. J., S. M. Austin and W. Beneson. Effective interaction and the reactions $^{7}Li(p, p')^{7}Li$ (478 keV) and $^{7}Li(p, n)^{7}Be$ (431 keV). Physical Review Letters 19:1141-1144. 1967.

26. Love, W. G. and G. R. Satchler. Core polarization and the microscopic model of inelastic scattering. Nuclear Physics A101: 424-448. 1967.

27. McManus, H., R. Petrovitch and D. Slanina. Inelastic scattering of medium-energy protons from nuclei. (Abstract) Bulletin of the American Physical Society, Ser. 11, 12:AD12. 1967.

28. Madsen, V. A. A formulism for direct inelastic scattering and charge exchange. Nuclear Physics 80:177-197. 1966.

29. Messiah, Albert. Quantum mechanics. Vol. II. Amsterdam, North-Holland, 1962. p. 507-1136.

30. Poletti, A. R. and E. K. Warburton. Relative phases of E2 and M1 matrix elements in 1p-shell nuclei. Physical Review 155: 1096-1104. 1967.

31. Reif, R., J. Slotta and J. Höhn. Excitation of non-normal parity states in inelastic proton scattering. Physics Letters 26B: 484-488. 1968.

32. Rose, H. J., O. Häusser and E. K. Warburton. Evidence for a nuclear tensor force from mass-14 beta- and gamma-ray data. Reviews of Modern Physics 40:591-610. 1968.

33. Rosenfeld, L. Nuclear forces. Amsterdam, North-Holland, 1948. 543 p.

34. Satchler, G. R. Inelastic scattering and the nuclear shell model. Nuclear Physics 77:481-512. 1966.

35. _____ Some studies of the effective interaction for the inelastic scattering of nucleons. Nuclear Physics A95:1-37. 1967.

36. Stevens, J., H. F. Lutz and S. F. Eccles. Elastic and inelastic scattering of protons by ^{18}O. Nuclear Physics 76:129-144. 1966.

37. Tamura, Taro. Analyses of the scattering of nuclear particles by collective nuclei in terms of the coupled-channel calculations. Reviews of Modern Physics 37:679-708. 1965.

38. True, William W. Nitrogen-14 and the shell model. Physical Review 130:1530-1537. 1963.

39. Visscher, William M. and Richard A. Ferrell. Beta decay of C^{14} and nuclear forces. Physical Review 107:781-796. 1957.

40. Warburton, E. K. and W. T. Pinkston. Shell model assignments for the energy levels of C^{14} and N^{14}. Physical Review 118:733-754. 1960.

41. Wong, C. et al. $C^{14}(p, n)N^{14}$ reaction and the two-body force. Physical Review 160:769-774. 1967.

APPENDIX

Optical Model Parameters

The general form of the optical potential used in this work is,

$$V(r) = -V_o f_o(r) - iW_v f_v(r) - i4a_s W_s(-\frac{df_s}{dr}) - V_{so}(\vec{\ell}\cdot\vec{\sigma})(\frac{\hbar}{m_\pi c})^2(-\frac{1}{r}\frac{df_o}{dr}) \quad \text{(A. 1)}$$

where

$$f_x(r) = [1+e^{(\frac{r-R_x}{a_x})}]^{-1}$$

for $x = o$, v, or s. All strengths are positive, and m_π is the pion rest mass.

For all DWBA calculations and the coupled channel calculation, with the exception of the $N^{14}(p, p')$ and $C^{14}(He^3, t)$ reactions, $W_v = 0$, $R_o = R_s = 1.25 \times A^{1/3}$, $a_o = .65$ and $a_s = .47$ fm. In addition, except for the coupled channel calculation $V_{so} = 0$ MeV. The values of the other parameters used are displayed in Table 14. Strengths for the real and imaginary parts of the potential are given for incident and final channels, along with the incident proton energy, the Q-value, and the final state energy for each reaction. For the most part, the parameters were obtained from Reference (4) and private communication.[5] Certain compromises were made however. For example, for the C^{14} reactions, an average Q-value was used for both the ground state and 3.95 MeV state transitions in order that a single set of

[5] Private communication with C. Wong.

Table 14. Optical model parameters (see Appendix for additional parameters). All values in MeV.

Reaction, transition	E_p	Q	$V_o(i)$	$V_o(f)$	$W_s(i)$	$W_s(f)$
$C^{14}(p, n)$ $(0^+ \rightarrow 1^+)$ (g. s.)	13. 7	-2	46. 0	50. 6	9. 0	6. 26
$C^{14}(p, n)$ $(0^+ \rightarrow 1^+)$ (3. 95)	13. 7	-2	46. 0	50. 6	9. 0	6. 26
$N^{14}(n, n')$ $(1^+ \rightarrow 0^+)$ (2. 31)	24. 5	-2. 31	51. 9	51. 9	5. 95	5. 95
$N^{15}(p, n)$ $(\frac{1^-}{2} \rightarrow \frac{1^-}{2})$ (anal.)	18. 8	-3. 54	46. 0	50. 0	9. 5	7. 5
$N^{15}(p, n)$ $(\frac{1^-}{2} \rightarrow \frac{3^-}{2})$ (6. 15)	18. 8	-9. 65	46. 0	50. 0	9. 5	7. 5
$O^{17}(p, n)$ $(\frac{5^-}{2} \rightarrow \frac{5^-}{2})$ (anal.)	13. 5	-3. 55	52. 0	50. 0	6. 25	4. 16
$O^{18}(p, n)$ $(0^+ \rightarrow 1^+)$ (g. s.)	11. 7	-2. 45	52. 0	50. 5	9. 0	5. 0
Exchange calc.						
$C^{14}(p, n)$ $(0^+ \rightarrow 1^+)$ (g. s)	13. 7	- . 628	46. 0	50. 6	12. 42	8. 66
$C^{14}(p, n)$ $(0^+ \rightarrow 1^+)$ (3. 95)	13. 7	-4. 58	46. 0	50. 6	12. 42	8. 66
$O^{18}(p, n)$ $(0^+ \rightarrow 1^+)$ (g. s.)	11. 7	-2. 45	52. 0	50. 5	12. 46	6. 92
Coupled channel calc.						
Initial channel is C^{14} + p	13. 7	a	47. 0	47. 0	7. 0	7. 0

[a] Q-values used were -. 628, -2. 94, and -4. 57 MeV for ground and first and second excited states in N^{14}.

distorted waves could be used for both transitions.

For the coupled-channel calculation, the spin-orbit potential was included with a strength V_{so} = 6 MeV. A single average optical potential was used in all channels (7, 36).

For the N^{14}(p, p) reaction, the parameters used were derived from values given in private communication.[6] The radii and diffuseness parameters were, a_o = .57, a_s = .61, R_o = 2.90, and R_s = 2.92 fm for both incident and final channels.

For the $C^{14}(He^3, t)$ calculation, volume absorption was used, rather than surface absorption, to conform with calculations by Ball (6). For the incident channel, W_v = 12.6 MeV, R_o = 2.94, R_v = 4.39, a_o = .569, and a_v = .795 fm. For the final channel, W_v = 11.37 MeV, R_o = 2.89 fm, R_v = 4.29 fm, a_o = .565 fm, and a_v = .811 fm.

Shell-Model Wave Functions and Bound State Parameters

For all bound states calculated in a Woods-Saxon potential, the diffuseness parameter was, a = .65 fm, and the radii were $R = 1.25 \times A^{1/3}$ fm. The binding energy, E, the potential depth, V, and the spin-orbit strength, C_{LS}, are given in Table 15. The 9. MeV binding of the $1p_{1/2}$ state is an average of the neutron separation energies in C^{14} and N^{14}, while the 6 MeV difference between the

[6] Private communication from S. M. Austin.

$1p_{1/2}$ and $1p_{3/2}$ states is approximately the splitting seen in N^{15} and O^{15}(41). The binding energies given for the $1d_{5/2}$ and the $2s_{1/2}$ states are found from the neutron separation energies of O^{17} and the first excited $1/2^+$ state in O^{17}, respectively (1).

In all cases, except for the A = 14 nuclei, the nucleon states were assumed to be pure jj-coupled shell-model states. For the A = 14 system, the intermediate-coupling wave functions of Visscher and Ferrell were used (39). The reasons for not using configuration mixed wave functions for the O^{18}(p, n) reaction have been discussed in Reference 4.

Range and Shape Effects of Potentials

Equivalent Gaussian and Yukawa potentials may be found by equating two-body matrix elements for $V_g(r) = V_g e^{-(\beta r)^2}$ and $V_y(r) = V_y \frac{e^{-\alpha r}}{\alpha r}$. Two particle harmonic-oscillator wave functions may be recoupled in relative co-ordinates so that two-body matrix elements may be expressed as one-body matrix elements.

$$\langle j_3 j_4 JT | V | j_1 j_2 JT \rangle \sim \sum_{\substack{\ell\ell' \\ nn'}} \langle n'\ell' | V | n\ell \rangle \qquad \text{(A. 2)}$$

where,

$$I = \langle n'\ell' | V | n\ell \rangle = \int R_{n'\ell'} R_{n\ell} V r^2 dr. \qquad \text{(A. 3)}$$

For short range (large α),

$$I \approx \int r^{\ell+\ell'} V(\alpha r) r^2 dr$$

$$\approx \frac{1}{\alpha^{\ell+\ell'+3}} \quad . \tag{A. 4}$$

The two-body matrix element will normally be proportional to $\frac{1}{\alpha^3}$ for short range, since those terms with the smallest ℓ and ℓ' will contribute. For $\ell = \ell' = 0$, equate Gaussian and Yukawa potentials (22).

$$\int V_g e^{-(\beta r)^2} r^2 dr = \int V_y \frac{e^{-\alpha r}}{\alpha r} r^2 dr. \tag{A. 5}$$

This equality implies $V_g/V_y = 2.25$ for $\alpha = \beta$.

The range and form dependence has been noted for some special cases using numerical methods. Two matrix elements have been looked at in detail.

$$\text{M2S} = \left\langle [\varphi_{2s}, \varphi_{2s}]_{J=0} \middle| V \middle| [\varphi_{2s}, \varphi_{2s}]_{J=0} \right\rangle \tag{A. 6}$$

$$\text{MDS} = \left\langle [\varphi_{2s}, \varphi_{2s}]_{J=0} \middle| V \middle| [\varphi_{1d}, \varphi_{1d}]_{J=0} \right\rangle \tag{A. 7}$$

Define n by, $M = V\alpha^{-n}$ where V and α^{-1} are the strength and range used in computing the matrix element M. M is M2S or MDS. For α varying from .5 to 1.5 fm^{-1}, n was found to

vary from 2.1 to 2.6 for M2S and from 1.7 to 2.5 for MDS. This result is valid for both Gaussian and Yukawa potentials, and compares with a short range value of 3 for n. For equal values of the inverse range α, the ratio, V_g/V_y, varied from 1.7 to 1.8 for M2S and from 1.4 to 1.6 for MDS. Recall that the short range value of this ratio is 2.5.

To obtain a more complete feeling for these effects, n was also determined for fits to the 15 effective matrix elements (refer to Chapter IV) in the 1p shell. A central Yukawa force with arbitrary exchange and a tensor force were assumed. There are four central exchange terms, triplet-even, singlet-even, triplet-odd, and singlet-odd. Each potential strength was then determined for two values of the inverse central range, $\alpha = .578$ and $2.\ \mathrm{fm}^{-1}$. A parameter, n_i, was determined from these strengths for each exchange term in the potential with the assumption that $V_i \sim \alpha^{n_i}$. The four values of n_i were $n_{TE} = 2.38$, $n_{SE} = 2.23$, $n_{TO} = 3.21$, and $n_{SO} = 4.25$. The larger values of n_i for the odd parts of the potential show that the matrix elements fall off faster with decreasing range for odd states. This result is expected, since the probability of finding two particles close together for an odd state is smaller than for an even state. For even and odd forces, average values for n_i of $n_E \sim 2.3$ and of $n_O \sim 3.7$ are convenient values for use in comparisons of calculations which use different ranges.

A similar procedure has been applied to DWBA amplitudes, both direct and exchange. Amplitudes were computed for three inverse ranges, $\alpha = .5, .7,$ and $3.$ fm^{-1} for a simple Yukawa force. This was done for the $L = 2$ ground state transition, and the $L = 0$ and $L = 2$ 3.95 MeV transitions in the $C^{14}(p, n)$ reactions. The parameter n was determined from $A \sim \alpha^{-n}$ where A is the DWBA amplitude. One value of n was computed for the inverse range $\alpha = .5$ to $.7$ fm^{-1} using the amplitudes computed from these two inverse ranges. A second value for n was computed for the inverse range $\alpha = .7$ to $3.$ fm^{-1}. The results are tabulated in Table 16.

Two things should be noted for the direct values. First, n increases toward the short-range value of 3 as α increases; second, the value of n is smaller for $L = 2$ than for $L = 0$. For the exchange amplitudes, n behaves in a nearly identical fashion; although, the magnitudes are somewhat smaller for exchange.

Hole Particle Transformations

In the use of configuration mixed wave functions and in the determination of the signs of potential strengths and matrix elements, it is important to obtain correct phase relationships in the calculations (32). This problem is more difficult when, as in this work, holes and particles appear. The problem will be discussed first for

Table 15. Single-particle bound state parameters (see Appendix for additional parameters). All values in MeV.

State	V	E	C_{LS} [a]
1p 1/2	48.1	9.00	.18
1p 3/2	49.0	15.00	.18
1d 5/2	48.0	4.15	.10
2s 1/2	48.0	3.28	.10

[a] The usual spin-orbit strength is $V_{SO} = V\left(\frac{C_{LS}}{2}\right)$.

Table 16. Range dependence of direct and exchange amplitudes. n_i is found from $A \sim a^{-n_i}$ where A is the amplitude. i = 1, 2 for two ranges.

Transitions in C^{14}(p, n)	Direct			Exchange		
	g. s. L=2	3.95 L=0	3.95 L=2	g. s. L=2	3.95 L=0	3.95 L=2
n_1, for a = .5 to .7	1.88	2.61	1.96	1.69	2.38	1.76
n_2, for a = .7 to 3.	2.31	2.62	2.24	2.25	2.46	2.25

scattering calculations and second in relation to two-body matrix elements.

In nucleon-nucleus scattering, the projectile is always a particle while the nucleus may be described in terms of holes or particles. For this problem, attention may be confined to the spectroscopic amplitude (see Equation (3. 26)):

$$S(I_n I_{n'}, I;\ T_n T_{n'}, T;\ j_1 j_2) = \frac{\langle J_{n'}, T_{n'} \| A_{I\tau}(j_1 j_2) \| J_n T_n \rangle}{\hat{I}\hat{\tau}} \qquad \text{(A. 8)}$$

where

$$A_{IK\tau\rho}(j_1 j_2) = \sum_{\substack{a_1 a_2 \\ m_1 m_2}} C(\tfrac{1}{2}\tfrac{1}{2}\tau;\ a_1 - a_2 - \rho)(-)^{1/2-a_1} C(j_1 j_2 I;\ m_1 - m_2 - K) \times (-)^{j_1 - m_1} a^{\dagger}_{j_2 m_2 a_2} a_{j_1 m_1 a_1} \qquad \text{(A. 9)}$$

To find the spectroscopic factor for holes, first commute the a's by use of the anticommutation relation

$$\left[a^{\dagger}_{j_2 m_2 a_2},\ a_{j_1 m_1 a_1} \right]_+ = \delta_{j_2 j_1} \delta_{m_2 m_1} \delta_{a_2 a_1}. \qquad \text{(A. 10)}$$

Now define the hole-creation and hole-destruction operators

$$b^{\dagger}_{jma} = (-)^{j+m} (-)^{1/2+a} a_{j-m-a} \qquad \text{(A. 11)}$$

and

$$b_{jma} = (b^{\dagger}_{jma})^{\dagger}. \qquad \text{(A. 12)}$$

With these definitions, it follows that

$$A_{IK\tau\rho}(j_1 j_2) = \sqrt{2}\,\hat{j}_1 \delta_{j_1 j_2} \delta_{\tau 0} \delta_{I0} \delta_{\rho 0} \delta_{K0}$$

$$+ (-)^{j_1+j_2-I-\tau} A^{h}_{IK\tau\rho}(j_2 j_1). \qquad \text{(A. 13)}$$

$A^{h}_{IK\tau\rho}$ is defined by exactly the same relation as for $A_{IK\tau\rho}$ except that particle operators $a^{\dagger}$ and a are replaced by the hole operators $b^{\dagger}$ and b. Now take reduced matrix elements of both sides of Equation (A. 13) to obtain

$$S(I_n I_{n'} I;\ T_n T_{n'} \tau;\ j_1 j_2) = (-)^{j_1+j_2-I-\tau} S^{h}(I_n I_{n'} I;\ T_n T_{n'} \tau;\ j_2 j_1) \qquad \text{(A. 14)}$$

for any transition between distinct initial and final states where

$$S^{h}(I_n I_{n'} I,\ T_n T_{n'} \tau;\ j_1 j_2) = \frac{\langle J_{n'} T_{n'} \| A^{h}_{I\tau}(j_1 j_2) \| J_n T_n \rangle}{\hat{I}\hat{\tau}}. \qquad \text{(A. 15)}$$

One can find spectroscopic factors for hole-states, then, simply by treating the holes as particles, reversing j_1 and j_2, and multiplying by the appropriate phase factor.

In order to compare two-body matrix elements deduced from hole-states with those found from particle states, one needs to know the connection between particle and hole interactions. This problem is discussed by Visscher and Ferrel (39). If $V(1, 2)$ is a two-body interaction for particles in co-ordinates 1 and 2, they show that an equivalent hole interaction is

$$V^h(1, 2) = \sigma_{y1}\sigma_{y2}\tau_{y1}\tau_{y2}V^{\dagger *}\tau_{y1}\tau_{y2}\sigma_{y1}\sigma_{y2} \qquad \text{(A. 16)}$$

where σ_{yi} and τ_{yi} are the y components of the Pauli spin matrices for spin and isospin respectively which act on coordinate i. For Hermitian, time-reversal invariant interactions, such as, 1, $\vec{\sigma}_1 \cdot \vec{\sigma}_2$, $\vec{\tau}_1 \cdot \vec{\tau}_2$, $\vec{\ell} \cdot \vec{S}$, and S_{12}, $V^h = V$.

In this work, Equation (A. 16) is not strictly true. If a two-body matrix is calculated between two two-particle states with orbital angular momentum ℓ_1, ℓ_2 and ℓ_3, ℓ_4, then the particle and hole-matrix elements will differ by an additional factor of $(-)^{\ell_1+\ell_2+\ell_3+\ell_4}$. This factor arises because $Y_{\ell m}$'s have been used in the description of single particle states, rather than the time-reversal invariant functions $i^{\ell} Y_{\ell m}$. However, all matrix elements in this work have been calculated entirely in the 1p or 2s-1d shell, and $(-)^{\ell_1+\ell_2+\ell_3+\ell_4} = +1$.

Potential Transformations

In this work the two-body potential is written in two different forms:

$$V = V_{00} + V_{10}\vec{\sigma}_1 \cdot \vec{\sigma}_2 + (V_{01}+V_{11}\vec{\sigma}_1 \cdot \vec{\sigma}_2)\vec{\tau}_1 \cdot \vec{\tau}_2 \qquad \text{(A. 17)}$$

and

$$V = V_{TE}P_{TE} + V_{SE}P_{SE} + V_{TO}P_{TO}+V_{SO}P_{SO}. \qquad \text{(A. 18)}$$

The strengths in these two representations will now be related.

Projectors onto singlet and triplet spin states are given by

$$P_0^{\sigma} = \frac{1}{4}(1-\vec{\sigma}_1 \cdot \vec{\sigma}_2) \tag{A. 19}$$

and

$$P_1^{\sigma} = \frac{1}{4}(3+\vec{\sigma}_1 \cdot \vec{\sigma}_2). \tag{A. 20}$$

P_0^{τ} and P_1^{τ} are defined in the same way for isospin space. P_E^{r} and P_0^{r} will denote even and odd space projectors. Note that for antisymmetric states

$$P_E^{r} = P_1^{\sigma} P_0^{\tau}, \tag{A. 21}$$

so that

$$P_{TE} \equiv P_1^{\sigma} P_E^{r} = P_1^{\sigma} P_0^{\tau} = \frac{1}{16}(3+\vec{\sigma}_1 \cdot \vec{\sigma}_2)(1-\vec{\tau}_1 \cdot \vec{\tau}_2). \tag{A. 22}$$

P_{SE}, P_{TO}, and P_{SO} may be re-expressed in a similar fashion. These relations and Equation (A. 18) allow one to write

$$V = \frac{1}{16}\{(3V_{TE}+3V_{SE}+9V_{TO}+V_{SO}) + (V_{TE}-3V_{SE}+3V_{TO}-V_{SO})(\vec{\sigma}_1 \cdot \vec{\sigma}_2)$$
$$+ (\ldots)\vec{\tau}_1 \cdot \vec{\tau}_2 + (\ldots)(\vec{\tau}_1 \cdot \vec{\tau}_2)(\vec{\sigma}_1 \cdot \vec{\sigma}_2)\}. \tag{A. 23}$$

A comparison of Equations (A. 17) and (A. 23) gives the desired relation, most easily expressed in matrix form:

$$\begin{pmatrix} V_{00} \\ V_{10} \\ V_{01} \\ V_{11} \end{pmatrix} = \frac{1}{16} \begin{pmatrix} 3 & 3 & 9 & 1 \\ 1 & -3 & 3 & -1 \\ -3 & 1 & 3 & -1 \\ -1 & -1 & 1 & 1 \end{pmatrix} \begin{pmatrix} V_{TE} \\ V_{SE} \\ V_{TO} \\ V_{SO} \end{pmatrix} \tag{A. 24}$$

Also, the inverse matrix is

$$\begin{pmatrix} 1 & 1 & -3 & -3 \\ 1 & -3 & 1 & -3 \\ 1 & 1 & 1 & 1 \\ 1 & -3 & -3 & 9 \end{pmatrix}$$

Note that these relations are valid only in the space of totally anti-symmetric functions.

Code for Particle Model Coupling Matrix Elements

The following equation has been derived for the coupling matrix elements (see Chapter III and in particular Equation (3. 19)):

$$V_{n_f n_i} = \sum_{II'L} C(II'L,\ n_i n_f) X(II'L,\ n_i n_f) \tag{A. 25}$$

where I, I', and L designate the total, spin and orbital angular momentum transfers, and n_i and n_f denote initial and final channels with their associated quantum numbers. The code to be

described calculates the X's for configuration-mixed shell model wave functions for an effective two-body potential of the form

$$V(r) = [(V_{00}+V_{10}\vec{\sigma}_1\cdot\vec{\sigma}_2)+(V_{01}+V_{11}\vec{\sigma}_1\cdot\vec{\sigma}_2)\vec{\tau}_1\cdot\vec{\tau}_2]v_C(r) + V_T S_{12}\vec{\tau}_1\cdot\vec{\tau}_2 V_{12}(r). \quad \text{(A. 26)}$$

V_{00}, V_{10}, V_{01}, V_{11}, and V_T are the four central and one tensor strengths. The radial parts are

$$v_C(r) = \frac{e^{-ar}}{ar} \quad \text{(A. 27)}$$

and

$$V_{12}(r) = E(a_T r) - (\frac{\beta}{a})^3 E(\beta_T r) \quad \text{(A. 28)}$$

where

$$E(ar) = (\frac{1}{(ar)^2} + \frac{1}{(ar)} + \frac{1}{3})\frac{e^{-ar}}{ar} \quad \text{(A. 29)}$$

The bound states may be calculated in a harmonic-oscillator or Woods-Saxon potential.

For convenience in coding, the following expressions have been used for X:

for non-definite isospin,

$$X = \sum_{\substack{j_1 j_2 \\ a_1 a_2 \\ T'}} SS' \overline{\alpha} z \quad \text{(A. 30)}$$

where

$$\bar{\mathcal{I}} = C(T'T'\tau'; \bar{p}_n - \bar{p}_{n'} - \rho')(-)^{T'-\bar{p}_n} \mathcal{I}(a_1 a_2 \tau'\rho'); \qquad \text{(A. 31)}$$

for definite isospin

$$X = \sum_{j_1 j_2} SS' \bar{\mathcal{I}} z \qquad \text{(A. 32)}$$

where

$$\bar{\mathcal{I}} = C(T'T'\tau'; \bar{p}_n - \bar{p}_{n'} - \rho')(-)^{T'-\bar{p}_n}$$

$$\times C(T_n T_{n'} \tau; P_n - P_{n'} - \rho)(-)^{T_n - P_n} \mathcal{I}(\tau\rho; \tau'\rho') \qquad \text{(A. 33)}$$

The quantities S and S', the nuclear and projectile spectroscopic factors, and $\mathcal{I}$, an isospin factor, have been defined in Chapter III. z is the sum of central and tensor form-factors also defined in Chapter III:

$$z = z_C + z_T \qquad \text{(A. 34)}$$

with

$$z_C = V_{I'\tau'} D_C(II'L; j_1 j_2) \bar{g}_L^{j_1 j_2} \qquad \text{(A. 35)}$$

and

$$z_T = V_T \sum_{\lambda} D_T(II'L\lambda; j_1 j_2) \bar{g}_L^{j_1 j_2}. \qquad \text{(A. 36)}$$

The D's are defined by

$$D_C = (-)^I COM(L, L) \tag{A. 37}$$

and

$$D_T = [2\sqrt{\frac{2\pi}{3}}(-)^L \langle \lambda \| Y_2 \| L \rangle \; W(11L\lambda;\; 2I)\delta_{I'1}] COM(L, \lambda) \tag{A. 38}$$

with

$$COM(L, \lambda) = (-8\pi) \frac{\hat{j}_1 \hat{j}_2 \hat{I}\hat{I}'}{\hat{L}} \langle \ell_2 \| Y_\lambda \| \ell_1 \rangle \begin{pmatrix} j_1 & \frac{1}{2} & \ell_1 \\ j_2 & \frac{1}{2} & \ell_2 \\ I & I' & \lambda \end{pmatrix} . \tag{A. 38}$$

The $\bar{g}$'s are closely related to the g's in Chapter III:

$$g_L^{j_1 j_2} = -(-)^L (4\pi) \bar{g}_L^{j_1 j_2} \tag{A. 40}$$

and

$$g_{L\lambda}^{j_1 j_2} = \frac{(-4\pi)}{3\sqrt{5}} \langle \lambda \| Y_2 \| L \rangle \; \bar{g}_L^{j_1 j_2} . \tag{A. 41}$$

A list of the cards and variables needed to operate the program is given below. The appropriate Fortran format is given at the right. It is convenient to display the data in five parts.

Part 1.

S TP PP (4F10)

1	I_1	T_1	P_1	π_1	
2	I_2	T_2	P_2	π_2	
.	.	.	.	.	(i1, 9X 5F10)
.	.	.	.	.	
.	.	.	.	.	
n	I_n	T_n	P_n	π_n	
Blank					

Part 2.

ISPIN IPINDX ITNSR (3i5)

SP $n_1 \ell_1 j_1 \alpha_1$ $n_2 \ell_2 j_2 \alpha_2$ $E_1 E_2$ (10X, 4F5, 10X, 4F5, 2F10)

I I (6X, i2)

S	S1	S2	n_f, n_i	τ
S	.	.	.	.
S	.	.	.	.
I	.	.	.	.
S	.	.	.	.
S	.	.	.	.
SP	.	.	.	.
.	.	.	.	.
.	.	.	.	.
Blank				

(10X, F10, 5X, F10, 5X, i1, 1X, i1, 7X, i1)

Part 3.

V_O V_{COUL} C_{LS} a R AM (6F10)

NPT NCONTRL H (2i5, F10)

α_C α_T β_T (3F10)

Part 4.

V_{00} V_{10} V_{01} V_{11} V_T (5F10)

Part 5.

N1 N2 N3 KG KX KTNSR (6i10)

End of Data

Part 1. The first card contains the projectile spin, S, isospin, TP, and z-component of isospin PP.

The following cards, terminated by a blank card, contain information for the various channel states:

n = channel number.

I_n = spin of nucleus.

T_n, P_n = nuclear isospin and z-component.

π_n = parity.

The value of π_n is ignored. The values of T_n and P_n are ignored if target isospin is not specified to be a good quantum number (see below).

Part 2. The first card contains three controls:

1. ISPIN = { 1 target isospin is definite.
           { 2 non-definite.

2. IPINDX = { 1 X's are computed for both I' = 0, 1.
2 only I' = 0 terms calculated.
3 only I' = 1 terms calculated.

3. ITNSR = { 0 does not calculate tensor coefficients, D_T to save time.
not 0 calculation normal.

The remaining cards in part 2., which are terminated by a blank card, give spectroscopic information which describes the coupling. Each card must begin with the letters SP, I, or S.

The SP card designates a single-particle transition, $(n_1 \ell_1 j_1 \alpha_1) \rightarrow (n_2 \ell_2 j_2 \alpha_2)$:

$n_1 \ell_1 j_1 \alpha_1$ = The radial quantum number, the orbital angular momentum, the total angular momentum, and the z-component of isospin for the initial single-particle states,

$n_2 \ell_2 j_2 \alpha_2$ = The corresponding final state quantum numbers.

α is .5 or -.5 for neutrons or protons respectively. The numbers α_1 and α_2 are ignored if the nuclear isospin has been chosen as definite. E_1 and E_2, both positive, are the single-particle binding energies.

Each SP card must be followed by an I card specifying the total angular momentum transfer. Each I card must be followed by one or more S cards which give all spectroscopic factors for the

single-particle transition and angular-momentum transfer just specified on the SP and I cards.

S1 is the value of the spectroscopic factor.

n_f, n_i are integers which specify the final and initial channels.

Important, $n_f \leq n_i$. If this requirement is not met, the X's will not be stored properly.

$(T = 0, 1)$ is the nuclear isospin transfer. This parameter is ignored if the nuclear isospin was designated as non-definite.

Often for a given single-particle transition, specified by $(n_1 \ell_1 j_1 a_1) \rightarrow (n_2 \ell_2 j_2 a_2)$, it is troublesome to require a separate SP card for both the $(\ell_1 j_1) \rightarrow (\ell_2 j_2)$ and the $(\ell_2 j_2) \rightarrow (\ell_1 j_1)$ transitions. Under the special circumstances given below. S2 may specify the spectroscopic factor which corresponds to the inverse single-particle transition $(\ell_2 j_2) \rightarrow (\ell_1 j_1)$:

1. for definite nuclear isospin, $n_1 = n_2$ or
2. for non-definite isospin, both $n_1 = n_2$ and $a_1 = a_2$.

These requirements insure that

$$g_{L\lambda}^{j_1 j_2 a_1 a_2} = g_{L\lambda}^{j_2 j_1 a_1 a_2}. \qquad \text{(A. 42)}$$

In any other circumstances the value of S2 is ignored.

Part 3. These cards supply parameters for the bound state wave functions and values for the ranges of the two-body force. The parameters on the first card follow in order:

V_0 = potential depth for Woods-Saxon potential well.

V_{coul} = coulomb strength (not currently implemented)

C_{LS} = spin-orbit strength.

a = diffuseness parameter.

R = well radius (if R is 0, a harmonic oscillator potential is assumed).

AM = reduced mass of bound particle.

All the above values are positives. Units are in MeV and Fermis. The second card contains the number of mesh points to be calculated, NPT; a control parameter, NCONTRL; and the mesh size, H in Fermis. NCONTRL controls the printing of the bound state wave functions and the type of energy convergence:

NCONTRL = { even bound state functions are printed.
odd no print.

NCONTRL = { ≥ 0 The binding energy E is fixed, and V_0 is changed to provide an eigenfunction with energy E. The value of V_0 read in is used as a first guess for the potential.

$$\text{NCONTRL} = \begin{cases} < 0 & \text{The well depth } V_0 \text{ is fixed, and the binding energy} \\ & \text{is changed. The value of E read in is used as a} \\ & \text{first guess for the binding energy.} \end{cases}$$

The third card contains the central range a_C and the two tensor ranges a_T and β_T. A check is made on a_T. If a_T is zero the calculation of tensor form-factors, $g_{L\lambda}^{j_1 j_2}$, is bypassed.

Part 4. A single card specifies the four central and one tensor strength in order:

$$V_{00} \quad V_{10} \quad V_{01} \quad V_{11} \quad V_T.$$

Part 5. A single card controls the printing of the g's and X's. These functions are output for the mesh points from n_1 to n_2 in steps of n_3.

If KG $\neq$ 0, then the $g_{L\lambda}^{j_1 j_2}$'s are printed.

If KX $\neq$ 0, then the X's are printed.

If KTNSR $\neq$ 0, then tensor parts of $g_{L\lambda}^{j_1 j_2}$ are printed as well as central parts.

Two control routines KRNLMAIN and XMAIN operate the program. The $g_{L\lambda}^{j_1 j_2}$'s are computed in KRNLMAIN and stored on unit 6. From there XMAIN uses them, along with the potential strengths in part 4 of the data, to compute X's, which are stored on unit 7.

Part 5 of the data is used in XMAIN for output control. If one wants to recompute the X's where only the potential strengths have been changed, all that is necessary is to add new data for parts 4 and 5 and rerun XMAIN. The $g_{L\lambda}^{j_1 j_2}$'s do not have to be recomputed. A number of coefficients and tables which are also passed from KRNLMAIN to XMAIN are saved on unit 3 and are also used again if only XMAIN is rerun.

KRNLMAIN uses, directly or indirectly, the following subroutines: INPUT, TABLE, DEE GEE, GC BSWF2, BESSL, and a package of coupling subroutines which include, COFCG COF9J,COFW, and BICO. XMAIN uses two subroutines: EX and OUTPUT. A brief description of these routines will now be given in the order they are listed.

INPUT: This routine inputs and stores part 1 of the data.

TABLE: The most important function of this routine is to provide control. It creates tables which are passed to GEE, GC, EX, and, OUTPUT to provide efficient sequencing for these routines. For example, each $g_{L\lambda}^{j_1 j_2}$ is computed only once regardless of how many coupling matrix elements it may enter.

TABLE also inputs the spectroscopic information in part 2 of the data. This data not only provides numerical values, but its order also provides a control for the program.

Values for I are input, and values for I' are specified by TABLE according to the value of IPINDX. For each I and I' all values of L satisfying the triangle relationship $\Delta(II'L)$ are computed. Those that do not satisfy $(-)^{\ell_1+\ell_2+L} = +1.$ are discarded. Each distinct set of II'L values is entered in a table, IT, which is later stored along with the X on unit 7. At the same time TABLE also stores a table, NNA, which identifies and addresses the X's stored on unit 7.

All values of $SS'\overline{\mathcal{J}}$ (see Equations A. 30-A. 33) that occur are computed and stored for later use by the EX routine. $S'(I', T')$ (Equation 3. 25) is set equal to +1. for all arguments. A simple modification would allow other values since the array already exists.

Finally TABLE computes and stores the D's (see Equations (A. 35-A. 38)) for use in the EX routine.

DEE: DEE calculates the D's for TABLE.

GEE: GEE, with the aid of GC, calculates the functions $\overline{g}_{L\lambda}^{j_1 j_2}$ (see Equations (A. 40, A. 41)) and stores them on unit 6. GEE also reads part 3 of the data and calculates the bound state wave functions by use of BSWF2. To make space for the wave functions while GEE is operating, KRNLMAIN temporarily saves a large block of tables on unit 3. GEE also uses unit 5 for scratch.

GC: The numerical integrations involved in the calculations are done by the GC using Simpson's rule. GC also calls BESSL to compute the necessary spherical Bessel and Hankel functions.

BSWF2: Bound state solutions are found for the differential equation

$$[\frac{\hbar^2}{2m}(-\frac{d^2}{dr^2}+\frac{\ell(\ell+1)}{r^2})+V(r)-E]u(r)=0 \qquad (A.43)$$

where

$$V=-V_o[F(r)-C_{LS}(\frac{\vec{\ell}\cdot\vec{\sigma}}{2})\lambda_\pi^2\frac{1}{r}\frac{dF(r)}{dr}] \qquad (A.44)$$

and

$$F(r)=[1+e^{(\frac{r-R}{a})}]^{-1}. \qquad (A.45)$$

λ_π is the pion compton-wave length. If $R = 0$, however, the routine uses a harmonic-oscillator potential:

$$V=-V_o[1-(\frac{r}{a})^2]. \qquad (A.46)$$

The harmonic oscillator strength, $\hbar w$, is given by $\hbar w=\frac{2}{a}\sqrt{\frac{\hbar^2}{2m}V_o}$.

The routine first integrates inward until the function turns over. The function is then integrated outward and matched to the results of the inward integration. Either V_o or E is adjusted until the match provides a smooth curve. E is altered if a control parameter NCONTRL is negative. Otherwise V_o is altered. If on the inward integration, the function fails to turn over, NCONTRL is set to 10 and

BSWF2 returns to the calling program. Also, if a smooth match is not made after ten tries, NCONTRL is set to 20 and BSWF2 returns to the calling program. After the solution is found, the number of nodes is counted. If the number does not agree with the input data the following message is printed: wrong number of nodes, node = n, where n is the number counted.

BESSL: The routine calculates the Bessel and Hänkel functions of a complex argument, $i^{\ell} j_L(ix)$ and $i^{\ell} h_L^{(1)}(ix)$. Higher L values are formed by upward recurrence and results lose significance as L increases, especially for small arguments, x.

COFCG, COF9J, COFW, BICO: The first three calculate Clebsch-Gordan, 9j, and Racah coefficients respectively. BICO is a binomial coefficient subroutine.

EX: First the potential strengths in part 4 of the data are read. These strengths are combined with the D coefficients and the $SS'\overline{\ell}$ factors previously calculated by TABLE. These combined factors are multiplied by the functions $\bar{g}_{L\lambda}^{j_1 j_2}$ stored on unit 6 and the appropriate sums are done (see Equations (A. 30-A. 36)). The final results, denoted by X are stored on unit 7.

OUTPUT: This routine can print the X and $\bar{g}$ functions directly from unit 7. If only the X's are to be printed, the routine needs no

other information except that on unit 7. In order to print the $\bar{g}$'s, certain information in tables is required so that the routine must operate with the rest of the program.